Manual for the Milner to Murphy Reach Gain Forecast Tool Version 1.1

DRAFT Final

October 2020

Idaho Department of Water Resources

Adapted from CH2M Hill's Final Signed Document (May 31, 2017)

Contents

Executive Summary

CH2M worked closely with staff at the Idaho Department of Water Resources (IDWR) to develop two spreadsheet-based tools to forecast reach gains in the Snake River. These two spreadsheets are referred to collectively as the Swan Falls Forecast Tool (SFFT).

- **Forecast Target.** The forecast target of the Swan Falls Forecast Tool (SFFT) is the daily gain in the Milner to Murphy reach of the Snake River, which is equivalent to the Adjusted Average Daily Flow (AADF) when no flow is passing Milner Dam. There is no intent to use the tool to forecast the AADF at the Snake River near Murphy, Idaho stream gage (USGS Station 13172500, referred to herein as the "Murphy Gaging Station") when there are releases from Milner Dam, as this flow is impacted by upstream reservoir operations that are difficult to predict. Further information regarding the AADF calculation is provided in the *Streamflow Measurement and Monitoring Plan* (Swan Falls Technical Working Group, 2014).
- General Description and Functionality of the Forecast Tools
  - The SSFT was set up in two Microsoft Excel spreadsheets. One spreadsheet is utilized to run the forecast in January (Jan-SSFT) and the other spreadsheet is set up to be run in May (May-SSFT).
  - As described in Section 2, gains in the Milner to Murphy reach of the Snake River are comprised of three components: discharge from the eastern Snake Plain aquifer (ESPA), reach gains from non-ESPA sources, and consumptively used diversions.
  - As described in Section 3, ESPA discharge is estimated using the Enhanced Snake Plain Aquifer Model (ESPAM) version 2.1 (IDWR, 2013) response functions, allowing the user to generate a forecast without having to run the aquifer model. ESPA discharge is calculated using four components: starting aquifer head surface, forecasted incidental recharge for the irrigation season, estimated groundwater pumping, and managed recharge that has occurred since the starting aquifer head was measured. Each forecast generated from the SFFT is based on the existing condition of the aquifer. The starting aquifer head surface for the Jan-SSFT is based on post-irrigation season water level measurements taken in late October/early November. The starting aquifer head surface for the May-SSFT is based on pre-irrigation season water level measurements taken in late March/early April. Incidental recharge is forecasted based on water supply predictor variables for three irrigation entities: North Side Canal Company, American Falls Reservoir District 2, and Big Wood Canal Company. Groundwater pumping for the upcoming irrigation season is estimated using the average monthly 2001 through 2010 net consumptive groundwater use for four groundwater irrigation entities identified in the Final Report for ESPAM 2.1 (IDWR, 2013): IEGW501, IEGW507, IEGW508, and IEGW509. Managed recharge volumes that have occurred since water levels were measured and that are expected to occur over the remainder of the season are entered into the SSFT for seven different managed recharge locations on the eastern Snake Plain: Southwest Irrigation District, Milner-Gooding Main Canal, Milner-Gooding Shoshone, Milner-Gooding Milepost 31, North Side Main Canal including Wilson Lake, Twin Falls Canal Company Murtaugh Canal, Big Wood Canal Company Richfield, Milepost 29, Wilson Canyon, and any future managed recharge locations may be added to this list.

- As described in Section 4, non-ESPA reach gains comprise three components: discharge into the Snake River from four major tributary streams (Rock Creek, Salmon Falls Creek, Malad River, and Bruneau River), irrigation return flows from diversions above Milner, and non-ESPA inflows from springs and returns in the Milner to Kimberly reach of the Snake River. Tributary inflows are forecasted based on the Surface Water Supply Index (SWSI) for the Big Wood River Basin and the Malad River.
- The tool estimates irrigation drainage discharge ($Q_{Returns}$) from the North Side Canal Company and Twin Falls Canal Company based on the median of the historic measurements of discharge.
- As described in Section 5, diversion measurements below Milner Dam on the Snake River are not readily available. Therefore, calculations in the forecast tool assume that any excess diversions below Milner Dam will return to the Snake River. The tool utilized the median consumptive diversion estimate from 2003 through 2016 to determine the consumptive diversion amount for the forecast. **Forecast Tool Input.** The State of Idaho must update the tool with new well water level data and surface water supply index (SWSI) data each year, then other users can use the forecast tool with the following inputs:
- **Forecast year –** the year the user wants to forecast.
- **Number of wells in the head surface interpolation scheme –** the number of points used to interpolate a head surface across the model grid ESPA Model version 2.1.
- **Anticipated Managed Recharge Volumes** – anticipated monthly managed recharge volumes at seven managed recharge locations.

- **Forecast Tool Output**. Both the January and May SFFTs generate the following, given the user inputs for the remainder of the calendar year:
  - The median value (50% exceedance) of ESPA daily discharge to the Kimberly to King Hill reach of the Snake River.
  - ESPA daily discharge in the Kimberly to King Hill reach of the Snake River
  - The median value (50% exceedance) of the daily reach gains in the Milner to Murphy reach of the Snake River.
  - Daily reach gains in the Milner to Murphy reach of the Snake River

1.Project Goals, and Project Team

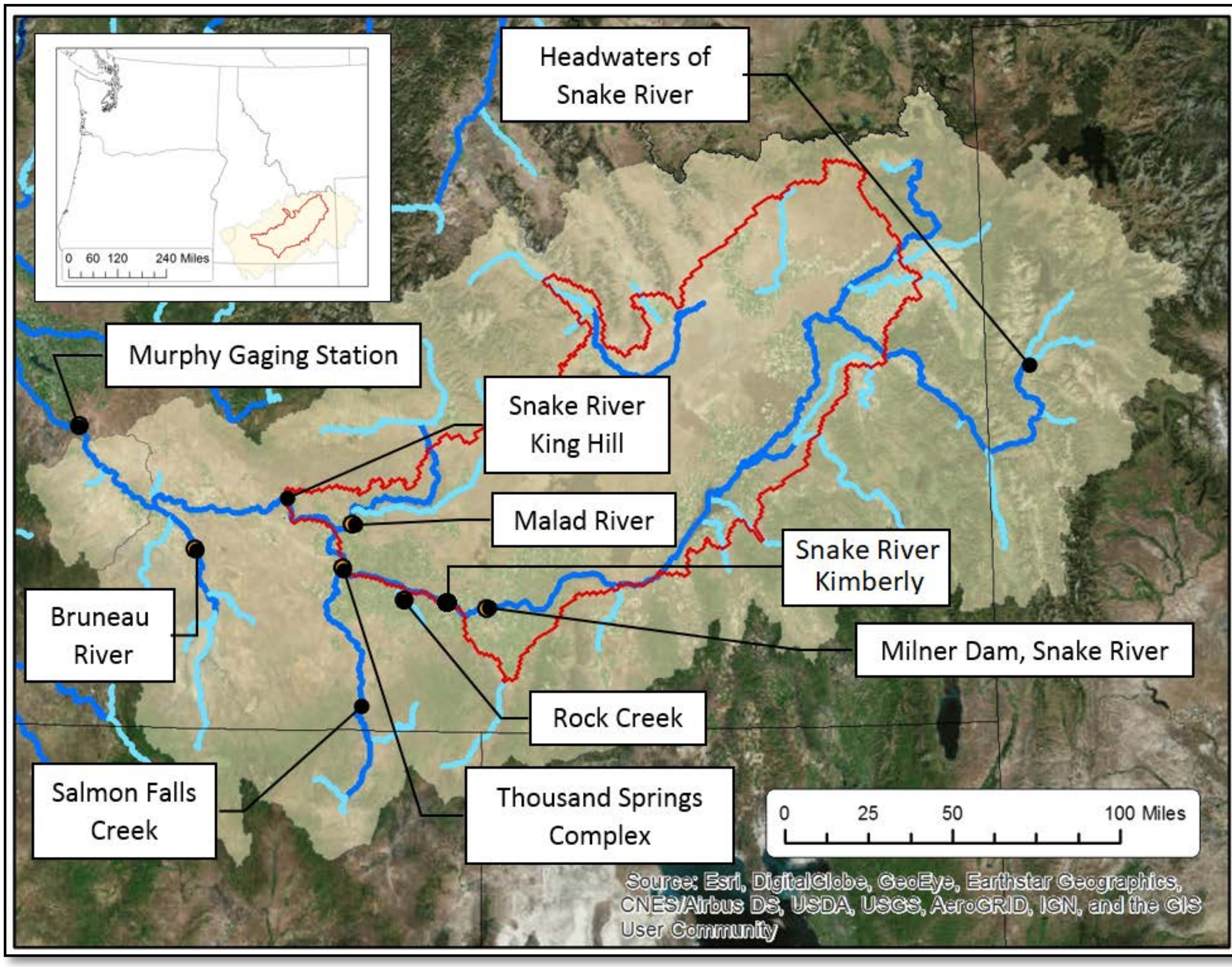

Figure 1-1. Map of the Eastern Snake River Plain and other relevant points of interest

1.1. Project Goals

The goal of this project is to provide water managers with a tool for forecasting the gains in the Milner to Murphy reach of the Snake River. The term *reach gain* refers to the increase in discharge between two measurement points on a river. Milner Dam is located at the head of the Milner to Murphy reach (see Figure 1-1). Since no discharge passes Milner Dam during the critical low flow period in the summer (Swan Falls Technical Working Group, 2014), the Milner to Murphy reach gain is equivalent to the flow at the Snake River at the Murphy Gaging Station during the low flow period.

1.2. Project Team

CH2M HILL worked closely with a subcontractor, the Henry's Fork Foundation, specifically Rob Van Kirk and Gary Johnson, to complete this work. In addition, the following state staff contributed significantly to this forecasting effort:

- Sean Vincent – Managed the project for the State of Idaho and provided the State's perspective throughout the forecast tool development process.
- David Hoekema and Dan Stanaway – developed historic consumptive diversion estimates and return flow estimates to include in the forecasting tool.
- Jennifer Sukow, Mike McVay, Wesley Hipke, Liz Cresto, and Allan Wylie – provided insight and data throughout the forecast tool development process.

Members of the Swan Falls Technical Working Group provided insight and review comments on the forecasting procedure.

2. Forecast Tool Target

The forecast target is the baseflow in the Milner to Murphy reach of the Snake River defined as the natural flow of the Snake River past Murphy gaging station minus Snake River flows past Milner Dam, which is equivalent to the Adjusted Average Daily Flow (AADF) at the Murphy Gaging Station when no flow is passing Milner Dam (Figure 2-1 to 2-3). The AADF calculated flow past Murphy minus flows past Milner would have been the ideal target for this analysis, but the AADF has only been calculated since 2014. Since there was not enough data to validate the forecasts to the AADF, a simplified version of the AADF minus Milner flows was developed and used as the validation target for this analysis. The simplified AADF was calculated as the which was estimated as 7-day moving average of the daily discharge past the Murphy gaging station minus the daily discharge of the Snake River past Milner Dam two days prior. The 2-day lag on the flow past Milner is applied to account for travel time from Milner to Murphy. The 7-day average was assumed to remove most of the Idaho Power Company's reservoir adjustments from the baseflow. The 7-day average is very similar to the AADF calculation when flow passing over Milner is removed. In this analysis the Murphy minus Milner flow is referred to as the Milner to Murphy reach gain. Figures 2-1, 2-2, and 2-3 compare the AADF (grey line) to the forecast target (black line). Where the grey line departs from the blackline, flow is passing Milner Dam.

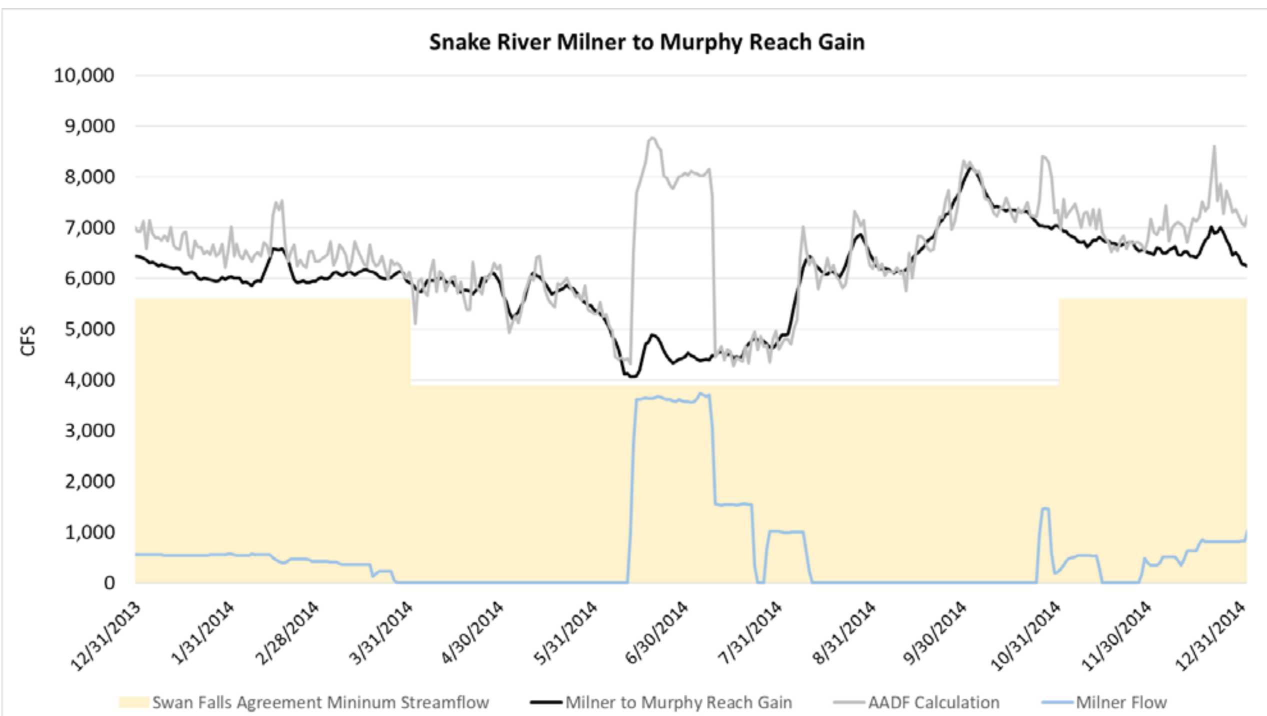

Figure 2-1. 2014 Snake River Milner Dam to the Snake River at Murphy Gaging Station Reach Gain compared to the 2014 AADF Calculation.

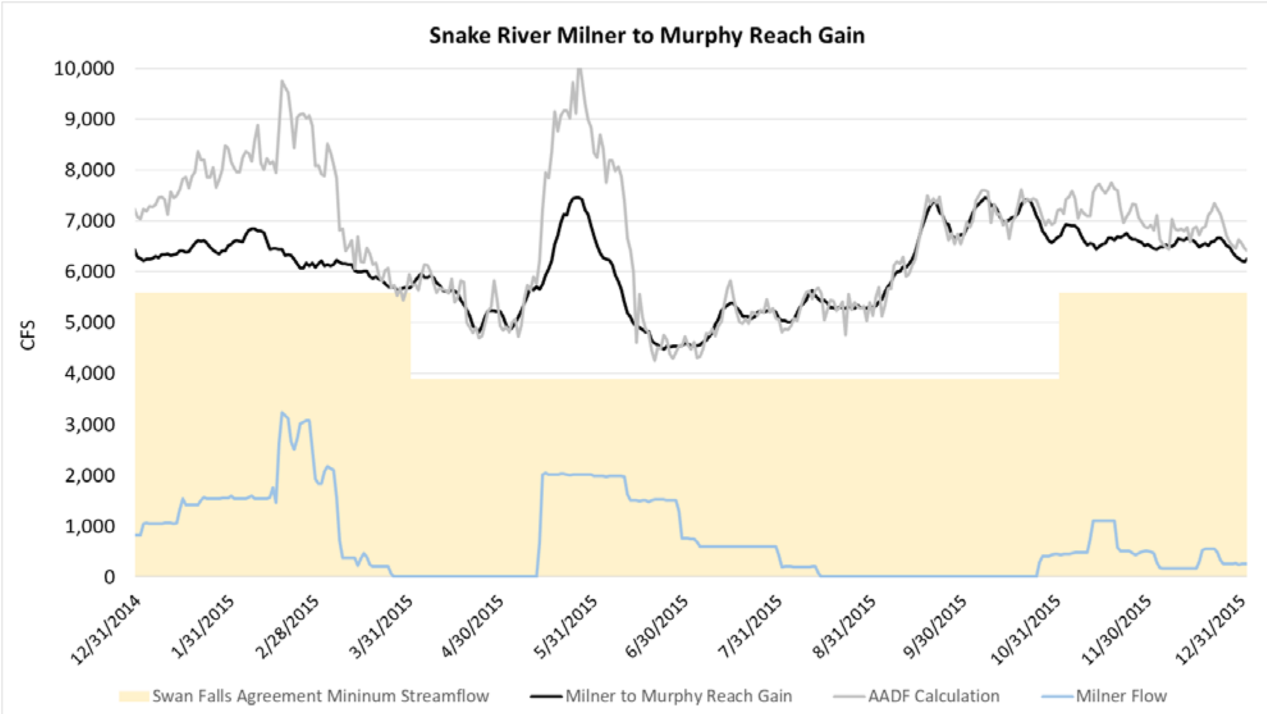

Figure 2-2. 2015 Snake River Milner Dam to the Snake River at Murphy Gaging Station Reach Gain compared to the 2015 AADF Calculation.

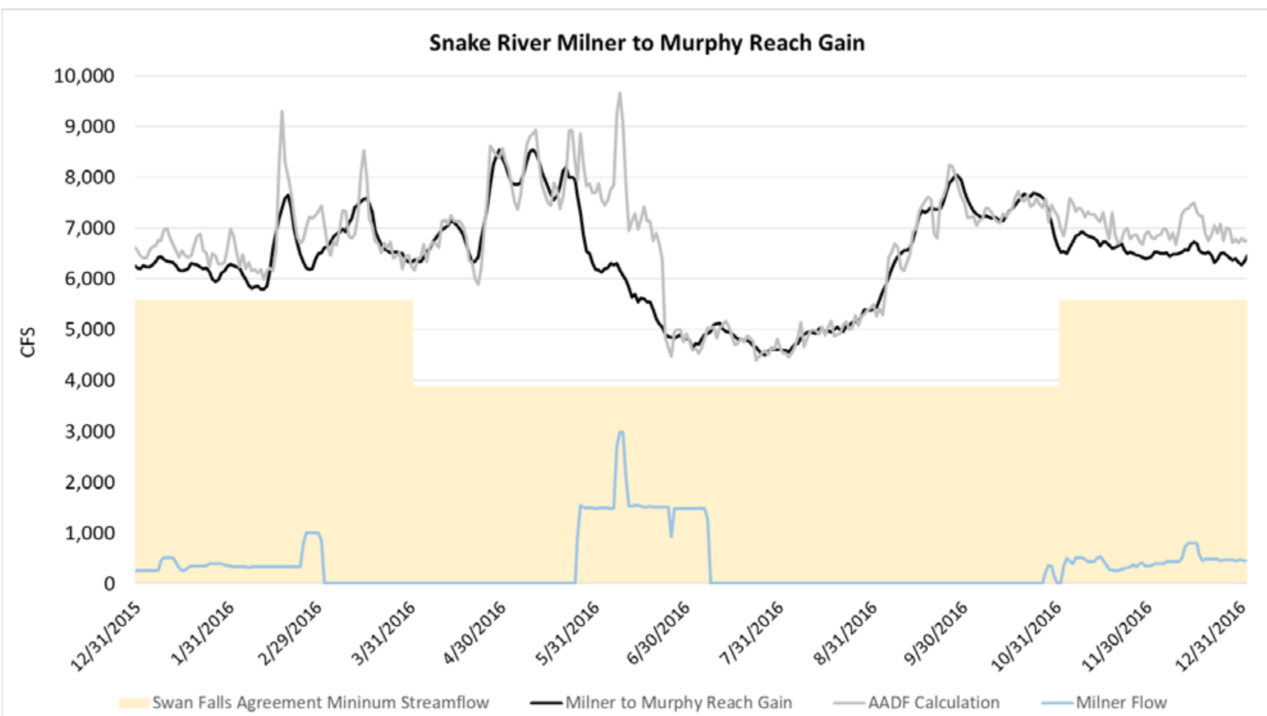

Figure 2-3. 2016 Snake River Milner Dam to the Snake River at Murphy Gaging Station Reach Gain compared to the 2016 AADF calculation.

Gains in the Milner to Murphy reach of the Snake River ($RG_{Milner2Murphy}$) are comprised of three components: discharge from the eastern Snake Plain aquifer (Q_{ESPA}), reach gains from non-ESPA sources ($Q_{non\text{-}ESPA}$), and consumptively used diversions (Q_{DivET}). In equation form, the forecast target is:

$$RG_{Milner2Murphy} = Q_{Murphy} - Q_{Milner} = Q_{ESPA} + Q_{non\text{-}ESPA} - Q_{DivET} \qquad (2\text{-}1)$$

where,

Q_{Murphy} = discharge at the Snake River near Murphy Gaging Station (USGS 13172500)

Q_{Milner} = discharge at the Snake River at Milner Dam Gaging Station (USGS 13088000)

Q_{ESPA} = discharge from the ESPA between Milner Dam and King Hill$Q_{non\text{-}ESPA}$ = Milner to Murphy reach gains from non-ESPA sourcesQ_{DivET} = Milner to Murphy consumptive use

3. Aquifer Discharge Forecast Methods and Procedures

This section details each component used to generate a forecast of ESPA discharge (Snake River reach gains between Kimberly and King Hill), including starting heads, recharge incidental to irrigation, managed recharge, and pumping. Each component of the discharge forecast is based on response functions from ESPAM 2.1. Moving forward, if a new ESPA model is approved, the response functions within the forecast tool will be updated appropriately and as soon as practical.

3.1. General Response Function Concepts

Cause and effect relationships in groundwater hydrology can be described by response functions, also termed response ratios, impulse responses, algebraic technologic functions (Maddock 1972), and transfer functions. Response functions can be thought of as the system response to an external stress. There is extensive information on response ratios in the literature, including a detailed mathematical derivation (Maddock 1972, Morel-Seytoux and Daly 1975); a description of MODSRP, which is a modified version of MODFLOW that was developed to generate response functions (Maddock and Lacher 1991); a report on the integration of surface-water and ground-water flow models (Fredericks and Labadie 1995); and details of the development of transient response functions using a numerical model (Cosgrove and Johnson 2004).

Response functions are mathematical descriptions of cause and effect in systems governed by diffusive processes. As applied here, a response function is the mathematical description of the relationship between a stress to an aquifer at a specified location (the cause, or the stress) and an in impact (the effect, or the response) elsewhere the aquifer system. The response function, for example, could be a curve describing stream depletion over time, resulting from a unit stress. Each response function models the response of a specific river reach or aquifer water level to a unit stress at a specified location. By multiplying the response function curve by the magnitude of the stress, a curve can be created that depicts stream depletion or drawdown over time. Response functions can also be used to describe the response of the system at steady state, when the impact of the stress has been fully realized.

Response functions are typically based on a unit stress and represent the ratio of the effects exhibited at a specific river reach over time to the total applied stress. Aquifer properties (transmissivity, storativity, and river conductance) govern the shape of the response function. The magnitude and timing of surface water response to aquifer stress also depends on the proximity of the stress (pumping well, for example) to the surface water body. Stresses to the aquifer that are close to a river reach have more immediate impacts (shorter lag times) and relatively high peak magnitudes compared to stresses at greater distances. For example, river baseflow and spring discharge may increase following aquifer recharge events. If an aquifer stress, such as a recharge event, occurs at some distance from the aquifer discharge location, the associated aquifer discharge that occurs may be lagged by months or years relative to the timing of the aquifer stress. This lag develops as the stress propagates through the aquifer. However, the magnitude of the aquifer stress is also dampened as the stress moves through the aquifer.

3.2. Starting Heads Component of the ESPA Discharge Forecast

The groundwater level in the ESPA adjacent the Kimberly to King Hill reach of the Snake River rise and fall based on an annual cycle of aquifer recharge and discharge that is driven by the irrigation season and spring runoff. Aquifer discharge follows the rising and falling pattern in aquifer head. When water levels rise/fall in the ESPA, spring discharges increase/decrease within the Kimberly to King Hill reach of the Snake River. These increased/decreased spring discharges persist into the future, confounded by the effects of subsequent aquifer recharge and pumping events. The peak aquifer head in the annual cycle generally occurs in November at the end of the irrigation season is the aquifer “carryover”. This carryover or persistence effect provides some level of opportunity to forecast aquifer discharge to the river in future months. This projection is subsequently combined with forecasts of aquifer recharge from forecasted irrigation activities to provide a more accurate estimate of future aquifer discharge.

The January forecast tool uses measured aquifer water levels that were measured after the previous irrigation season in late October or early November. These measurements, which are generally centered on November 1, capture the peak of the aquifer water level hydrographs, and are used to estimate carryover effects of the previous irrigation season on Snake River gains between Kimberly and King Hill in the following spring and summer. The May forecast tool uses measured heads in the spring, generally centered on April 1. Carryover, pumping and aquifer recharge effects are estimated using version 2.1 of the Enhanced Snake Plain Aquifer Model (ESPAM 2.1) because the individual effects cannot be physically separated. Estimates produced by aquifer models are inexact because models are an imperfect representations of the real physical system. The model, however, incorporates our best understanding of the physical characteristics of the aquifer and it’s interconnections with the Snake River.

3.2.1. General Procedure for Estimating the Impact of Aquifer Heads on Future Gains

The Jan-SFFT is used to estimate effects of November aquifer heads, as measured at available wells, on aquifer discharge in the Kimberly to King Hill reach for the following 12 months. The procedure is the same for May-SSFT, but water levels measured in late March and early April are used instead of November water levels. The spreadsheet performs the following operations:

1. Determines the difference in aquifer head from November or April 2008 and the November or April aquifer head for the forecast year. The depth to water is used to calculate difference in aquifer head. Depth to water measurements are stored in a database in the spreadsheet for heads in November and April years 1980 to the present.
2. Interpolates measured head differences to each ESPAM 2.1 model grid cell in the southwest portion of the ESPAM model domain up to the approximate location of the Great Rift (represented approximately by column 100). The Great Rift is an imprecise hydrologic feature identified by steep groundwater contour lines in the ESPA that represent a divide between the upper and lower portions of the ESPA.

3. Multiplies the interpolated head by a set of predetermined head response functions from ESPAM 2.1 to estimate the contribution of each cell to future discharge of the Kimberly to King Hill reach of the Snake River.
4. Sums the products determined in step 3 to determine the forecasted difference in gains from 2008-09.
5. Adds the values from step 4 to the simulated Kimberly to King Hill gain recession determined from November, or April, 2008 heads with no subsequent aquifer recharge and discharge to forecast the effect of the November or April heads on Kimberly to King Hill gains in the remaining months of the forecast year.

This heads worksheet is integrated into a larger spreadsheet to forecast Kimberly to King Hill gains from multiple components.

3.2.2. Mathematical Description of Head Component Computational Methods

As described above, the carryover effect of November and April aquifer heads on Q_{ESPA} was determined through the application of initial head response functions developed from the ESPAM 2.1 model. The contribution of November aquifer head to Q_{HEADS} is determined as:

$$Q_{HEADS,t} = \Delta Q_t + Qref_t, \qquad (3\text{-}1)$$

where,

$$\Delta Q_{HEADS,t} = \Sigma_{\text{all cells}} (\Delta H_{i,j} * RF_{i,j,t}), \text{ and} \qquad (3\text{-}2)$$

$\Delta Q_{HEADS,t}$ is the calculated change in Snake River gains between Kimberly to King Hill resulting from the departure of specific year's November or April aquifer head values from November or April 2008 head values, evaluated at elapsed time t from November 1 or April 1, respectively,

$Q_{HEADS,t}$ is the estimated total November or April aquifer head contribution to river gains in a specific year at any elapsed time t, excluding any incidental recharge and groundwater pumping effects after November or April 1,

$\Delta H_{i,j}$ is the interpolated change in November aquifer head from the 2008 reference at any grid cell i,j,

$RF_{i,j,t}$ is the initial head response function for the grid cell i,j at time t, and

$Qref_t$ is the simulated gain contribution at elapsed time t from the ESPAM 2.1 2008 November or April aquifer heads.

These values were obtained by running two ESPAM 2.1 simulations, one with initial heads set to the November 2008 ESPAM 2.1 calibration result and simulating a one year period with no incidental recharge or groundwater pumping effects, and another simulation set to the April 2008 ESPAM 2.1 calibration result and simulating a one year period with no incidental recharge or groundwater pumping effects.

Of particular interest is the summation term in equation 3-2, $\Sigma (\Delta H_{i,j} * RF_{i,j,t})$, which represents the difference in a particular forecast year's November or April carryover effect from that occurring in 2008.

An example of this computational procedure is illustrated for November 2015 (Figure 3-1). In the example year 2015, the river gains from the reference year heads (November, 2008), shown by the dashed red line ($Qref_t$), diminish from about 5,900 cfs to about 5,400 cfs. This decrease in aquifer discharge to the Snake River occurs because, in the absence of any aquifer recharge from surface water irrigation or discharge from groundwater pumping, storage in the aquifer is depleted and aquifer water levels and discharge decrease with time. The computed difference in aquifer discharge to the Milner to Murphy reach relative to the 2008 heads (ΔQ_t computed from initial head response functions times head difference) is negative and is shown by the blue line plotted against the right hand axis. These negative values result from observed heads in November of 2015 being less than those of November 2008, resulting in a decreased aquifer discharge. The sum of the 2008 reference gains, and change in gains for 2015 results in the black line, which is the estimated gains that result from November 2015 heads if no incidental aquifer recharge or groundwater pumping occurred after that time ($Q_{HEADS,t}$).

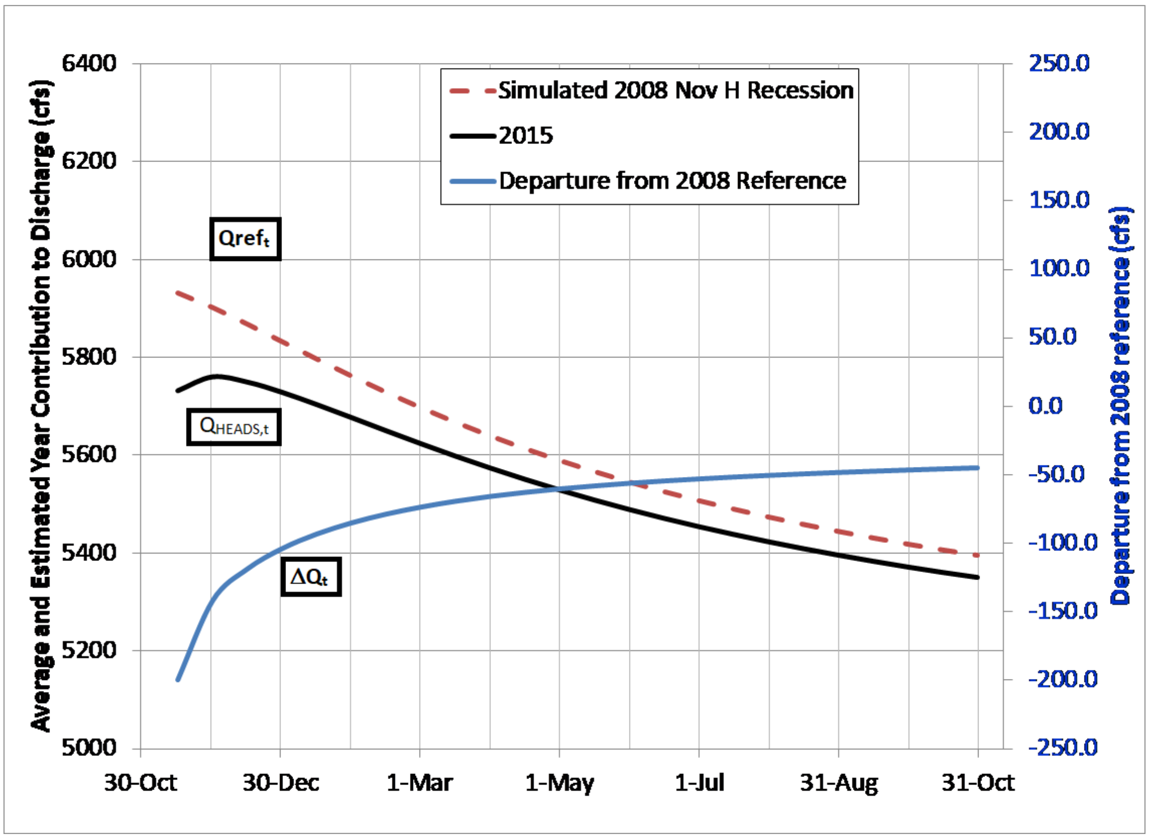

Figure 3-1. Simulated effects of November 2015 aquifer heads on Snake River gains between Kimberly to King Hill

3.2.3. Head Response Functions

Response functions have been used to estimate effects of changes in aquifer recharge and pumping on gains and losses to surface water in the Snake River Plain and other locations (Maddock 1972, Morel-Seytoux and Daly 1975, Maddock and Lacher 1991, Fredericks and Labadie 1995, Cosgrove and Johnson 2004). Valid application of response functions requires that the aquifer system respond in a near linear fashion (that is, effects of one recharge event are independent of the effects of other events). This is often the case when aquifer thickness is near constant in time and discharge sites are perennial. Typically, response functions express the ratio of the change in natural aquifer discharge (or head dependent gain) to a change in aquifer recharge or pumping at a specific location. Transient response functions are a series of values describing how the response changes over time.

Conceptually, an instantaneous pulse of recharge (or pumping) is equivalent to an immediate change in volume of aquifer storage at a specific location. Since a change in the volume of aquifer storage is equivalent to the product of head change and aquifer storativity or specific yield over some defined area, one would expect that response functions can be applied to changes in aquifer head similar to their application to recharge. This application is useful in the procedure to forecast aquifer discharge in the Kimberly to King Hill reach of the Snake River as that procedure requires an accounting of the effects of aquifer heads on future river gains. The validity of head based response functions is demonstrated in Appendix A via two methods, a simple 10x10 hypothetical model, and with the use of ESPAM 2.1. The units on head response functions are discharge rate/length (head). In this case, the most convenient units are cfs/foot of head.

3.2.4. Initial Head Response Function Array Determination

Initial head response functions were determined from the ESPAM 2.1 transient superposition input data sets developed by IDWR. We modified input files slightly to create a one-year simulation divided into 24 equal-length timesteps in a single stress period. Head-dependent fluxes from the river and general head boundary packages were saved in a binary water budget file for each timestep. We used the MODFLOW utility program bud2smp (Doherty 1995) to extract, reformat, and interpret the data in the budget file. The ESPAM 2.1 superposition simulation used an initial head of zero at all active model cells. That condition was maintained except at a single cell where initial head was elevated to 100 feet. One hundred feet was chosen to reduce the significance of numerical model error relative to the magnitude of estimated river gains. River gains (general head boundary plus river package) were simulated and stored from the single elevated head. The elevated head was then moved to the next active model cell and the simulation and data processing was repeated. This cycle was repeated 11,236 times until elevated head had been simulated at every active model cell. The river gains were compiled and divided by 100 feet (the head perturbation) and 86,400 sec/day to obtain response functions for each cell and timestep (24 timesteps over a one-year period) in units of cubic feet per second of river gain (Kimberly to King Hill reach) per foot of initial aquifer head.

Conceptually, the initial head response functions estimate the change in river gains in the Kimberly to King Hill reach of the Snake River that is caused by a one-foot change in aquifer head over the area of a single model cell (one square mile). Because the simulation progresses forward in time from the initial head, the head response functions provide insight into the degree to which today's aquifer heads influence future river gains. If we sum the response functions at all cells for a given time increment (for example, three months after the initial head), we obtain an estimate of the magnitude of change in river gains to expect from an aquifer-wide increase or decrease in aquifer head. This allows us to gain a sense of the degree to which current aquifer water levels affect future river gains. This sum of the response functions can be considered a measure of sensitivity of river gains to current aquifer heads. That sensitivity changes over time (Figure 3-2). Of course, this only considers the effects of initial or present aquifer head and does not account for any future changes in aquifer recharge. For example, if present aquifer heads are about one-foot higher than average for this time of year then, in about 180 days, river gains can be expected to be about 10 cfs greater than average (if all other conditions remain average).

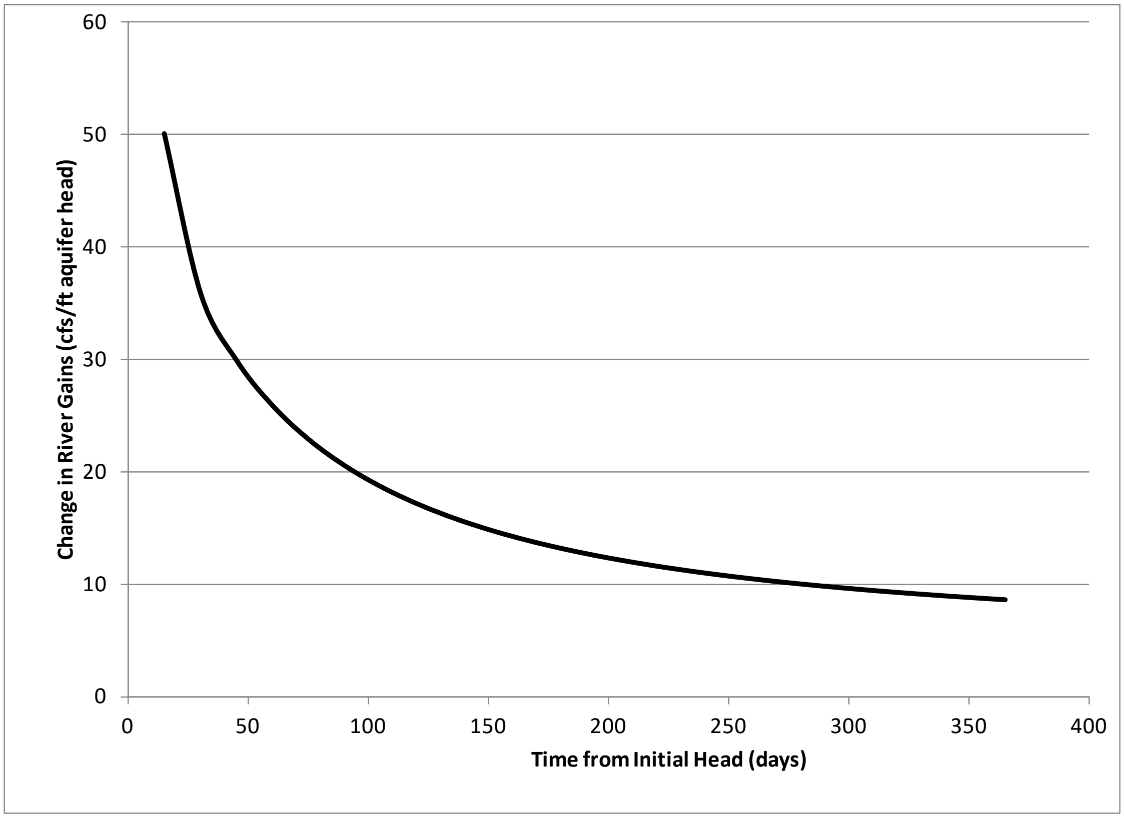

Figure 3-2. Sensitivity of future Kimberly to King Hill gains to current aquifer head

3.2.5. Determination of the Relevant Domain for Head Response Functions

The forecast tool becomes more efficient, and requires less water-level data, if the aquifer area used to evaluate November or April head impacts on subsequent spring discharge is limited in size. Forecasts of future gains to the Snake River in the Kimberly to King Hill reach depend on aquifer water levels at the time of the forecast. Water levels in more distant portions of the Snake River Plain aquifer, however, have a very small impact on near-term discharge in the Kimberly to King Hill reach due to lag and dampening of effects over distance and the distribution of the impact to other interconnected portions of the river. In the Snake River Plain aquifer, stresses more than approximately 60 km (37 miles) from the discharge location have little effect on seasonal discharge variability (Boggs et al. 2010). A similar evaluation was performed in this project using the updated ESPAM 2.1 aquifer model and initial head response functions. The area where aquifer head change is considered to produce a significant intra-year effect on Kimberly to King Hill gains is referred to as the relevant domain, and the area that can be excluded with negligible effect on forecasts is termed the exclusion zone. “Negligible effect” is a subjective term, but is considered to be less than five to ten cubic feet per second for the purpose of forecasting.

3.2.6. Procedure and Results of the Determination of the Relevant Domain for Head Response Functions

We implemented the following procedure to identify the area of the Snake River Plain aquifer that could be excluded from the analysis of observed November and April head effects on Snake River reach gains between Kimberly to King Hill the following July. Actual aquifer head change from an average November or April head in the excluded zone is not considered in estimation of gains meaning it is assumed to be zero.

Initial head response functions were determined for each model cell of the ESPAM 2.1 model grid as previously described. Those response functions express the effect of a one-foot variation in aquifer head over the area of the model cell on aquifer discharge in the Kimberly to King Hill reach of the Snake River at different time periods (cfs/foot of head). We selected a 9-month (274 days, representing November to July) response period for this analysis and sorted the response functions from smallest to largest for the 9 month response function. Because of the importance of distance in impacting response, smaller response functions tend to cluster at the more distant portions of the aquifer. A progressive cumulative response (that is, running total) was determined by summing 9 month response functions from smallest to largest for all model cells. One can interpret the cumulative response as the normalized error, per foot of aquifer head difference, associated with excluding all cells with lesser response functions in units of cfs/foot of head. Figure 3-3 shows the variation in cumulative response (normalized error) with the number of cells included in the sum, sorted smallest to largest 9-month response function. The error increases dramatically when more than about 8,000 model cells are excluded (Figure 3-3). When all 11,236 active model cells are excluded, the error is 100 percent of the predicted response, or 10.13 cfs per foot of aquifer head, after 274 days of head decay. When cells with ESPAM 2.1 column numbers greater than 100 are excluded, the error is 0.35 cfs per foot of head change, and more than 7,000 cells can be excluded from the initial head analysis, greatly simplifying our starting head procedure in the forecast tool.

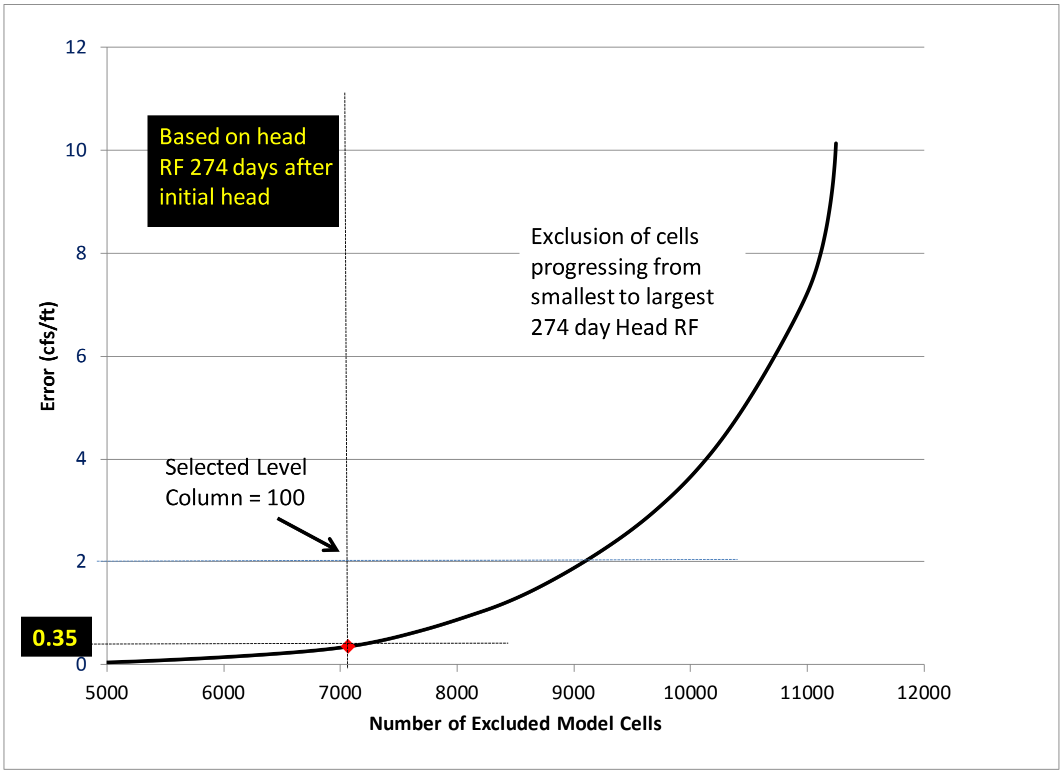

Figure 3-3. Relationship between the number of model cells excluded from an initial head analysis and the error induced in the Snake River gain between Kimberly to King Hill estimate
The error per foot of head difference from reference for the selected cutoff level of column 100 is also shown.

The relative error described in the previous paragraph is expressed in units of discharge (in cfs) per foot of uniform change in aquifer head from some reference value, in this case the November 2008 head distribution. In any given November or April, the variation from the 2008 reference will not be spatially uniform, and may vary between several feet below average to several feet above. Because the analysis presented here is based on idealized uniform conditions, the results cannot be quantitatively applied but are useful as a guide to understand the approximate magnitude of the error introduced by excluding a portion of the eastern Snake River Plain from evaluation of November aquifer head impacts on July river gains. In the worst case for the 1980-2015 period, aquifer head values in the relevant domain averaged nearly 28 feet above the 2008 reference in 1984. In that case, the estimated change in July gains (relative to 2008) in the Kimberly to King Hill reach of the Snake River is 274 cfs, and the error from excluding model columns greater than 100 is 9.8 cfs, or less than four percent. For most recent years, the absolute error is much smaller. In periods less than nine months, both the absolute and relative errors would be less.

3.2.7. Well Data used for Starting Heads Forecast Component

Depth to water measurements from wells in the southwest portion (ESPAM 2.1 column 100 or less) of the eastern Snake Plain aquifer are used to determine the difference in water levels from any November or April of interest and the reference values of November and April of 2008, respectively. These differences are then used to interpolate a “difference surface” at all ESPAM 2.1 model cells in column 100 or less. The best interpolated surface will result from a large number of uniformly distributed difference observations. Differences can only be established at wells that were measured in October or November of 2008 for the January forecast, or in March and April for the May forecast. The two-month window is set to provide a sufficient period to include an adequate number of wells. Observation dates in this window on average tend to occur about November 1 and April 1, which is consequently treated as the date of measurement for the respective forecast tool. IDWR staff (Mike McVay) provided a list of ESPA wells monitored during October and November and identified those wells in which observations appeared unrepresentative. From this list, 65 wells were: a) within the ESPAM 2.1 active model grid, b) in column 100 or less, and c) measured in October or November of 2008. Those wells and their model grid locations are given in Table 3-1. Following the same criteria, water levels in 60 wells were measured in the spring of 2008 (Table 3-2).

Many of the wells monitored in 2008 were not monitored in other years. The number of measurements in each year ranges from 24 in 1980 to 65 in 2008. Wells within this network must continue to be monitored for the forecasting tool to be used in the future. Although additional wells can be added to the network, they must have been monitored in fall of 2008 to determine a head difference with the reference year. Users should scrutinize the depth to water data of each year for which they are interested in making a forecast to ensure that no unrepresentative data are included.

Table 3-1. Selected Wells Measured in Fall 2008

Table 3-1. Selected Wells Measured in Fall 2008

Well Number	Altitude (ft msl)	IDTM Easting	IDTM Northing	ESPAM 2.1 Col	ESPAM 2.1 Row
05S 15E 35DBD2	3627	2447737	1304903	28	38
08S 24E 31DAC1	4227	2525237	1275694	60	78
09S 25E 03CAC1	4157	2538833	1274215	67	84
08S 25E 36DAA1	4209	2543147	1276060	69	84
09S 25E 23DBA1	4267	2540978	1269569	66	87
12S 21E 26CCD2	4435	2502551	1238321	36	91
10S 21E 28BCB1	4160	2499269	1258656	41	79
10S 21E 26AAA2	4154	2503776	1259168	43	80
08S 26E 03DCC1	4347	2549013	1283256	75	82
07S 26E 14CCC1	4403	2549625	1289800	77	79
12S 21E 02DAA1	4361	2504002	1245472	39	88
08S 14E 16CBB1	3177	2432018	1281521	12	45
07S 25E 19BAA1	4320	2534180	1289767	69	74
08S 15E 32CBB1	3308	2439955	1276681	15	50
12S 23E 06DCC1	4297	2515360	1244790	45	92
11S 21E 25AAA1	4376	2505612	1249466	41	86
05S 17E 26ACA1	3974	2467272	1306960	39	43

Table 3-1. Selected Wells Measured in Fall 2008

Table 3-1. Selected Wells Measured in Fall 2008

Well Number	Altitude (ft msl)	IDTM Easting	IDTM Northing	ESPAM 2.1 Col	ESPAM 2.1 Row
09S 29E 04BCA1	4227	2575456	1274856	86	95
07S 14E 33BBB1	3278	2432072	1287049	14	42
08S 17E 33DAD2	3822	2462011	1276110	26	58
06S 29E 15BBC1	4730	2576189	1300655	95	82
05S 14E 12AAA1	3609	2440267	1312524	27	31
12S 21E 25CCC1	4410	2504025	1238452	37	91
08S 14E 12CBC1	3272	2436872	1282918	15	46
09S 28E 18BAD1	4217	2563192	1271741	79	93
09S 29E 18CDA1	4249	2572902	1270942	84	96
08S 29E 34CBC1	4389	2576877	1276044	87	95
08S 28E 01AAA2	4495	2571981	1284979	88	89
05S 28E 26BBD1	4941	2568350	1307236	93	76
08S 14E 21ABA2	3190	2433125	1280861	13	46
08S 14E 23AAA1	3305	2436727	1280780	15	47
09S 16E 09CCA1	3508	2451433	1272919	20	56
09S 16E 11DDD2	3580	2455849	1272673	22	58
08S 16E 21AAA1	3582	2452675	1280422	23	52
08S 19E 05DAB1	4079	2479266	1284180	38	59
11S 23E 34CDC1	4271	2519882	1246220	47	92
09S 14E 03BAA1	3209	2434284	1275955	12	49
07S 20E 33AAA1	4293	2490960	1286444	45	62
06S 18E 07BCB1	3983	2469535	1302059	39	46
07S 14E 31ABA1	3193	2429856	1287263	13	41
12S 22E 35BCC1	4390	2512204	1237419	41	95
05S 25E 22DAD1	4583	2544511	1307835	80	68
09S 20E 30BCDD1	4018	2486605	1268025	37	70
08S 27E 07DBC1	4325	2553982	1282232	77	84
08S 16E 17CCC1	3490	2449643	1280705	21	51
06S 22E 28CDD1	4223	2512643	1296077	60	64
08S 30E 23DCC1	4512	2588972	1278904	95	97

Table 3-1. Selected Wells Measured in Fall 2008

Table 3-1. Selected Wells Measured in Fall 2008

Well Number	Altitude (ft msl)	IDTM Easting	IDTM Northing	ESPAM 2.1 Col	ESPAM 2.1 Row
03S 27E 24DDA1	4982	2561508	1327223	96	63
08S 18E 35BACD1	3908	2473856	1276646	33	61
08S 26E 33BCB1	4213	2546490	1276390	71	85
08S 27E 31DDA1	4203	2554326	1275460	75	88
06S 13E 23ABA2	3293	2428499	1299666	16	34
05S 13E 32DDC1	3297	2423811	1304711	15	30
09S 22E 16CDB1	4201	2509449	1270843	50	76
08S 25E 16DAC1	4243	2538092	1280719	68	80
02S 20E 01ACC2	4790	2497969	1342092	67	34
08S 28E 33ABA1	4330	2566854	1276927	82	91
07S 30E 24DDC1	4394	2590864	1288499	99	93
07S 29E 12CCC2	4565	2579929	1291636	94	88
06S 24E 32DBA1	4331	2531045	1295009	69	70
08S 17E 15CDC1	4010	2462682	1280567	28	56
01S 22E 18DBD2	4815	2509568	1348292	75	35
06S 15E 05DCC1	3587	2442766	1302972	25	37
09S 26E 13CCC2	4280	2551321	1270563	72	90
13S 22E 21CAA1	4495	2509668	1230960	37	97

Table 3-2. Selected Wells Measured in Spring 2008

Well Number	Altitude (ft msl)	IDTM Easting	IDTM Northing	ESPAM Col	ESPAM Row
05S 15E 35DBD2	3627.3	2447737	1304903	28	38
08S 24E 31DAC1	4226.5	2525237	1275694	60	78
09S 25E 03CAC1	4156.7	2538833	1274215	67	84
08S 25E 36DAA1	4209	2543147	1276060	69	84
09S 25E 23DBA1	4267	2540978	1269569	66	87
10S 21E 28BCB1	4159.6	2499269	1258656	41	79
10S 21E 26AAA2	4154.29	2503776	1259168	43	80
08S 26E 03DCC1	4346.5	2549013	1283256	75	82
07S 26E 14CCC1	4403.1	2549625	1289800	77	79

Table 3-2. Selected Wells Measured in Spring 2008

Well Number	Altitude (ft msl)	IDTM Easting	IDTM Northing	ESPAM Col	ESPAM Row
12S 21E 02DAA1	4361.3	2504002	1245472	39	88
08S 14E 16CBB1	3177.21	2432018	1281521	12	45
07S 25E 19BAA1	4320.4	2534180	1289767	69	74
08S 15E 32CBB1	3308	2439955	1276681	15	50
05S 17E 26ACA1	3974.02	2467272	1306960	39	43
09S 29E 04BCA1	4226.7	2575456	1274856	86	95
07S 14E 33BBB1	3277.5	2432072	1287049	14	42
08S 17E 33DAD2	3822	2462011	1276110	26	58
06S 29E 15BBC1	4730	2576189	1300655	95	82
05S 14E 12AAA1	3609	2440267	1312524	27	31
12S 21E 25CCC1	4409.6	2504025	1238452	37	91
08S 14E 12CBC1	3272	2436872	1282918	15	46
09S 28E 18BAD1	4216.8	2563192	1271741	79	93
09S 29E 18CDA1	4249.3	2572902	1270942	84	96
08S 29E 34CBC1	4389.3	2576877	1276044	87	95
08S 28E 01AAA2	4495	2571981	1284979	88	89
05S 28E 26BBD1	4941	2568350	1307236	93	76
08S 14E 21ABA2	3190	2433125	1280861	13	46
08S 14E 23AAA1	3305	2436727	1280780	15	47
09S 16E 09CCA1	3508	2451433	1272919	20	56
09S 16E 11DDD2	3580	2455849	1272673	22	58
08S 16E 21AAA1	3582	2452675	1280422	23	52
08S 19E 05DAB1	4078.94	2479266	1284180	38	59
11S 23E 34CDC1	4271.1	2519882	1246220	47	92
09S 14E 03BAA1	3209	2434284	1275955	12	49
07S 20E 33AAA1	4293.26	2490960	1286444	45	62
06S 18E 07BCB1	3983.05	2469535	1302059	39	46
07S 14E 31ABA1	3193	2429856	1287263	13	41
12S 22E 35BCC1	4390	2512204	1237419	41	95
05S 25E 22DAD1	4583.4	2544511	1307835	80	68
09S 20E 30BCDD1	4018.45	2486605	1268025	37	70

Table 3-2. Selected Wells Measured in Spring 2008

Well Number	Altitude (ft msl)	IDTM Easting	IDTM Northing	ESPAM Col	ESPAM Row
08S 27E 07DBC1	4325	2553982	1282232	77	84
08S 16E 17CCC1	3490	2449643	1280705	21	51
06S 22E 28CDD1	4222.7	2512643	1296077	60	64
08S 30E 23DCC1	4511.5	2588972	1278904	95	97
03S 27E 24DDA1	4982.1	2561508	1327223	96	63
08S 18E 35BACD1	3908.28	2473856	1276646	33	61
08S 26E 33BCB1	4212.7	2546490	1276390	71	85
08S 27E 31DDA1	4202.5	2554326	1275460	75	88
06S 13E 23ABA2	3293	2428499	1299666	16	34
05S 13E 32DDC1	3296.9	2423811	1304711	15	30
09S 22E 16CDB1	4201	2509449	1270843	50	76
02S 20E 01ACC2	4790.1	2497969	1342092	67	34
08S 28E 33ABA1	4330	2566854	1276927	82	91
07S 30E 24DDC1	4394.3	2590864	1288499	99	93
07S 29E 12CCC2	4565	2579929	1291636	94	88
06S 24E 32DBA1	4331	2531045	1295009	69	70
01S 22E 18DBD2	4815	2509568	1348292	75	35
06S 15E 05DCC1	3587	2442766	1302972	25	37
09S 26E 13CCC2	4280	2551321	1270563	72	90
13S 22E 21CAA1	4495	2509668	1230960	37	97

3.2.8. Head Interpolation

We used an inverse-distance-squared method to interpolate head differences (year of interest – reference year) at all grid cells (≤ ESPAM 2.1 column 100) between measured wells. The number of wells involved varies depending upon the number measured in both the year of interest and in the reference year (2008). We selected the inverse-distance-squared method because it is a simple method easily programmed into a spreadsheet, it is a widely-used method, it respects the differences determined at each well, and it does not produce any values larger or smaller than the observed differences. An option is included in the spreadsheet that allows the user to limit the number of neighboring wells used in the interpolation at a cell.

The inverse distance squared computation at each model cell is calculated in the spreadsheet by:

1. Calculating the IDTM easting and northing for the center of each model cell (≤ ESPAM 2.1 column 100)
2. Calculating the inverse square of the distance between the cell center and each well $1/(\Delta IDTM_{east}^2+\Delta IDTM_{north}^2) = w_i$
3. Ranking the distances between the cell and all measured wells and selecting those in the specified neighborhood
4. Calculating the interpolated head difference as $\Sigma(\Delta H_i*w_i)/\Sigma w_i$ for all wells in the neighborhood

These calculations are performed in a worksheet that is normally hidden from the user.

3.2.9. Reference Year (2008) Gains from Starting Heads

The 2008 reference year was chosen because a large number of wells (65) were measured in the spring and fall of 2008 in the southwest portion of the aquifer, and because it is the most recent year for which ESPAM 2.1 simulated head data were available. Simulated gains from a set of November or April heads could have been generated from either heads interpolated from measured values, or from heads resulting from the ESPAM 2.1 simulation. The latter was the preferred method because it is believed that the potential for significant error in gain estimates is greater when an initial head surface is determined from interpolated values. This is why the ESPAM 2.1 model calibration (and many other models) did not begin with head values interpolated from 1980 well measurements. Interpolation errors from head differences (year of interest – 1980 reference year) have significantly less potential for error because the values from well to well are more similar since they do not contain the potentially hundreds of feet of head difference due to background hydraulic gradients within the aquifer.

Head values from November 1, 2008 and April 1, 2008 were read from the binary head output file of the ESPAM 2.1 calibration and reformatted to a file with a format that was easier to view and work with. This file served as the starting head file for a one-year, single stress period, 24-timestep MODFLOW simulation that contained no head-independent aquifer recharge and discharge (removal of the .wel file). The Snake River gains between Kimberly to King Hill (drain and general head boundary files) generated for the January forecast simulation are shown in Figure 3-4. The graph appears as a recession as aquifer head declines from the initial head due to an absence of recharge.

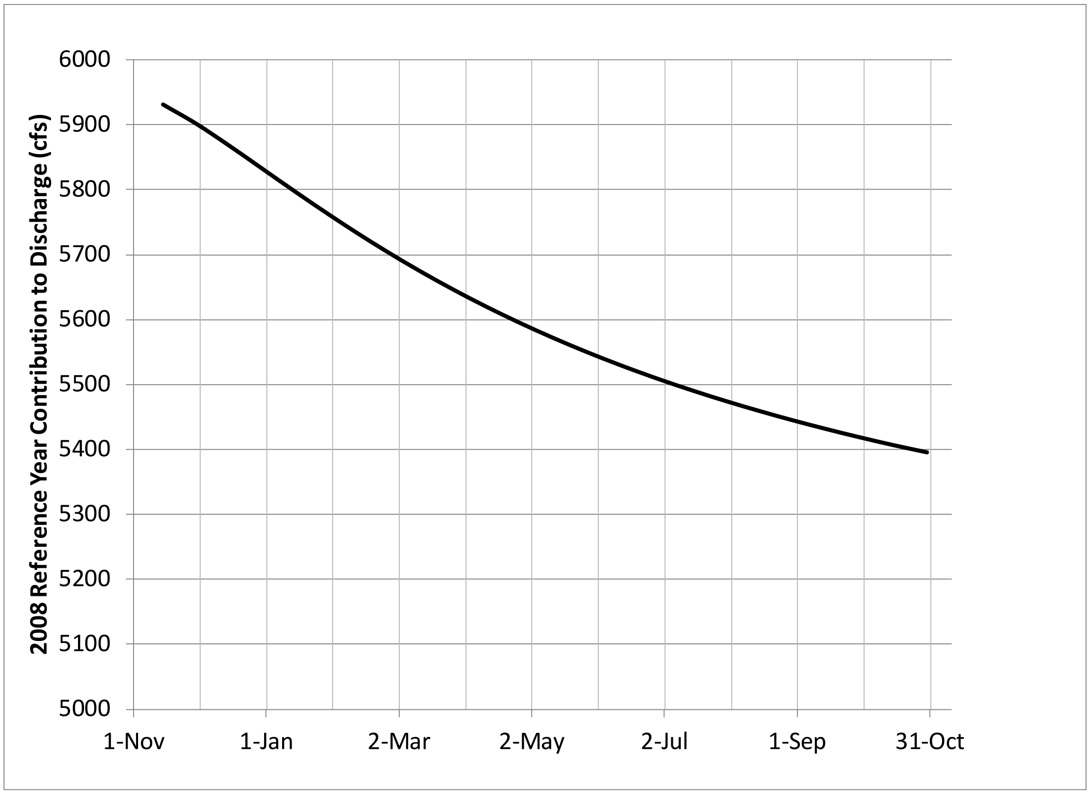

Figure 3-4. Simulated Snake River reach gains between Kimberly to King Hill resulting from November 2008 ESPAM 2.1 simulated heads with no subsequent aquifer recharge or discharge.
Dates shown after January 1 are in 2009

3.2.10. Estimated Gains for the 1980—2015 Period from Starting Heads

We used the procedure described above to calculate Snake River reach gains between Kimberly to King Hill for all years 1980-2015 (Figure 3-5). The number of measured wells in the reference well set (those measured in 2008) varied from 25 to 65 for the different years with generally the fewest wells in the earlier years. In each year, the cell-by-cell head interpolation was performed based on the nearest 10 neighboring wells. Results of the gains from head are compared to the ESPAM 2.1 simulated gains resulting from the model calibration. The gains estimated from November heads reproduce winter recession curves of the ESPAM 2.1 results well except in a few years. The differences may be due to a) failures of ESPAM 2.1 to reproduce the correct aquifer heads in some fall periods, b) recharge or pumping occurring during the late fall or winter periods that is not represented in the forecasting tool estimates of November head recessions, c) misrepresentative head measurements used in the November head estimates, and d) head interpolation error. A larger interpolation error is expected in the vicinity of the springs since the spring discharge tends to stabilize aquifer heads, which is not accounted for in the interpolation scheme. The effects of this error, however, will dissipate rapidly with time, well before the forecast period of interest in March or July. The similarity of the values estimated from November heads and those of the ESPAM 2.1 simulation lend support to the developed method.

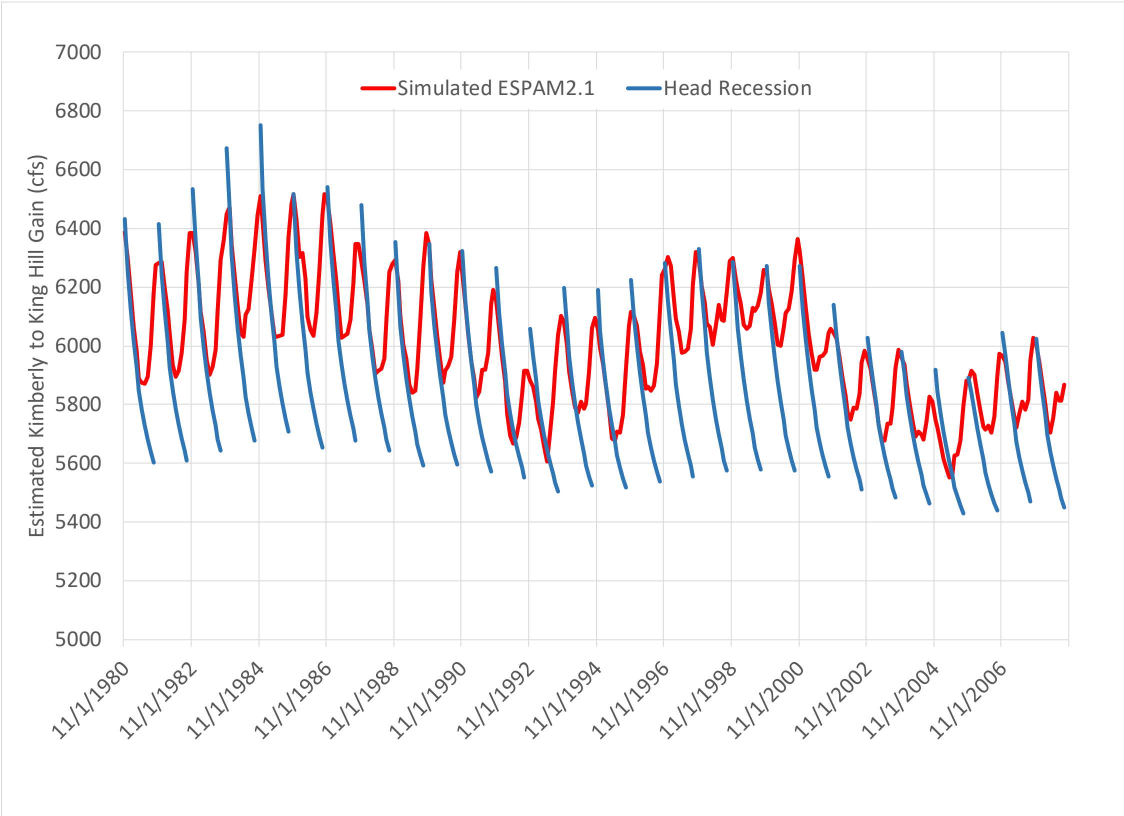

Figure 3-5. Gains estimated from November 1 aquifer head and ESPAM 2.1 simulated gains or the 1980–2008 period. The November 1 (labeled Head Recession) effects are assembled from individual years.

3.3. Recharge Incidental to Irrigation Component of the ESPA Discharge Forecast

3.3.1. Background

Recharge incidental to irrigation has two components: canal seepage and on-farm seepage. We calculated both of these components using algorithms taken directly from ESPAM 2.1. Canal seepage in each canal is a fixed fraction, taken from the ESPAM 2.1 documentation (IDWR 2013). The ESPAM 2.1 on-farm seepage algorithm is (see Appendix B in IDWR 2013):

$$\text{Rech} = (1 - \text{OFE}) \times \text{Dh} \times \text{DPin} + \text{Max}\,(\text{Peff} + \text{OFE} \times \text{Dh} - \text{ET} \times \text{A} - \text{Max}(\Delta\text{SM},0),\, 0) \times \text{DPex}, \qquad (3\text{-}3)$$

where,

Rech = deep percolation to ESPA aquifer (ft/month),

Peff = effective precipitation (ft/month),

OFE = maximum On-Farm efficiency (unitless),

Dh = farm headgate delivery (ft/month),

ET = evapotranspiration

A = ET adjustment factor (unitless),

ΔSM = change in soil moisture (ft/month),

Dpin = portion of initial loss to deep percolation (unitless), and

Dpex = portion of excess delivery to deep percolation (unitless).

3.3.2. Statistical Methods

Statistical modeling was used in three elements of the predictive tool:

1. Extension of the ESPAM-derived time series of evapotranspiration and precipitation data beyond 2008,
2. Prediction of upcoming irrigation-season diversion rates, and
3. Calibration of response-function predictions of monthly ESPA discharge to observed ESPA discharge (presented in Section 3.6).

All statistical analyses were implemented in R (R Core Team 2014), and outputs were then transferred to the spreadsheet environment. Development of predictive models for each of these three items was based on analysis of linear regression models with auto correlated residuals (Shumway and Stoffer 2011). The general form of these models is:

$$y(t) = \alpha + \sum_{i=1}^{m} \beta_i x_i(t) + \sum_{j=1}^{p} \phi_j \left[y(t-j) - \left(\alpha + \sum_{i=1}^{m} \beta_i x_i(t-j) \right) \right] + \varepsilon, \tag{3-4}$$

where,

$y(t)$ is the value of the response variable at time t,

α is the intercept,

$x_i(t)$ is the value of predictor i at time t (total of m predictor variables),

β_i is the regression coefficient for predictor i,

ϕ_j is the autoregressive coefficient of lag j (lags from 1 to p time steps), and

$\varepsilon(t)$ is an independent, identically distributed normal random variable with mean 0 and standard deviation σ.

In each application, we proposed a set of candidate models in the form of equation (3-4), based on preliminary descriptive data analysis and plausible physical mechanisms. All monthly data showed predictable seasonal variability, which we modeled with sine and cosine functions (trigonometric polynomials) of various frequencies. We then used Akaike's Information Criterion with small-sample correction (AICc) to rank models in the candidate set (Pawitan 2001; Burnham and Anderson 2002; Claeskens and Hjort 2008). After initial ranking, models containing "pretending variables"

(Anderson 2008) were removed and the remaining set ranked again. In most cases, we selected the model with lowest AICc value as the optimal model. However, because exceedance probabilities in discharge are based on quantiles of the normal distribution, we paid especially close attention to ensuring that model residuals met the assumptions of normality, independence, and constant variance. These assumptions were verified with residual plots. Models with data transformations were included in the candidate set when needed to improve residual properties. In some cases, the optimal model was not the one with highest ranking (lowest AICc value) but was selected based on residual properties and on precision of coefficient estimation. While selection of a lower-ranked model based on these criteria results in slightly lower predictive ability, models with more robust residual properties and more precisely estimated coefficients yield more realistic estimates of uncertainty based on distribution of the residuals. For this application, good estimates of uncertainty are more important than precision in estimating the expected value. Model performance was assessed with plots of observed versus fitted values and quantified with Nash-Sutcliffe Efficiency (NSE; Nash and Sutcliffe 1970).

3.3.3. Extension of Evapotranspiration and Precipitation Data

Calculation of on-farm seepage in ESPAM 2.1 requires values of monthly evapotranspiration (ET) and precipitation (PP) for each surface-water irrigation entity. Monthly ET and PP data used in ESPAM 2.1 were derived from spatial analysis and were available from May 1980 through September 2008. To extend this record to the period October 2008 through October 2016 without performing the full spatial analysis, we used regression models of the form of equation (3-4), using readily available ET and PP data as predictors. We first summarized monthly reference ET and PP data over the longest possible period of record at each of five currently operating AgriMet stations: Glenns Ferry, Fairfield, Picabo, Rupert, and Kimberly. We then compared monthly ET for the three irrigation entities, as reported in the ESPAM 2.1 documentation, to monthly reference ET at each of the five AgriMet stations. Monthly ET in all three irrigation entities was most highly correlated with monthly reference ET at Picabo ($r > 0.95$ for all irrigation entities). For each irrigation entity, the general model-selection procedure described above was used to determine the best regression model fit to the time period of overlap between the ESPAM 2.1 data and reference ET at Picabo. These models included a seasonal effect, modeled by trigonometric polynomials of frequencies 1, 2, 3 and 4 cycles per year, and autoregressive terms. Optimal ET models had very high NSE values (Table 3-3) and were used to extend the ET time series through October 2016 (Figure 3-6). An analogous modeling process was used for precipitation. Monthly PP from ESPAM 2.1 was most highly correlated with monthly precipitation at Kimberly ($r > 0.80$ for all irrigation entities), which was used as a predictor variable. These models also incorporated seasonal effects and autoregressive terms. Again, NSE values were high (Table 3-4), and the resulting models were used to generate PP values for water years 1989-2016 (Figure 3-7).

Table 3-3. Summary of regression models used to extend monthly evapotranspiration time series. All models were fit to monthly values for April 1993 through September 2008 (n = 186 months)

Irrigation Entity ID and Name	Maximum frequency of seasonal terms	Maximum lag of autoregressive terms	Nash-Sutcliffe Efficiency
IESW032 Northside	4 cycles/year	3	0.9999
IESW058 AFRD2	4 cycles/year	3	0.9999
IESW059 Gooding-Richfield	4 cycles/year	3	0.9999

Table 3-4. Summary of regression models used to extend monthly precipitation time series. All models were fit to monthly values for May 1990 through September 2008 (*n* = 221 months)

Irrigation Entity ID and Name	Maximum frequency of seasonal terms	Maximum lag of autoregressive terms	Nash-Sutcliffe Efficiency
IESW032 Northside	4 cycles/year	1	0.9999
IESW058 AFRD2	4 cycles/year	1	0.9999
IESW059 Gooding-Richfield	4 cycles/year	1	0.9998

The extended data sets consisted of monthly ET and PP values for the period May 1980 through October 2016, which were organized into irrigation-year format. The median across all irrigation years was used in the on-farm component of spreadsheet tool in calculating the 50% exceedance value of ESPA discharge (Figures 3-8 and 3-9). In calculating a given user-defined uncertainty range probability, the appropriate percentile across all irrigation years was used. For example, if the user specified the 90% exceedance flow as the output, the 10th percentile would be used for PP (90% of years had higher PP, i.e., were wetter; Figure 3-9), whereas the 90th percentile would be used for ET (90% of years had lower ET, i.e., were wetter; Figure 3-10). Higher ET and lower PP lead to lower on-farm seepage, which leads to lower recharge and hence lower aquifer discharge.

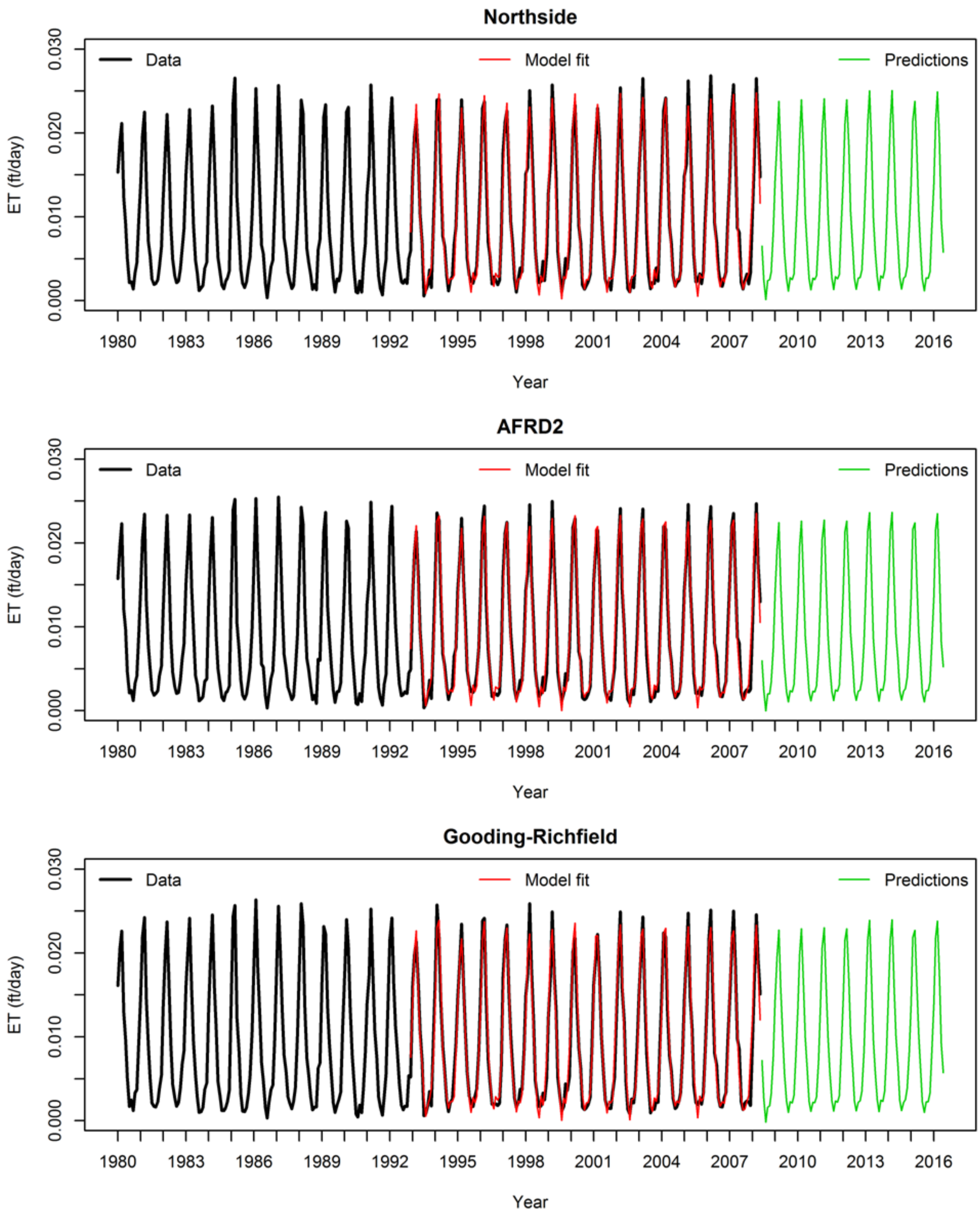

Figure 3-6. ESPAM 2.1 evapotranspiration data, fitted model, and prediction of extended time series

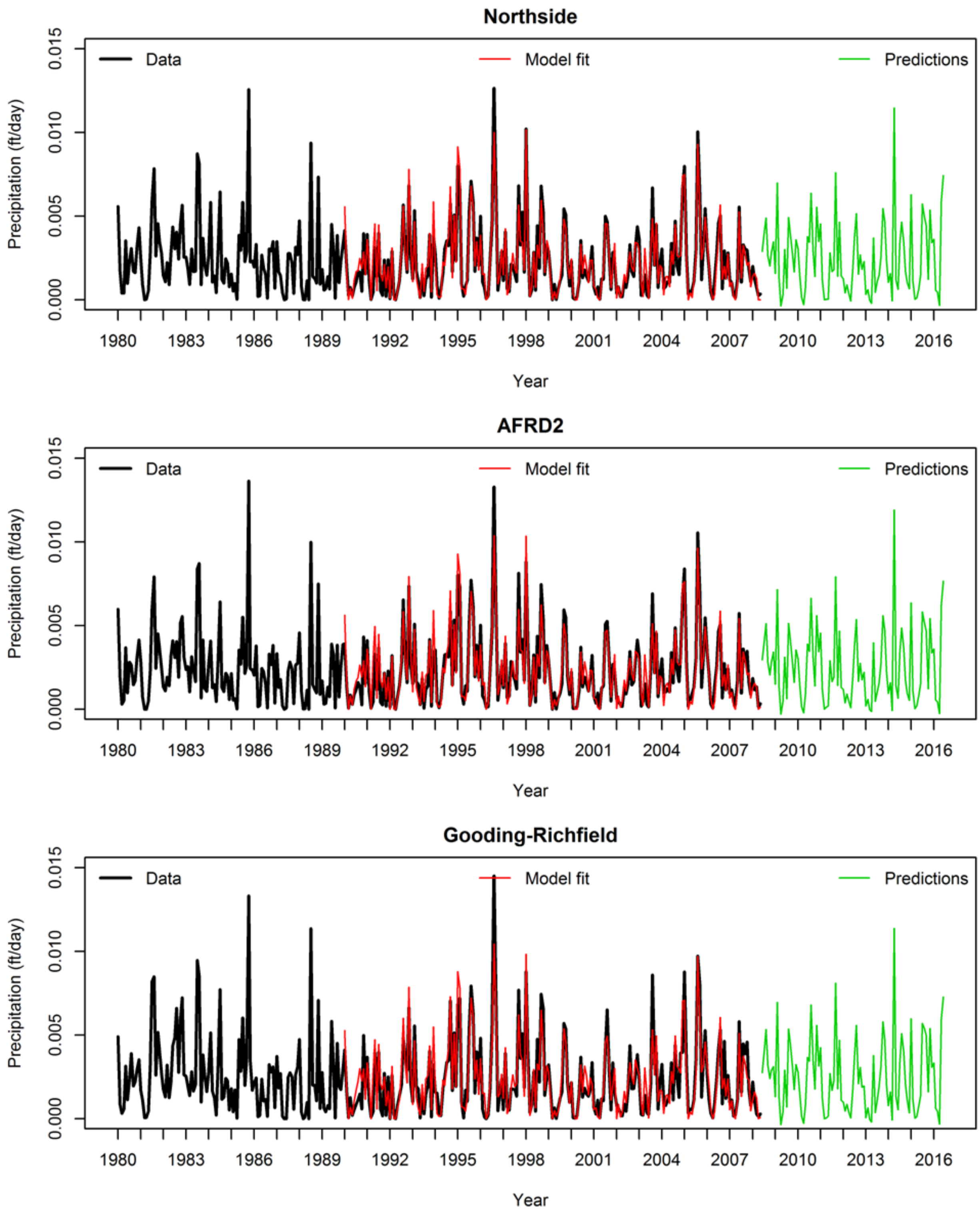

Figure 3-7. ESPAM 2.1 precipitation data, fitted model, and prediction of extended time series

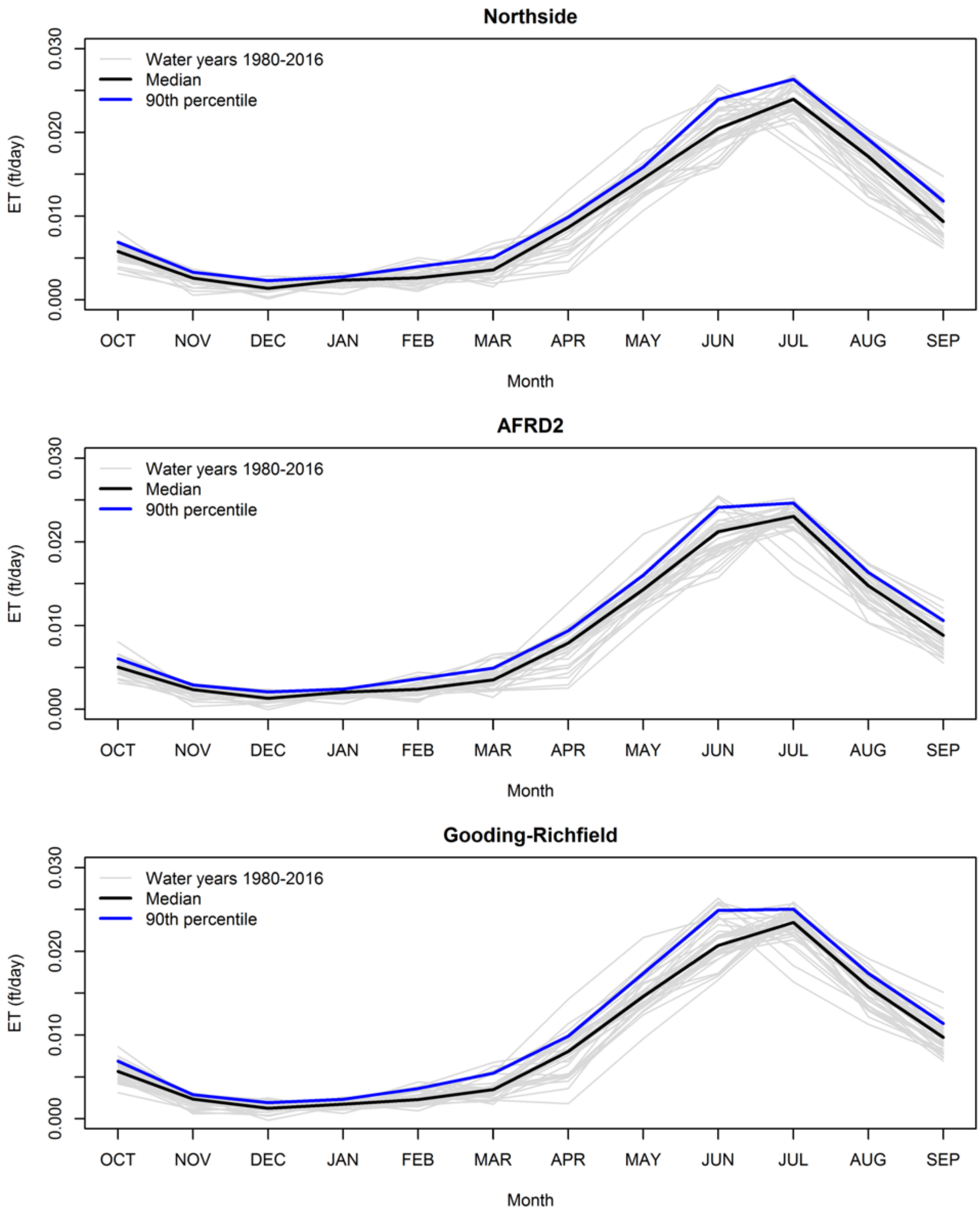

Figure 3-8. Water-year hydrographs of evapotranspiration, showing median and 90th percentile across all irrigation years in sample (year that is drier than 90% of all years)

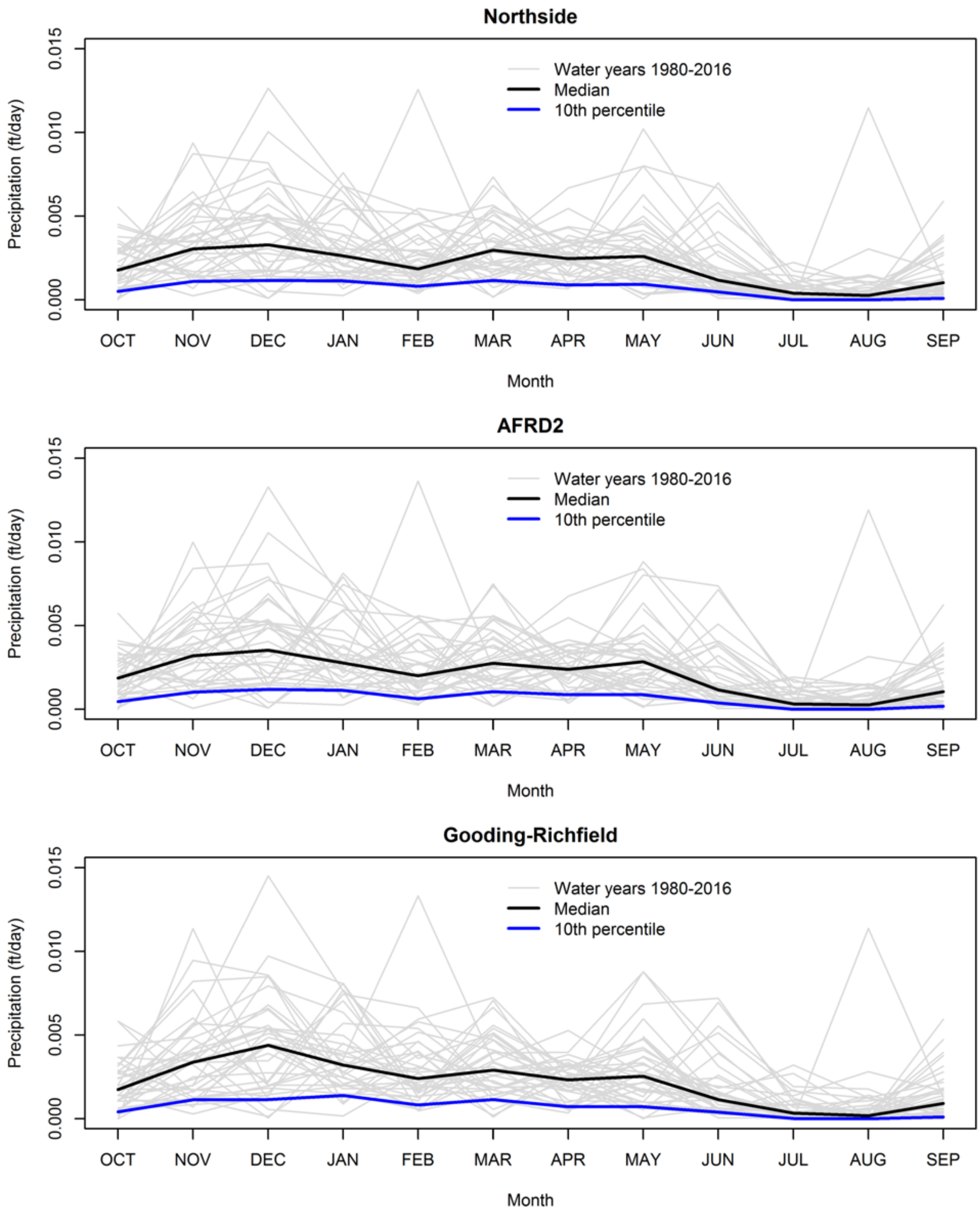

Figure 3-9. Water-year hydrographs of precipitation, showing median and 10th percentile across all irrigation years in sample (year that is drier than 90% of all years)

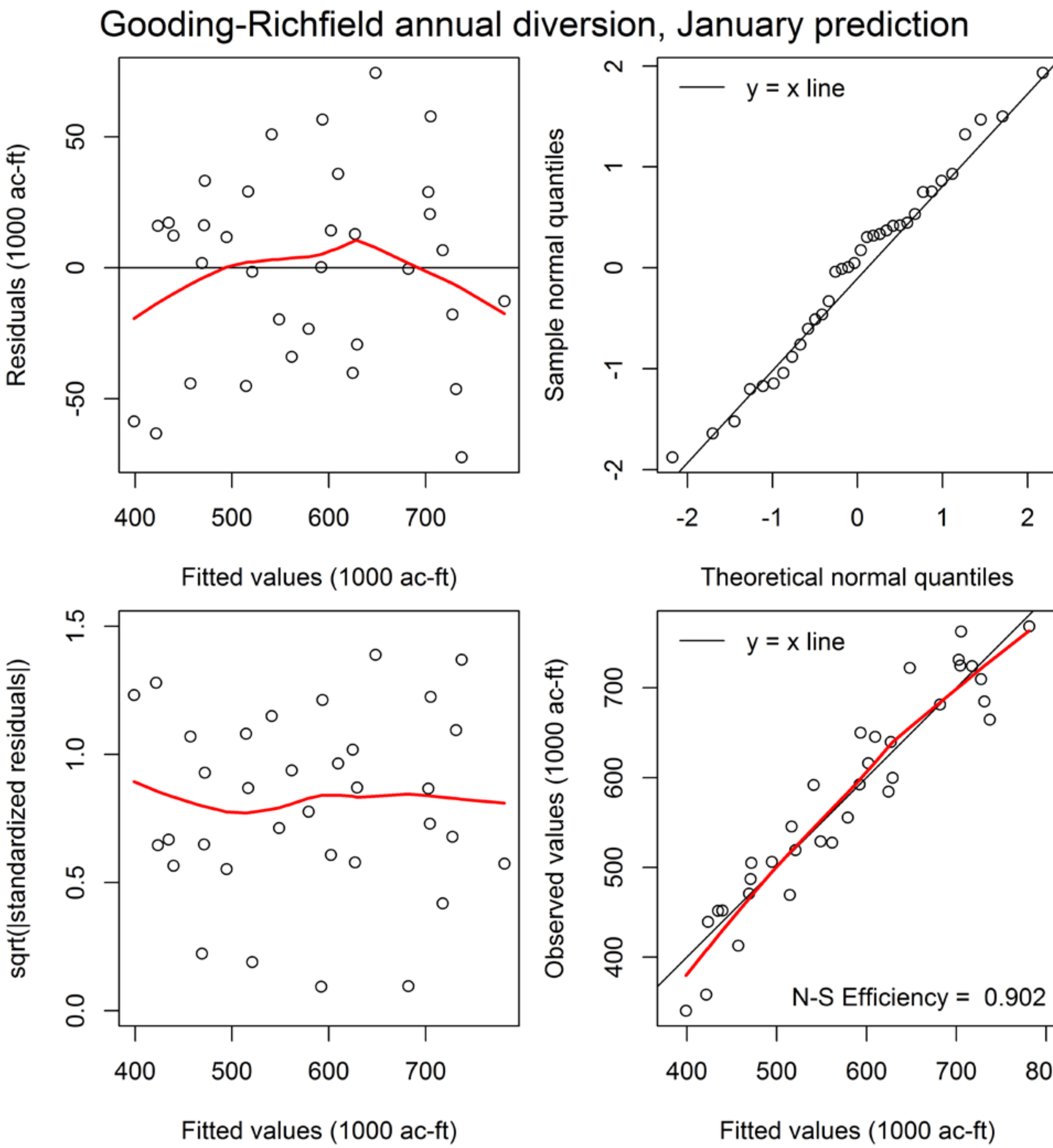

Figure 3-10. Diagnostic plots for January prediction of Gooding-Richfield annual diversion. Red curves are locally weighted scatterplot smoothing (LOWESS) fits (Helsel and Hirsch 1992)

3.3.4. Prediction of Irrigation Diversion

Predictions of monthly irrigation diversions for the upcoming year were made for each of the three surface-water irrigation entities: Northside Canal Company, AFRD2, and Big Wood Canal Company. Two such predictions were made, one based on information available on January 1 and a second based on information available on April 1.

The first step in the prediction of monthly diversion was to estimate total annual diversion volume. Potential predictors considered in the model-selection process were:

1. basin-averaged snow-water-equivalent (SWE),
2. surface water supply index (SWSI), and
3. reservoir storage.

For Northside and AFRD2, basin-averaged SWE was that reported by the Natural Resources Conservation Service as “Snake Basin above American Falls.” The other two predictors for these entities were Snake River at Heise SWSI and upper Snake Reservoir system storage (sum of contents in Jackson Lake, Palisades Reservoir, Henrys Lake, Grassy Lake, Island Park Reservoir, Ririe Reservoir, and American Falls Reservoir). The Milner pool and Lake Walcott were not included in total system storage since they function primarily as equalization and delivery reservoirs at the bottom of the system. For Big Wood Company, Big Wood basin SWE, Big Wood SWSI, and Magic Reservoir contents were used as predictors. All regression analyses used data from calendar years 1981-2014 (n = 34). The optimal models were used to predict total diversion values for 2015 and 2016, which were not yet available when we initially developed the response-function tool but were needed for final model calibration and for the 2017 prediction.

The strongest predictor of annual diversion across the three irrigation entities was SWSI, and all models included first-order (one-year) autocorrelation (Tables 3-5 and 3-6). Reservoir storage was a significant predictor only for the Northside irrigation entity. Nash-Sutcliffe efficiencies ranged from 0.434 for the Northside April prediction to 0.911 for the Big Wood April prediction but did not differ much between January and April predictions within each irrigation entity. The Big Wood models had excellent residual properties and fit, showing no evidence of bias, skewness or heteroscedasticity (e.g., Figure 3-10). The Northside models showed bias toward under-prediction at high values and mild right-skewness in the residuals (e.g., Figure 3-11). However, these deviations will have minimal effect on predictions, since the tool will used primarily to predict exceedance probabilities in the range of 50% to 90%. These correspond to normal quantiles between 0 and -1.28, in which range the residual distribution was close to normal (Figure 3-11). The AFRD2 models were slightly better in fit and residuals properties than the Northside models.

Table 3-5. Summary of regression models to predict upcoming irrigation-season diversion based on 1-January information. All models were fit to annual values for calendar years 1981-2014 (n = 34 years)

Irrigation Entity ID and Name	Predictors in model	Maximum lag of autoregressive terms	Nash-Sutcliffe Efficiency
IESW032 Northside	SWSI, reservoir storage	1	0.483
IESW058 AFRD2	SWSI	1	0.514
IESW059 Big Wood	SWSI	1	0.902

Table 3-6. Summary of regression models to predict upcoming irrigation-season diversion based on 1-April information. All models were fit to April-December diversion for calendar years 1981-2014 (n = 34 years)

Irrigation Entity ID and Name	Predictors in model	Maximum lag of autoregressive terms	Nash-Sutcliffe Efficiency
IESW032 Northside	SWSI, reservoir storage	1	0.434
IESW058 AFRD2	SWSI	1	0.512
IESW059 Big Wood	SWSI	1	0.911

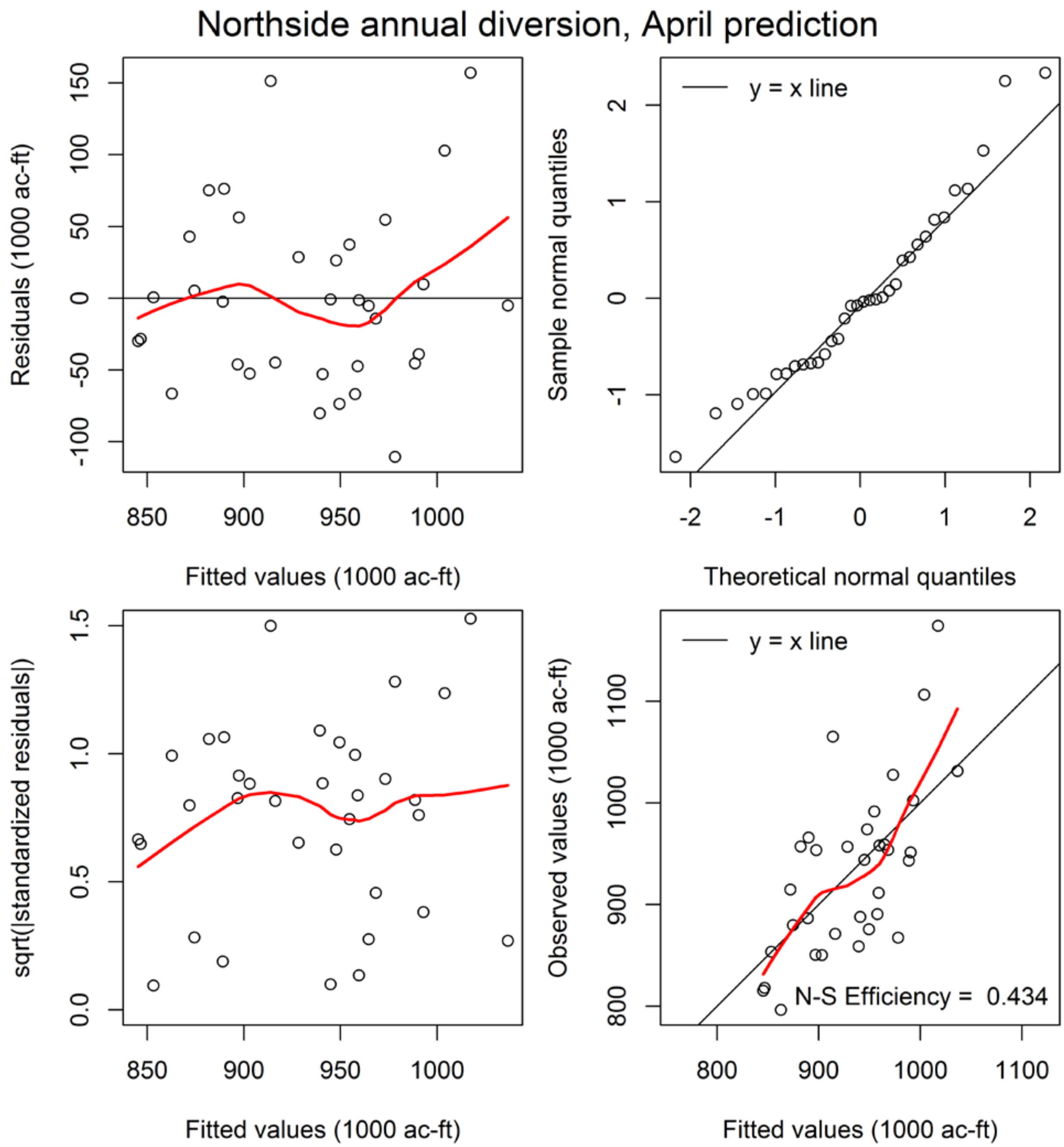

Figure 3-11. Diagnostic plots for April prediction of Northside annual diversion. Red curves are locally weighted scatterplot smoothing (LOWESS) fits.

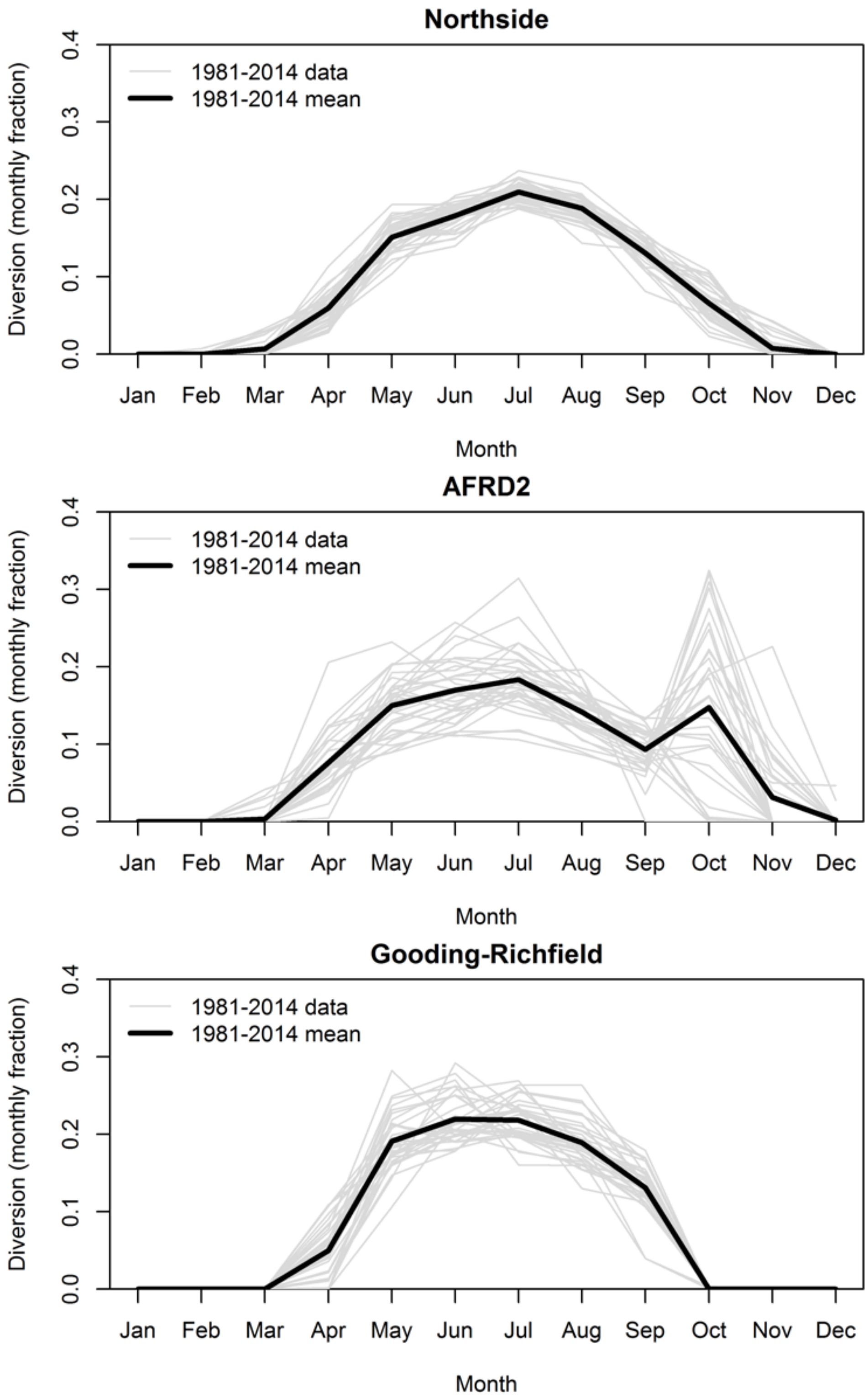

Figure 3-12. Distribution of annual diversion across months. The 1981-2014 mean is the unit hydrograph used in prediction of monthly diversion

3.3.5. Estimation of Monthly Diversion

Once annual diversion was estimated, the annual volume was distributed across months to obtain monthly values. Statistical modeling showed that the only significant predictors of temporal distribution of annual diversion were growing-season evapotranspiration and precipitation, which cannot be predicted with any certainty ahead of the irrigation season. Furthermore, variance-components analysis (Crawley 2007) showed that less than 11.1% of total variance in monthly diversion was due to variability in monthly distribution across years (Table 3-7). Thus, we calculated a unit diversion-hydrograph (monthly values sum to 1) as the mean monthly distribution of annual diversion (Figure 3-12). This unit hydrograph was then multiplied by the appropriate annual total to obtain monthly diversion (e.g., Figure 3-13).

Table 3-7. Variance-components analysis of monthly diversion over calendar years 1981-2014 (*n* = 408 months). Entries in table are percentages of total variance in monthly diversion explained by the given source. Residual variance is due to variability in monthly distribution across years

	Source of variance		
Irrigation Entity ID and Name	**Year**	**Monthly distribution within year**	**Residual**
IESW032 Northside	14.6%	74.3%	11.1%
IESW058 AFRD2	3.2%	85.6%	11.1%
IESW059 Big Wood	26.2%	63.6%	10.2%

3.4. Managed Recharge Component of the ESPA Discharge Forecast

Based on the results of the ESPA comprehensive aquifer management planning process (CAMP), adopted by the Idaho Water Resource Board (IWRB) in January 2009, there is a long-term goal of implementing a net annual ESPA water budget change of 600,000 acre-feet through a variety of management actions. To that end, the state has a goal of recharging 250,000 acre-feet per year to the ESPA through managed aquifer recharge. The State's managed aquifer recharge program is funded by the IWRB and is being implemented on behalf of the Board by the Idaho Department of Water Resources (IDWR). The program currently relies on existing canal systems to carry and deliver water under the Board's recharge water rights. The program varies year to year, based on willing participation by recharge entities, such as canal companies and irrigation districts.

The forecast tool incorporates the State's current managed recharge locations below American Falls, including:

- Southwest Irrigation District
- Milner Good Main Canal
- Milner Gooding – Shoshone
- Milner Gooding – Milepost 31

- Northside Canal Company Main Canal including Wilson Lake
- Twin Falls Canal Company – Murtaugh Canal
- Big Wood Canal Company – Richfield

There are placeholders in the spreadsheet forecast tool to add additional managed recharge locations in the future. There are other managed recharge locations on the ESPA, but they do not contribute significantly to reach gains to the Snake River between Kimberly to King Hill in the upcoming year given their distance from the river reach.

The forecast tool's user interface instructs the user to enter the anticipated monthly recharge volumes for the upcoming year. These values are multiplied by managed recharge location response functions to generate reach gains to the Snake River between Kimberly and King Hill for each managed recharge location.

3.5. Pumping Component of the ESPA Discharge Forecast

Aquifer pumping impacts reach gains to the Snake River between Kimberly and King Hill. Measured ESPA pumping data are not available. Therefore, the forecast tool incorporates an average pumping impact to river reach gains using information developed for the State's model of the ESPA, ESPAM 2.1.
We averaged monthly 2001 through 2010 net consumptive groundwater use (the crop irrigation requirement, or CIR) for four groundwater entities IEGW501, IEGW507, IEGW508, and IEGW509. These entities are close enough to the Kimberly to King Hill reach of the Snake River to impact river reach gains in the upcoming year. The forecast tool multiplies the average monthly pumping stresses by response functions for each of the four groundwater entities to generate the pumping impact to Snake River reach gains between Kimberly and King Hill. Moving forward, if a new ESPA model is approved, the pumping data within the forecast tool will be updated appropriately and as soon as practical.

The forecast tool can be updated to incorporate revised pumping stresses if measured pumping data becomes available in the future.

3.6. Calibration of Predicted Discharge to Observed Discharge

The response-function tool produced monthly estimates of ESPA discharge. We calibrated these outputs to observed ESPA discharge, which we define here to be the proposed ESPAM 2.2 calibration targets provided by IDWR. Because the response functions used in the predictive tool were taken directly from ESPAM 2.1 and the predictive tool incorporated the recharge and discharge components that have the greatest effect on ESPA discharge, raw output from the predictive tool matched output from the full ESPAM 2.1 model very well over the ESPAM 2.1 calibration period of 1981-2008 (Figure 3-14). Over the whole 1981-2015 record (n = 368 months for which both observed and predicted data were available), raw outputs from the predictive tool were unbiased and moderately correlated with observed discharge. Over those 368 months, mean monthly predicted discharge exceeded observed discharge by 11.1 cfs, a positive bias of only 0.76%. Correlation between observed and predicted discharge was 0.51

(Figure 3-15). These observations indicate that the predictive tool successfully approximated the output of the full ESPAM 2.1 model and, on average, produced unbiased monthly estimates of ESPA discharge.

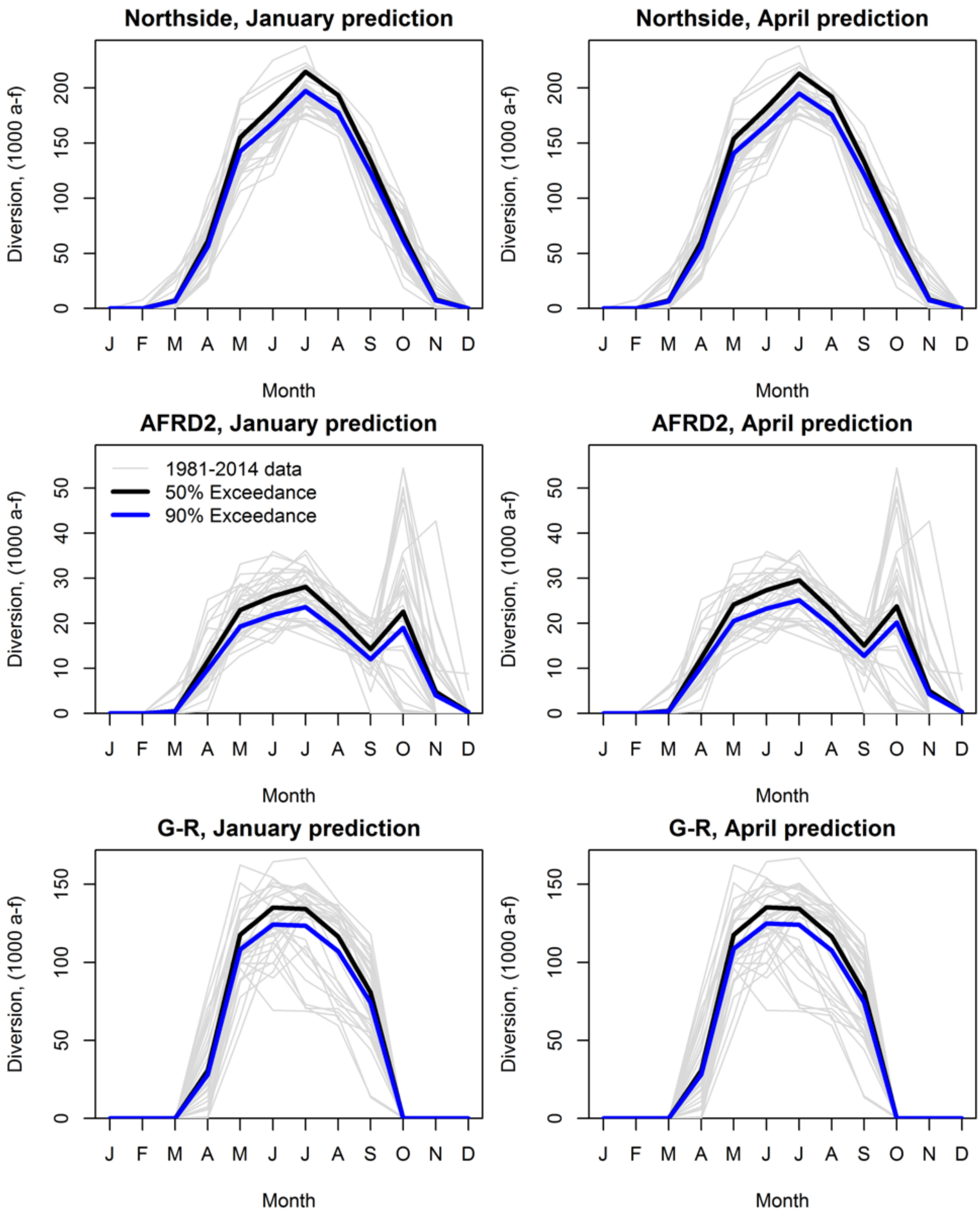

Figure 3-13. Example of predicted annual diversion hydrographs, overlaid on 1981-2014 data. Predictions shown here are 50% exceedance and 90% exceedance diversion hydrographs for 2016. Note: Figures have different y-axis scale and range.

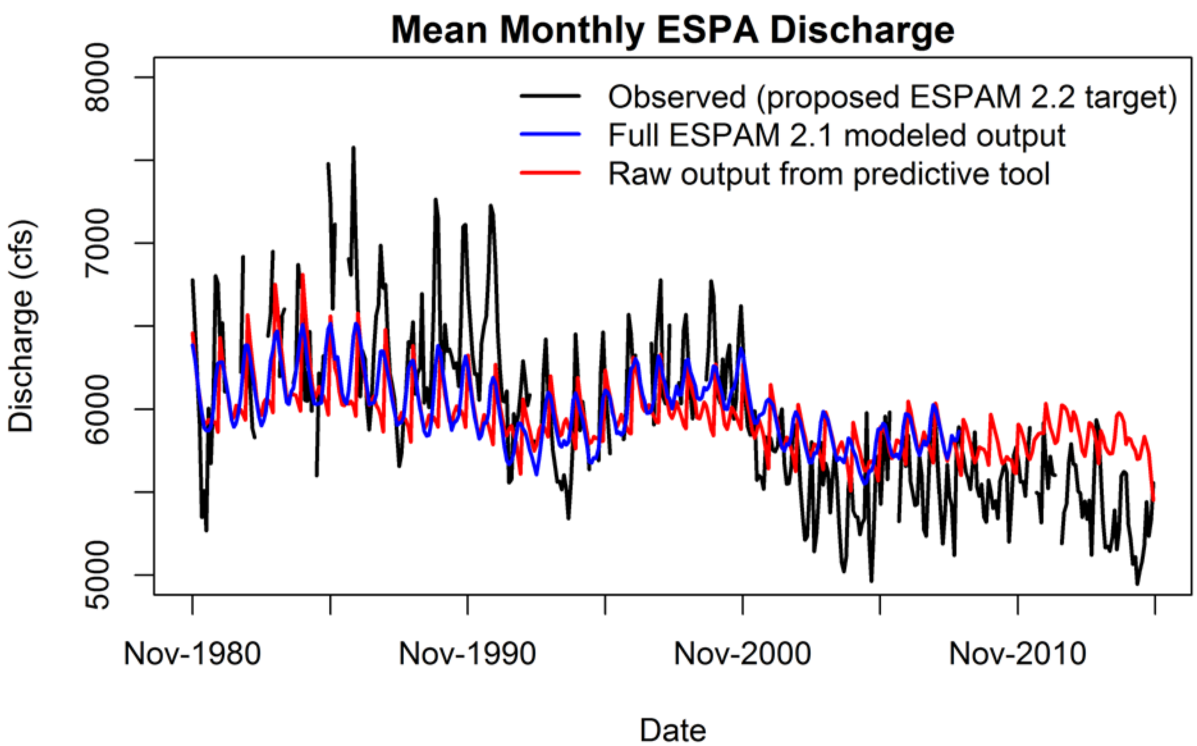

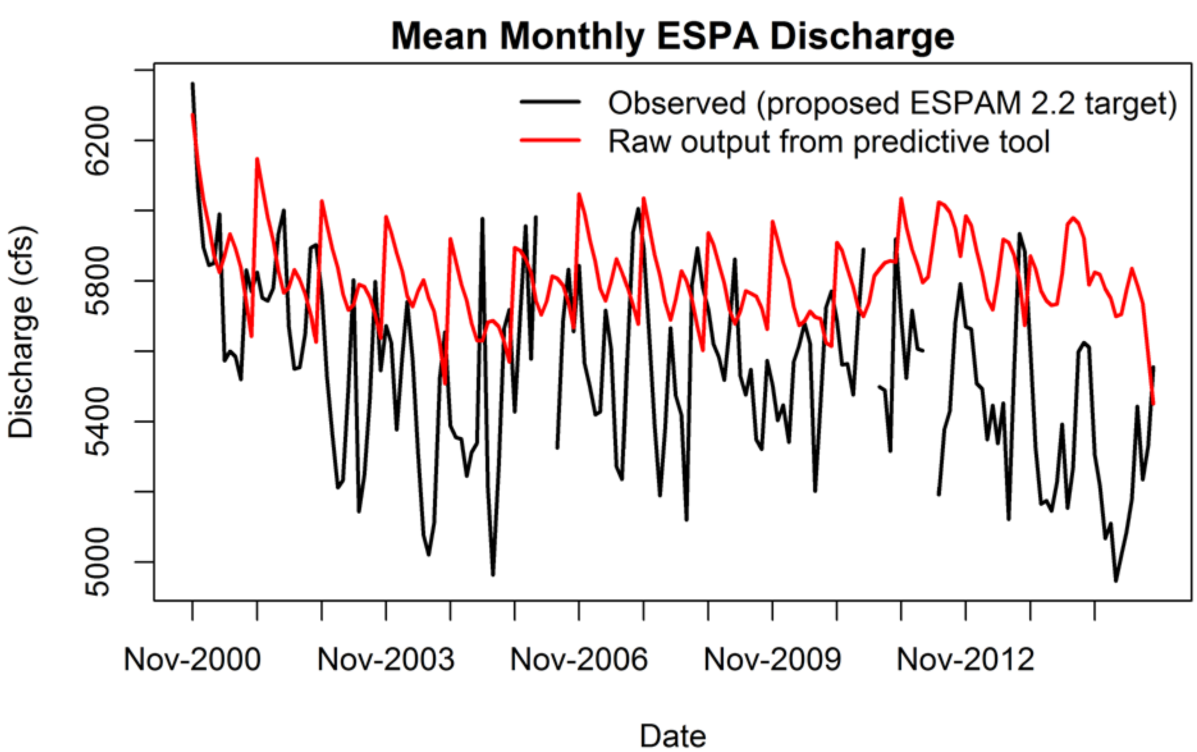

Figure 3-14. Time series of observed mean monthly ESPA discharge, full ESPAM 2.1 modeled discharge, and raw output from predictive tool (top). Bottom panel shows observed discharge and raw predictive-tool output over the predictive-tool calibration period of 2001-2015

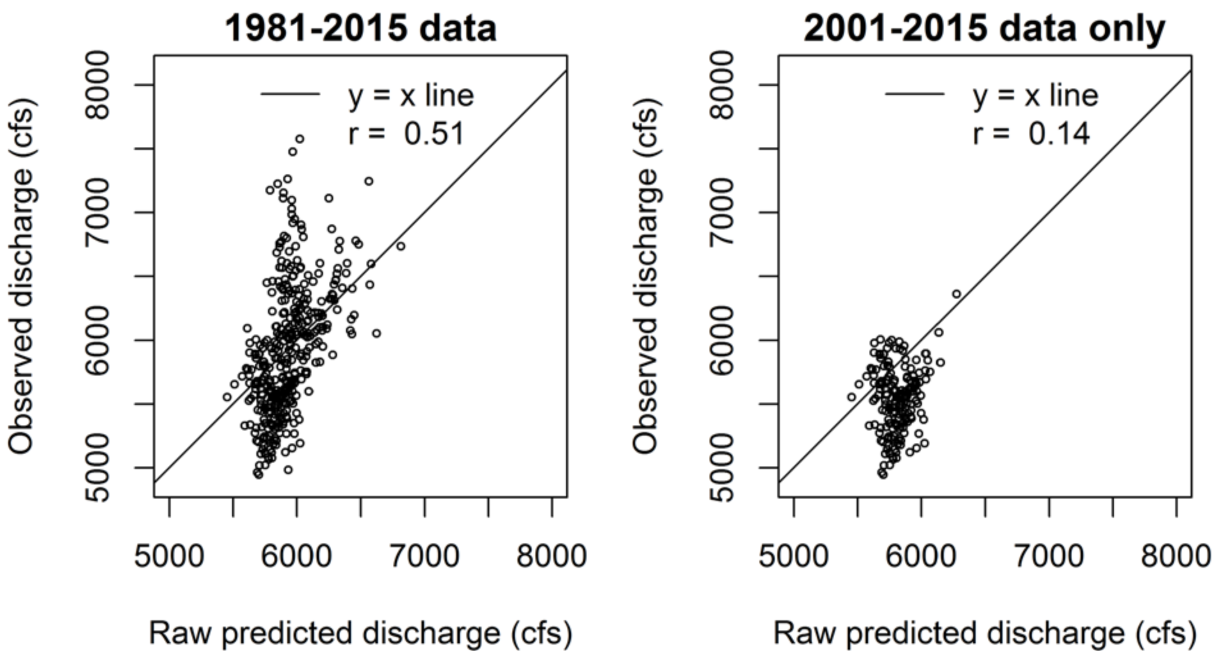

Figure 3-15. Scatterplots of observed versus raw predicted discharge over the full 1981-2015 period of record (left) and the 2001-2015 predictive-tool calibration period (right)

From 2000 through 2008, neither the full ESPAM 2.1 output nor the raw output from the predictive tool matched observed ESPA discharge well (Figure 3-15). The discrepancy between predictive-tool output and observed discharge was even greater over irrigation years 2009-2015 (Figure 3-14). Starting in irrigation year 2000, both ESPAM 2.1 and the predictive tool overestimated total discharge and underestimated the amplitude of annual cycles in discharge. Given long-term declines in ESPA water levels and discharge, as well as increased duration of drought, we chose to calibrate predictive-tool to irrigation years 2001-2015, which best represent most recent hydrologic conditions on the ESPA, despite poor agreement between model output and observed discharge (Figures 3-14 and 3-15). There were n = 173 months during this 15-year period for which observed data were available.

Calibration of predictive-tool output was done with the same general modeling procedures used for extension of the evapotranspiration and precipitation data sets. The response variable was monthly observed ESPA discharge, and the predictor was raw monthly discharge from the predictive tool. Trigonometric polynomials of various frequencies and autoregressive terms of various lags were also proposed. In this case, residual properties from the model with lowest AICc score were excellent, so we selected the model with lowest AICc score as the optimal predictive model. That model included a positive regression coefficient on the raw predicted discharge, trigonometric polynomials of frequencies of 1-3 cycles/year, and autoregressive coefficients of lags 1-3 months. Because annual cycles were an important component of the calibration model but only 15 full irrigation years were used in model development, we used leave-one-out cross-validation to assess model fit and estimate residual variance (Efron, 1982). The same model form as was selected from the AICc analysis was re-fit to a sample of 14 of the 15 irrigation years in the calibration period, and the resulting model used to predict monthly values for the 15th year. This process was repeated for all 15 different 14-year samples. These cross-validation fits were then used to calculate residuals and assess model performance. Model variance was calculated as sum-of-squares of the cross-validation residuals divided by residual degrees of freedom (sample size minus number of model parameters fit, including intercept and autoregressive coefficients).

The cross-validation fits displayed greatly improved agreement with observed data in both mean discharge and amplitude of annual cycles (Figure 3-16). Although Nash-Sutcliffe Efficiency for the cross-validation fits was only 0.259, residual properties were excellent (Figure 3-17). Deviations from optimal residual properties were caused by only two points, which were the largest two monthly discharge values in the calibration set (Figure 3-17). The predictive model slightly overestimated these two extreme values. Residuals had a nearly perfect normal distribution, so normal quantiles provide robust estimates of exceedance probabilities for future out-of-sample monthly discharge predictions. However, the final model used in the predictive tool was the one fit to all 15 years.

To interface with the model of surface-water inputs developed by Idaho Department of Water Resources, daily values of ESPA discharge were needed. Cubic-spline interpolation was used to estimate daily values from the final predicted monthly values. This was implemented directly in the spreadsheet tool using the “SRS1 Splines” Excel add-in (www.srs1software.com/SRS1CubicSplineForExcel).

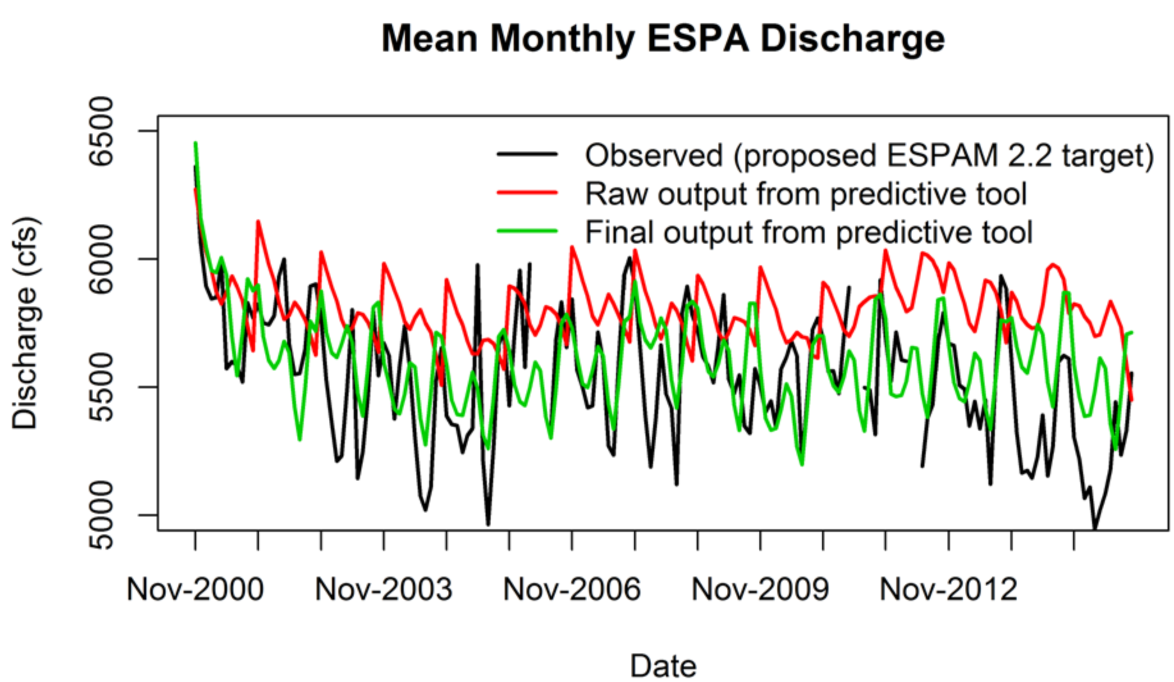

Figure 3-16. Time series of observed ESPA discharge, raw output from predictive tool, and final calibrated output from predictive tool

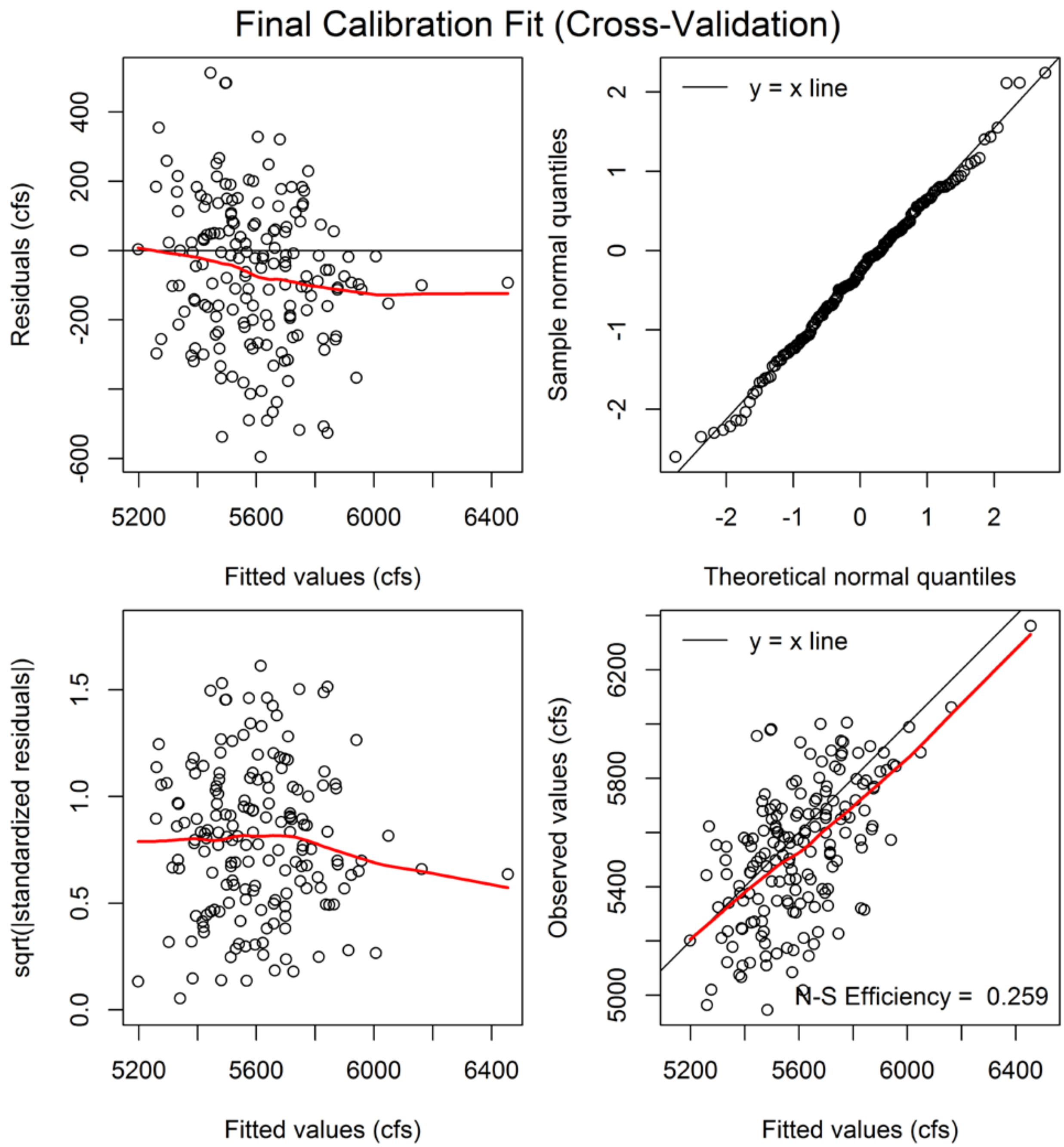

Figure 3-17. Diagnostic plots for the final calibrated model output. Fitted values were generated by fitting the model to every possible subset of 14 calibration years and then using that fitted model to predict values for the remaining year (leave-one-out cross-validation)

4. Estimation of non-ESPA Reach Gains

This section summarizes the procedures used in the SFFT to forecast non-ESPA reach gains ($Q_{non\text{-}ESPA}$). The term $Q_{non\text{-}ESPA}$ has three components per Equation 4-1: tributary discharge (Q_{Tribs}), return flow discharge ($Q_{ReturnFlow}$), and Snake River gains between Milner and Kimberly ($Q_{KimberlyGains}$).

$$Q_{non\text{-}ESPA} = Q_{Tribs} + Q_{ReturnFlow} + Q_{KimberlyGains} \qquad (4\text{-}1)$$

where,

Q_{Tribs} = discharge into the Snake River from four major tributary streams (Rock Creek, Salmon Falls Creek, Malad River, and Bruneau River).

$Q_{ReturnFlow}$ = irrigation return flow from diversions above Milner.

$Q_{KimberlyGains}$ = non-ESPA spring discharge and irrigation returns in the Milner to Kimberly reach of the Snake River (see Figure 4-1).

In the SFFT, forecasted or estimated hydrographs for each component of $Q_{non\text{-}ESPA}$ are constructed. The component hydrographs are statistical hydrographs constructed from percentiles of the historic data record. These component hydrographs are summed to create the $Q_{non\text{-}ESPA}$ forecast hydrograph. The component hydrograph construction and validation are described in this section in the order of Equation 4-1.

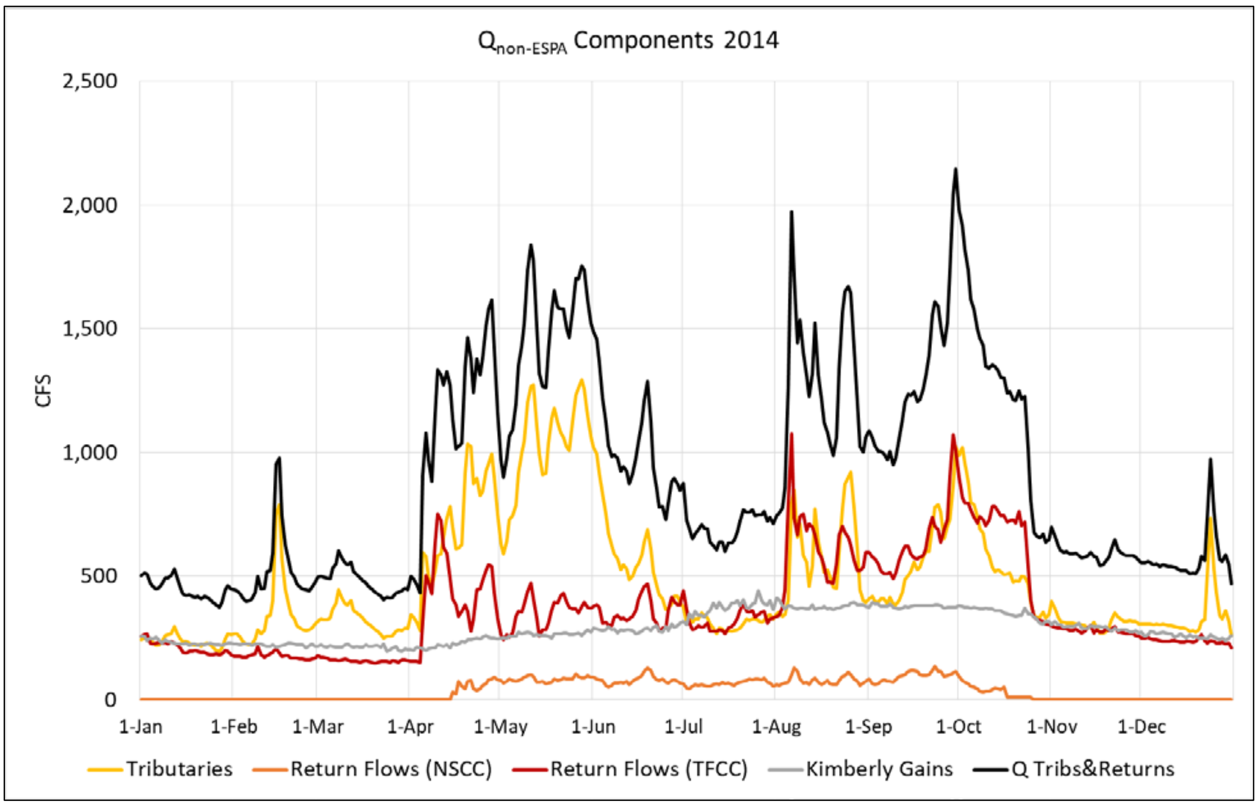

Figure 4-1. $Q_{non\text{-}ESPA}$ components observed data (2014).

4.1. Tributary Inflow Forecast

The tributary component of $Q_{non\text{-}ESPA}$ accounts for water supplied to the Snake River Milner to Murphy reach from its four major tributaries. The USGS Gaging Station number and period of record for each of the tributaries is shown in Table 4-1. The daily flow record for all tributaries is available from the USGS for the period of record of 1993 – 2016. The daily flow value is the sum of the statistical hydrograph from each tributary. Individual tributary hydrographs (period of record median) and the sum of the tributaries hydrograph is shown in Figure 4.2.

Tributary Name	USGS Gaging Station Number	Daily Flow Period of Record
Rock Creek	13092747	09/14/1992 - Current
Salmon Falls Creek	13108150	10/01/1986 - Current
Malad River	13152500	01/11/1987 - Current
Bruneau River	13168500	10/01/1986 - Current

Table 4-1. Major tributaries in the Milner-Murphy reach.

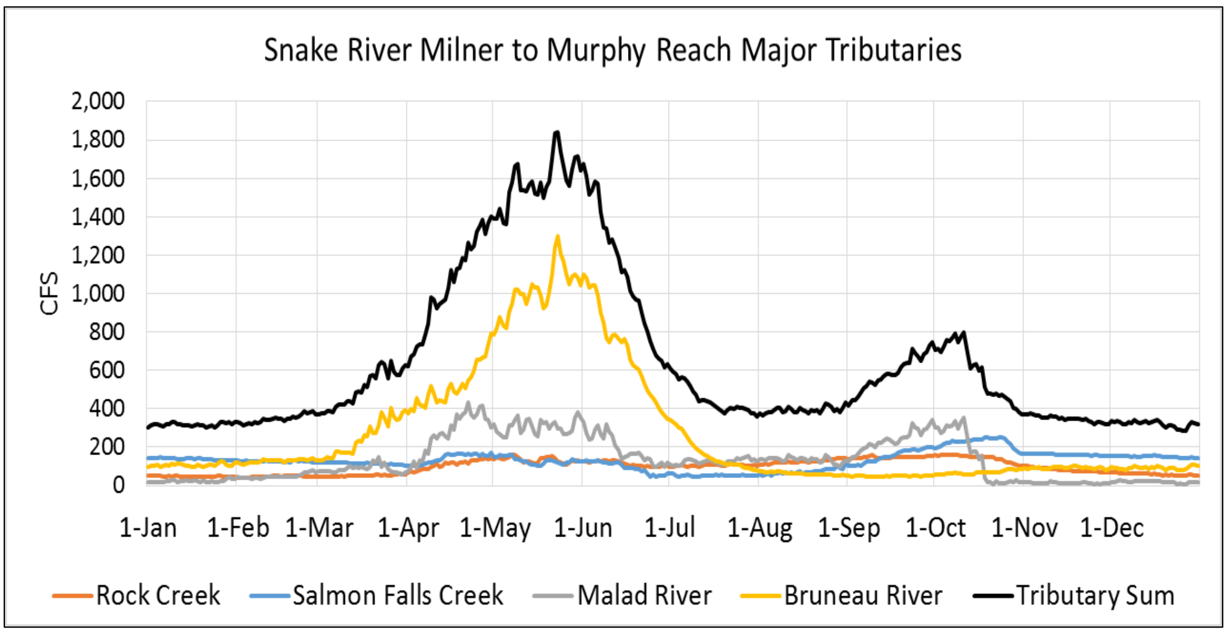

Figure 4-2. Median annual hydrographs for the major tributaries for the period 1993-2016.

The tributary forecast, Q_{Tribs}, is a statistical hydrograph that is the sum of the four tributaries' estimated hydrographs. The estimated hydrographs are calculated independently by calculating a median hydrograph by projected water supply (Bruneau River and Malad River) or the period of record median (Rock Creek and Salmon Falls Creek). The Bruneau River and the Malad River are the primary tributaries by volume and both systems are forecasted with the SWSI (Big Wood SWSI applies to the Malad River). The SWSI projects an April – September water supply volume and ranks the projection against past years. The estimated hydrographs are the median hydrograph of the six most similar years. Similar years are determined by the January or April SWSI value with the projected SWSI value ±3 years used to generate the estimated hydrograph. The SWSI ranges from -4.1 (excessively dry) to 4.1 (excessively wet) and is updated monthly. Salmon Falls Creek and Rock Creek estimated hydrographs are the period of record median. Both systems are heavily managed for irrigation return and are therefore predictable with low interannual variability. The median hydrograph maximum overestimation of flow is 133 cfs and 153 cfs for Salmon Falls Creek and Rock Creek, respectively. Flow underestimation is considerably larger however this error is of less concern for Swan Falls management.

Table 4-2. Big Wood SWSI and Percentiles

Tributary forecast fit to past years are shown in Figure 4.3. The plots compare observed versus forecasted hydrographs in three different years (1998, 2009, and 2013). The forecast hydrographs generalize the shape of the observed data and best fits the critical low flow period. The statistical method generally approximates the timing and magnitude of the runoff rising limb, peak, and receding but is not able to predict event-related anomalies such as early season spikes and multiple peaks.

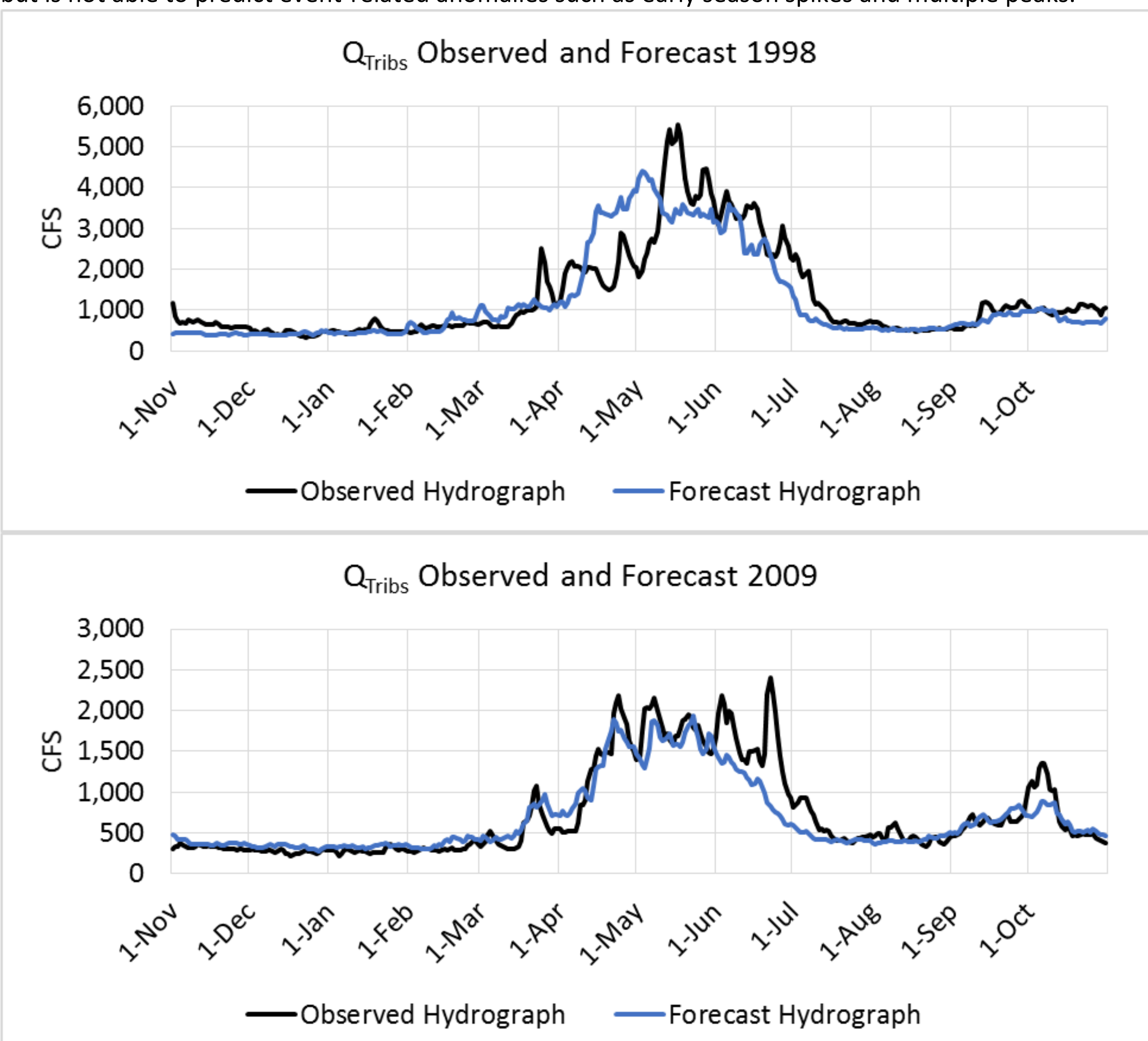

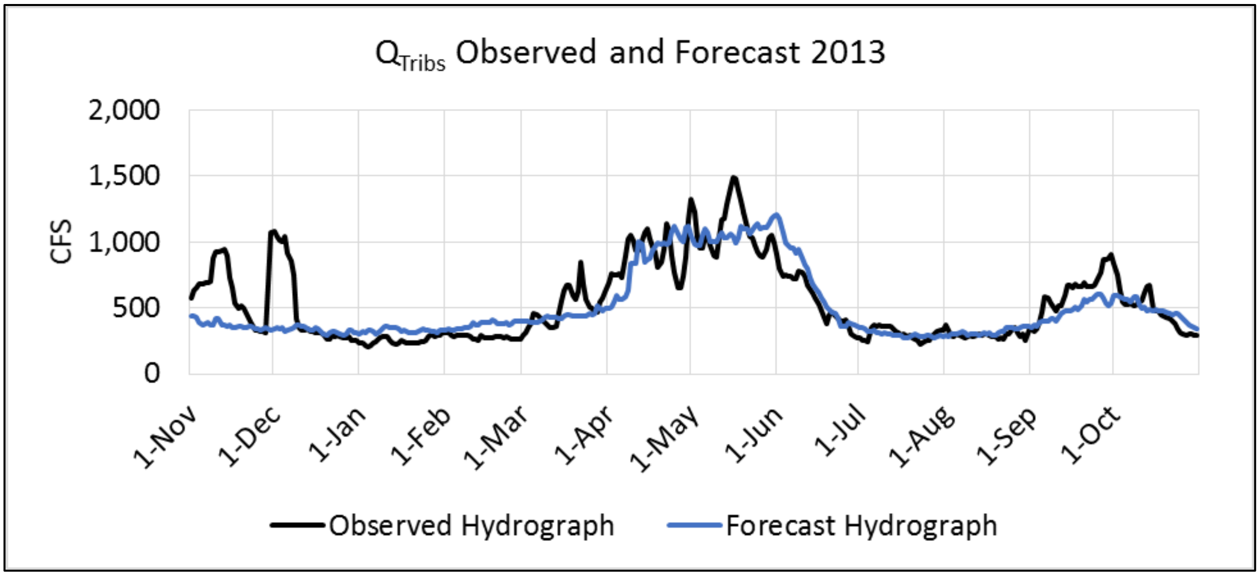

Figure 4-3. Observed and forecasted hydrographs for years 1998 (wet), 2009 (neutral), and 2013 (dry). Note: Figures have different y-axis scale and range.

4.2. Return Flow Estimation Procedure

Irrigation return flow originates from two canal companies: Northside Canal Company (NSCC) and Twin Falls Canal Company (TFCC). Both companies divert from the Milner pool, which is upstream of the forecast reach. However, some of the diverted water enters the forecast reach as return flow from irrigation drains and ditches. These return flows are a gain to the system and therefore must be explicitly tracked in the SFFT. Return flow is a single term in Equation 4-1 ($Q_{non\text{-}ESPA}$) that includes return flows from NSCC and TFCC that are forecasted independently. Losses from diversions below Milner are accounted for in the Q_{DivET} component of the reach gain equation.

The return flow networks are monitored and maintained by IDWR (TFCC and NSCC) and NSCC (NSCC only). The NSCC network has no flow in the non-irrigation season while the TFCC network has perennial flow. Return flow monitoring began in March 2002, however, not all sites within the current networks were monitored until April 2013 (NSCC) and June 2007 (TFCC). Daily average flow values at each monitoring station are available during the period of record. The total daily gain from each network is calculated as the sum of the network's monitoring sites. Statistics are performed on the composite datasets. Return flow data processing and forecast procedures are discussed below.

4.2.1. Return Flow Discharge Data Processing

Return flow data required processing to remove flow data that is accounted for by other forecast components and to complete the dataset due to incomplete monitoring networks. A number of return flow monitoring sites measure water that is discharged to a tributary or to the Snake River above Kimberly. This flow data was removed to avoid double accounting of the water. Secondly, prior to when all current monitoring sites were active ("complete network" in Figures 4-4, 4-5), an incomplete accounting of return flow gain is available ("incomplete network" in Figure 4-4, 4-5). A statistical procedure was developed to approximate missed flow in the incomplete network data record.

The TFCC has 13 total sites in their return flow discharge monitoring network. Nine of these sites are included in the TFCC return flow estimation within the SFFT. The reason that four of the sites were excluded from the return flow estimation is to avoid double-counting the water. Two of these sites discharge into Salmon Falls Creek above the Salmon Falls Creek discharge monitoring station near Hagerman, and the other two stations discharge into the Milner to Kimberly reach. Four of the nine return flow discharge records included in $Q_{ReturnFlow}$ from the TFCC were added to the network in 2007. These discharge sites had their records extended from back to 2002 by statistical methods.

The NSCC has 14 return flow discharge monitoring sites. Since three of these sites discharge into the Snake River within the Milner to Kimberly reach of the Snake River, they were excluded from the $Q_{ReturnFlow}$ estimation in the SFFT. Three of the eleven remaining sites had incomplete discharge records, since two site were added into the network in 2008 and one site in 2013. These three discharge monitoring sites had their records extended statistically to 2002.

Total daily return flow discharge in each network was estimated for the time period when not all monitoring sites were reporting. Total return flow was estimated during this time by applying a scale factor to observed data. The scale factor is > 1 and up-scales the daily flow from the incomplete network dataset to approximate total flow and account for missed flow. To calculate the scale factor the dataset is sub-setted to include only the period where all monitoring sites are active (TFCC: 6/8/2007 – 10/31/2016, NSCC: 5/23/2008 – 10/25/2015[1]). The scale factor is calculated using this subset as the ratio of the flow from all sites divided by flow from sites with a complete period of record. A scale factor was calculated for each day in the subset.

Daily scale factors were grouped by day of year and the median value calculated. The daily median scale factor specific to a day of year is applied to the incomplete network. The scale factor is multiplied by the sum of observed flow at the daily time step to estimate total return flow discharge.

Figures 4-4 and 4-5 compares the output of the scaled data to the measured return flow discharge for the NSCC and the TFCC from 2002 to the present. The measured discharge prior to April 2008 (NSCC) and June 2007 (TFCC) is the sum of flow from incomplete networks. Measured flow after this date is the sum of all measured flow in the network from sites included in the return flow statistical analysis. Scaled data is used prior to the completion of the networks and the forward cast is shown for validation.

[1] NSCC is assumed complete in 2008 to increase the sample size.

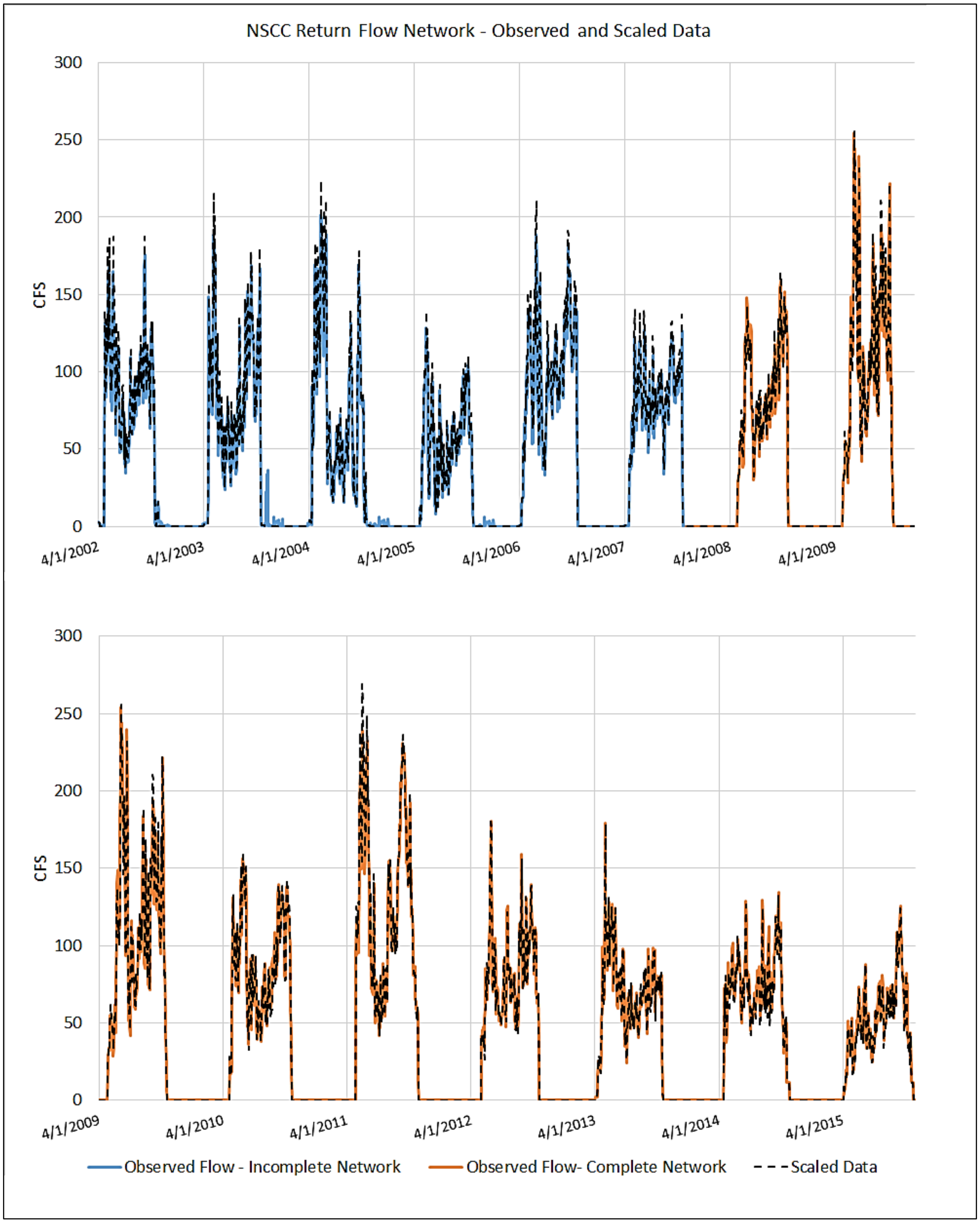

Figure 4-4. Measured and estimated discharge from the North Side Canal Company (NSCC) return flow network (2002-2016).

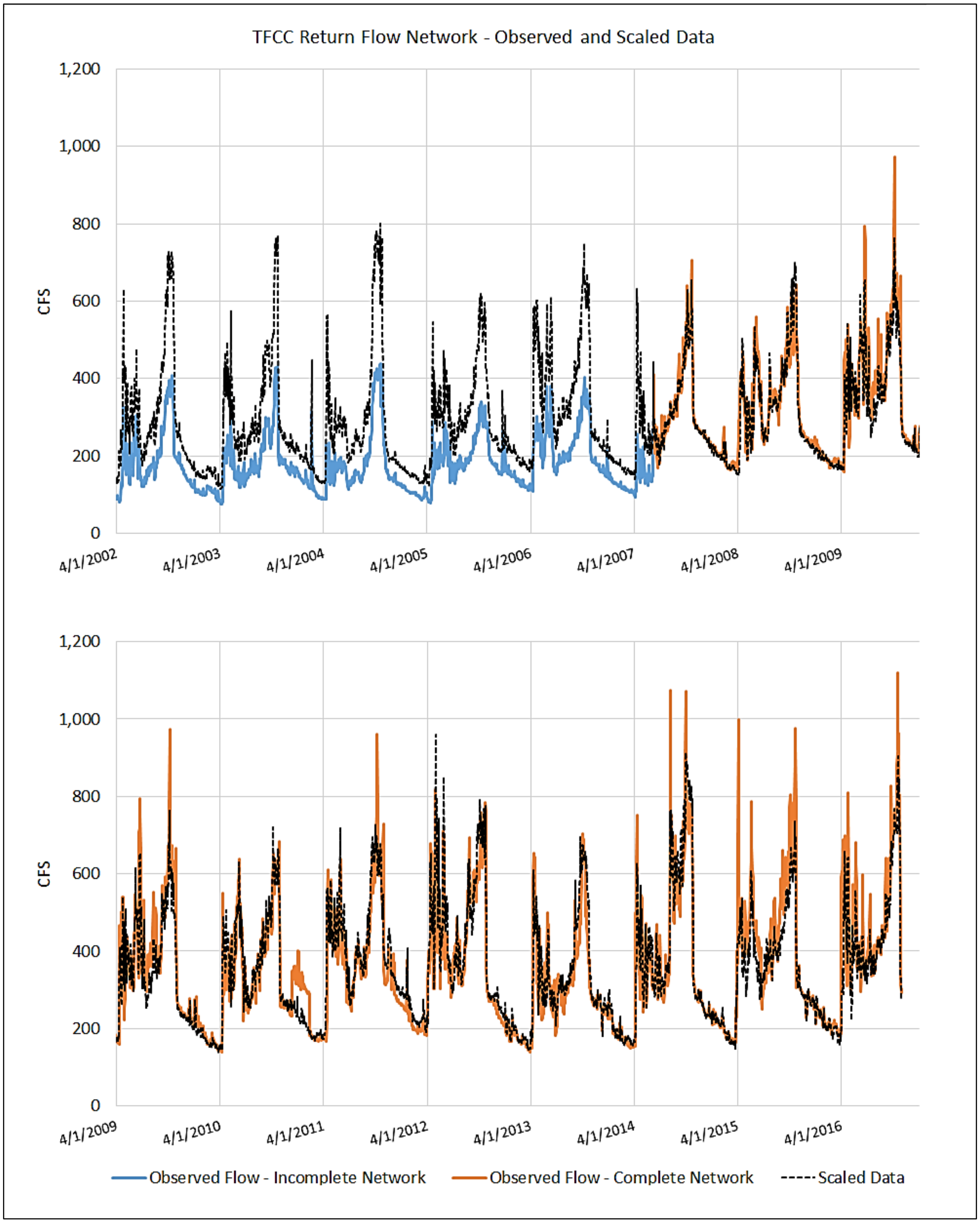

Figure 4-5 Measured and estimated discharge from the Twin Falls Canal Company (TFCC) return flow network (2002-2016).

4.2.2. SFFT Return Flow Estimation

The estimated return flow hydrographs are the median of the historic dataset and each canal company is treated independently (Figures 4.6 and 4.7). The median is the estimated hydrograph no water supply predictor variable was found to be correlated with return flows.

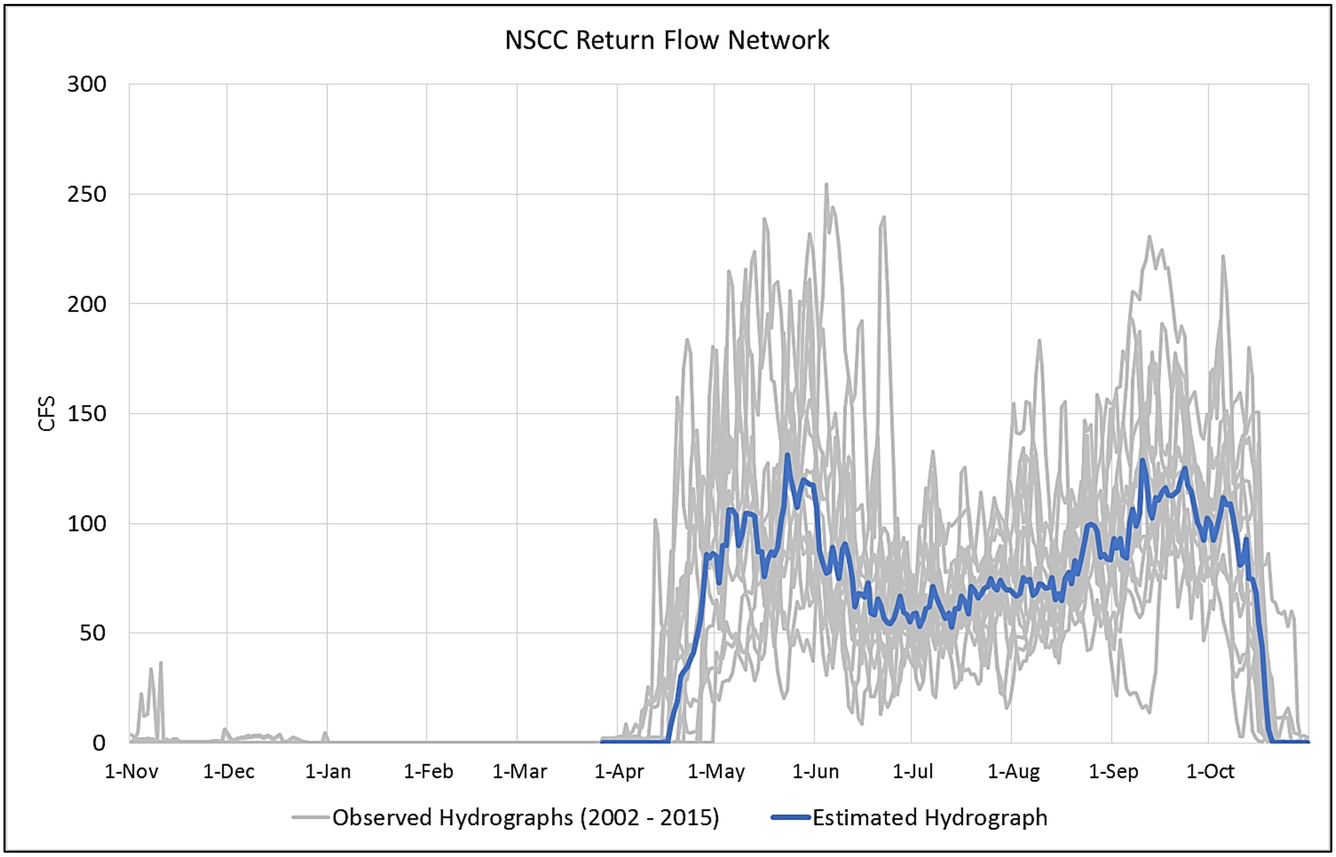

Figure 4-6. NSCC return flow network annual hydrographs and daily median value shown in blue, which is the estimated value used in the SFFT.

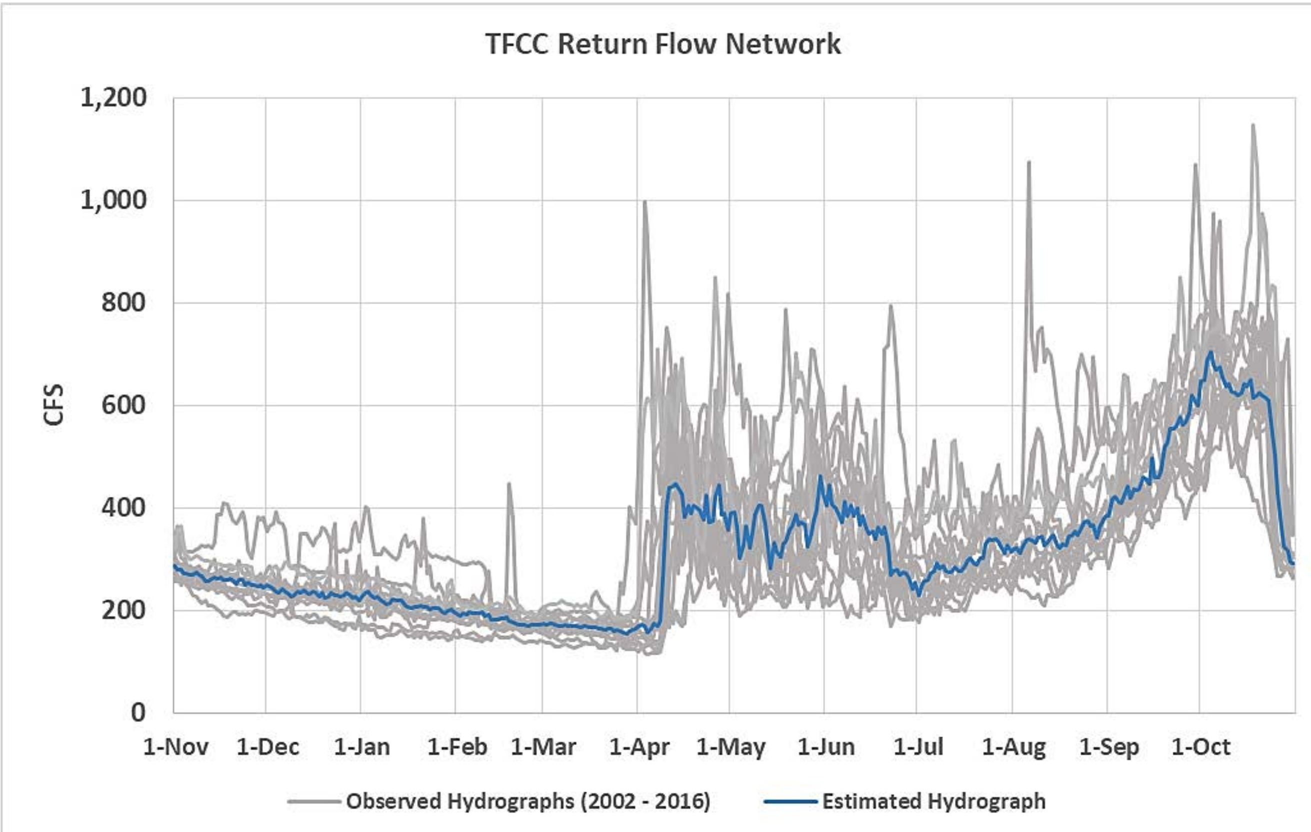

Figure 4-7. TFCC return flow network annual hydrographs and daily median value.

4.3. Kimberly Gains Estimation Procedure

The Kimberly gains are a component in the $Q_{non\text{-}ESPA}$ equation and is non-ESPA spring discharge and minor irrigation return flows that enter the system between Milner Dam and the Snake River at Kimberly gaging station. Daily gains are calculated by subtracting the Snake River at Kimberly gage from the Snake River at Milner gage for WY 1993 – 2016. This period of record is consistent with the tributary forecast. The Kimberly gains estimation is the median statistical hydrograph of the daily gage calculation.

The Kimberly gains are calculated as the gage difference between Snake River at Kimberly and Snake River at Milner. Milner data is lagged by one day to account for travel time[2]. Daily gains are then filtered to include only days when the gain is greater than 10% of Kimberly flow. The 10% of Kimberly flow filter criteria is based on the "good" rating of the gage by Idaho Power[3] and is used to identify gains that are greater than gage uncertainty. A "good" rating indicates that 95% of the daily discharge values are within 10% of the true value[4]. After filtering for gage uncertainty, outlying values were identified and removed. Outliers are identified as a daily gain value outside of 2 standard deviations of the mean and

2 Travel time from Milner to Kimberly is approximately 20 hours at flow of 5,000 cfs. *Streamflow Monitoring and Measurement Plan*, Table 5, page 90

3 http://www.idahopower.com/pdfs/ourEnvironment/waterResourcesdata/WaterResourcesData2011.pdf (pg. 37)

4 https://wdr.water.usgs.gov/current/documentation.html#stage

are artifacts of gage differencing. Once the gage uncertainty and outlier filters were applied, the daily record for statistical analysis had between 12-24 data points (years). The daily median value was calculated and smoothed with a 5 day centered average (Figure 4-8).

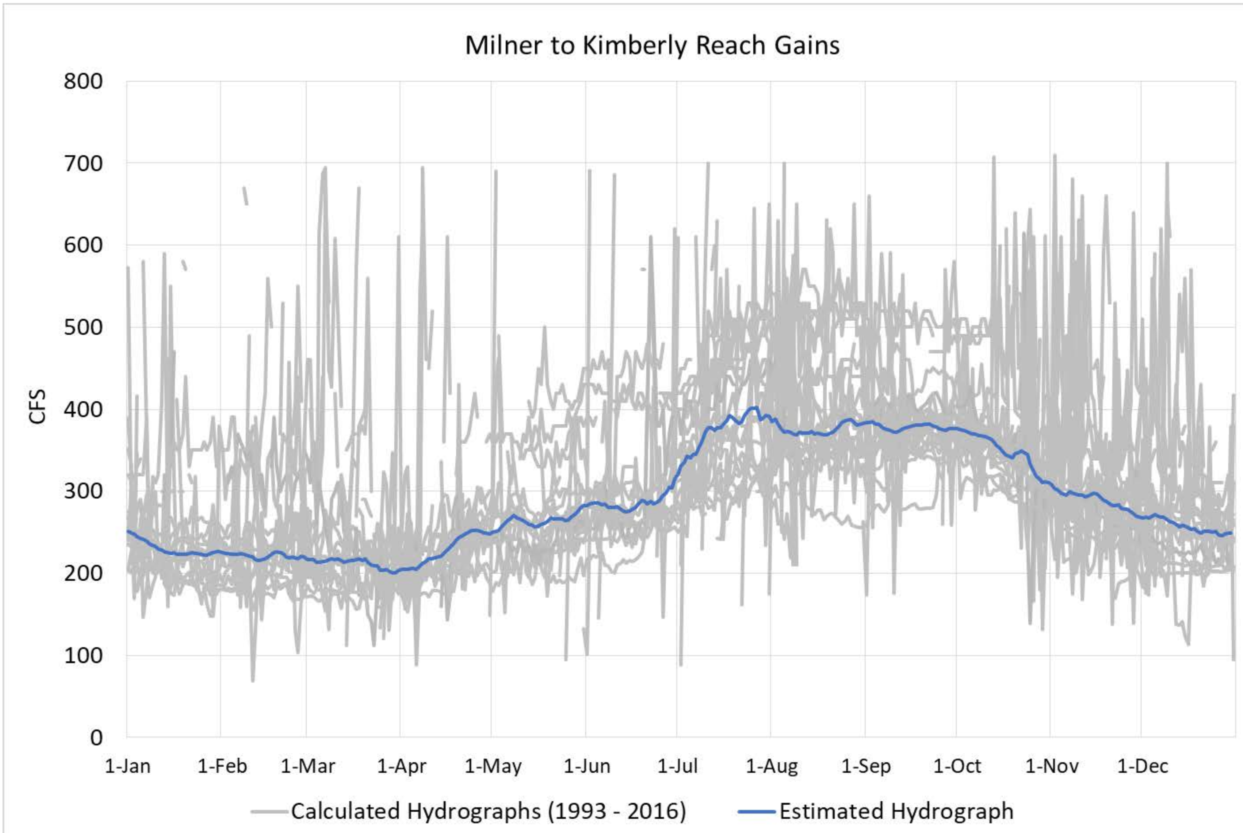

Figure 4-8. Kimberly gain estimation in the SFFT

4.4. $Q_{non\text{-}ESPA}$ Summary

The $Q_{non\text{-}ESPA}$ forecast is shown in Figure 4-9 for the 2009 forecast. The forecast is the sum of the estimates for tributary inflows, return flows, and Kimberly gains. The daily flow value is added to the ESPA discharge forecast to account for total water supply in the system. The Q_{Tribs} hydrograph is the sum of the four major tributaries in the Milner to Murphy reach constructed as the median of the dataset. The tributary hydrograph will change for each forecast correspondent to the surface water supply index. The irrigation return flow hydrographs are constant in the SFFT and the period of record will be extended in time. The Kimberly gain hydrograph is constant.

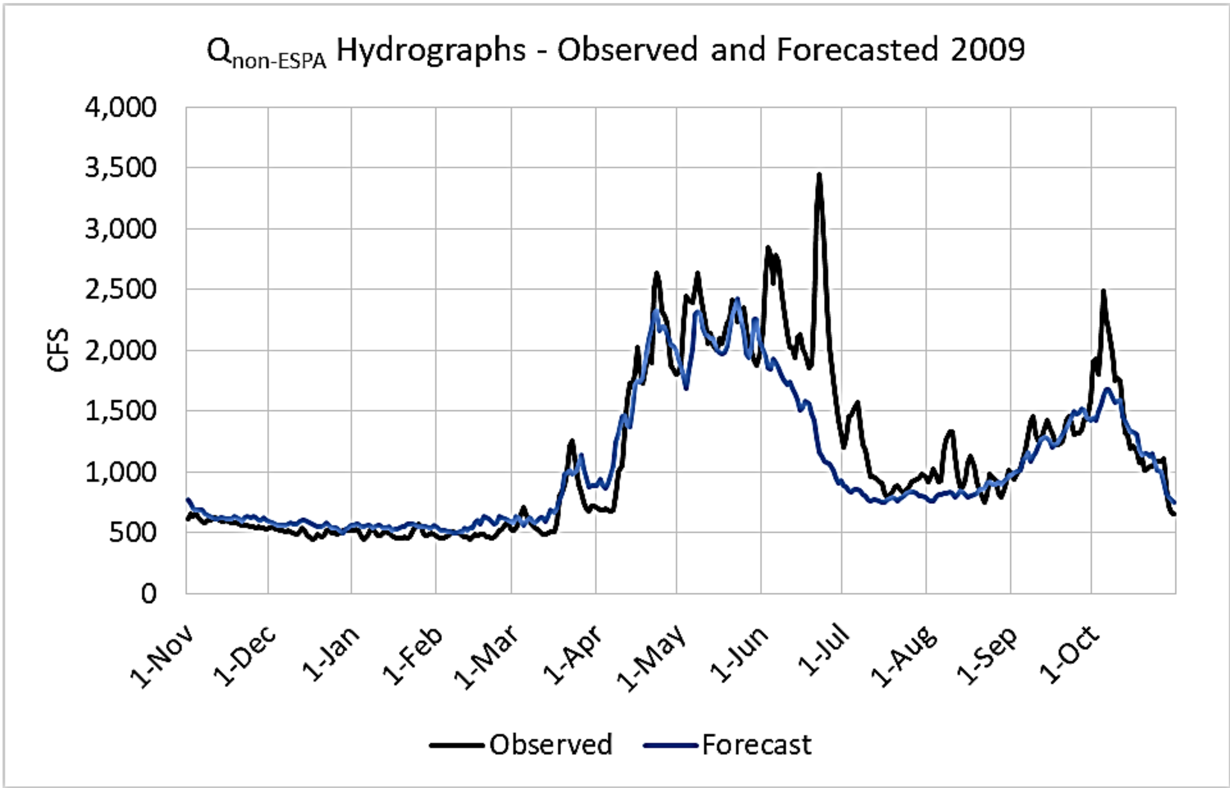

Figure 4-9. $Q_{non\text{-}ESPA}$ Observed and Forecast Hydrographs 2009.

4.5. $Q_{non\text{-}ESPA}$ Performance

A volumetric analysis and a residual analysis were used to quantify method performance. Performance is quantified by hindcasting of years 2002 – 2017 and comparing the estimated flow to the observed flow. Hindcast hydrographs were estimated using the period of record median and the January Big Wood River and Bruneau River SWSI values. The hindcasted year was removed from the Bruneau River and Malad River datasets. The Kimberly gain is omitted from the hindcast because the lack of a continuous dataset of observed values.

The volumetric analysis compares irrigation season (April 1 – October 31) observed and estimated volumes (Figure 4-10). Hindcasted volumes are not biased greater or less than observed volumes in the 16 years analyzed with 8 hindcasts less than observed volume and 8 hindcasts greater than observed volume. The forecast is within 5% of the observed volume in 4 years. The greatest volume difference occurs in two very wet years, 2011 and 2017. Interesting, hindcast overestimation generally occurs in the early part of the dataset (years 2002 – 2008) and underestimation occurs in the latter years. These years correspond to return flows that are less than the median value that is used to estimate this component and may result from a change in irrigation management. Hindcast overestimation can also result from the Big Wood SWSI value for years with high reservoir carryover. High reservoir contents can increase the SWSI value not correspondent to runoff volume. For instance, the 2007 January Big Wood SWSI value was -1 and is a combination of above average reservoir contents and below average streamflow forecast of 60K AF. A Big Wood SWSI value with a streamflow forecast in this range and average or below reservoir contents is typically ≤ -1.9.

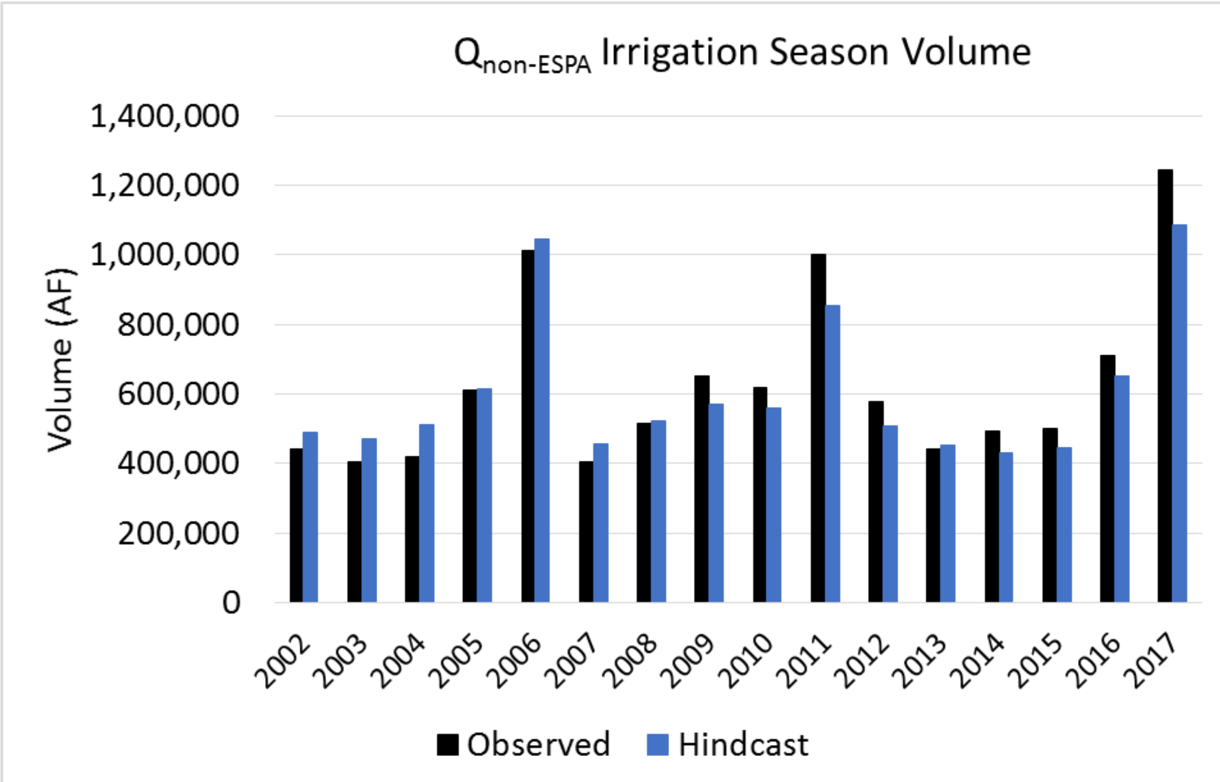

Figure 4-10. Irrigation season observed and forecast volume of combined tributary and return flow discharge to the Snake River between Kimberly and Murphy.

The residual analysis is the interquartile range of the difference between the daily flow value of the observed hydrograph and the hindcasted hydrograph for all years 2002 – 2017 (Figure 4-11). The interquartile range is the middle 50% of data and is bounded by the 25^{th} and 75^{th} percentiles. Negative values result when the estimated hydrograph underestimates observed values. Likewise, positive values result with overestimation of observed data. The width of the band corresponds to uncertainty and a deviation of the band from 0 results from a consistent forecast bias.

The greatest $Q_{non\text{-}ESPA}$ uncertainty occurs during the runoff period of mid-March to the end of June. This is an expected result because the inter-annual variability of runoff timing and magnitude is difficult to predict with deterministic statistics many months in advance. The residual interquartile range during this time is large relative to other times in the year but no strong bias is evident. $Q_{non\text{-}ESPA}$ estimation performance increases when the system enters its “baseflow” condition of July – mid March. This result is important because the greatest potential for a minimum streamflow shortfall occurs at the critical low flow period in the Snake River Milner to Murphy reach during the peak of summer. SFFT model fit during this time is the priority.

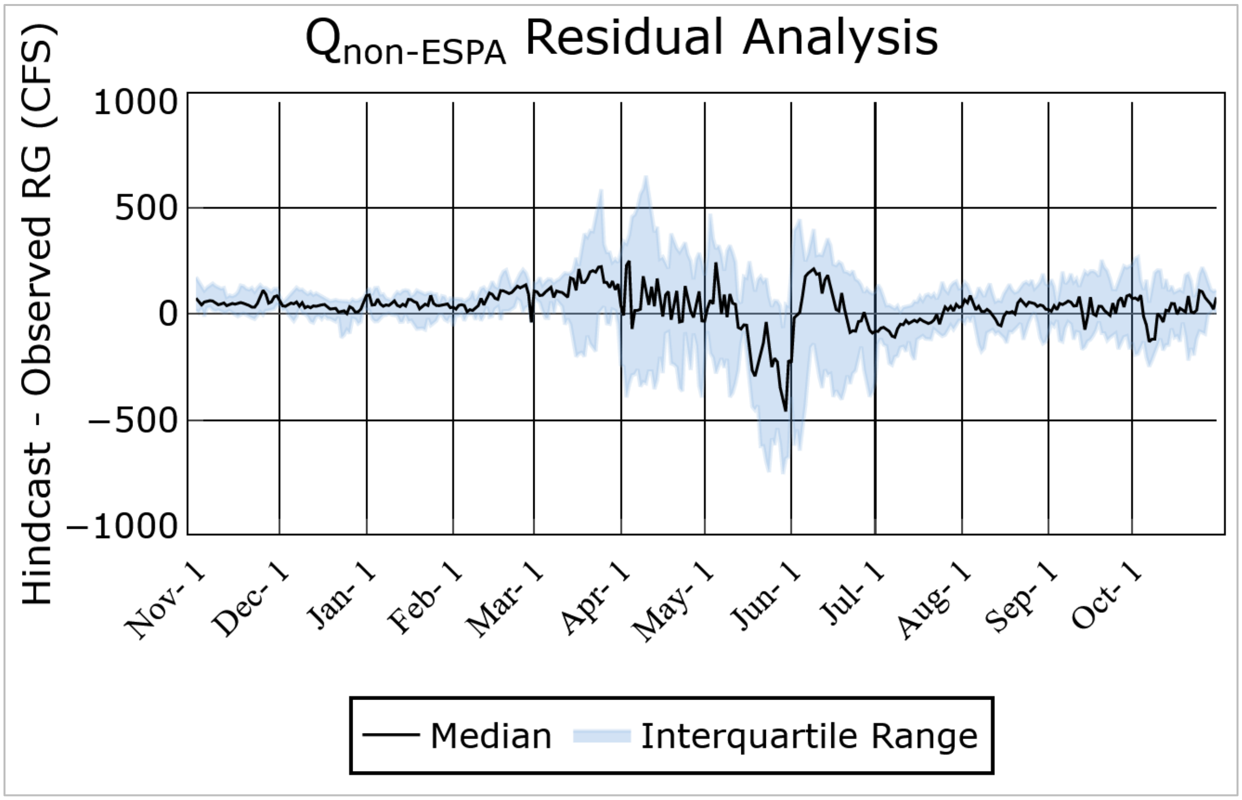

Figure 4-11. Residual analysis hydrograph showing the interquartile range of the daily difference between observed and hindcasted values for years 2002 – 2017.

4.6. Conclusions

Tributary inflow, irrigation return flow, and Kimberly gains supply water to the Snake River Milner to Murphy reach and sum to the $Q_{non\text{-}ESPA}$ term in the SFFT. A simple statistical approach is applied to forecast $Q_{non\text{-}ESPA}$. An annual hydrograph is constructed for each of the three components in $Q_{non\text{-}ESPA}$. The tributary inflow forecast uses the median hydrograph of similar years are used to estimate Malad River and Bruneau River hydrographs while the period of record median is used to estimate Salmon Falls Creek and Rock Creek because of low inter-annual variability. The return flow and Kimberly gain estimates are the period of record median. The different methods used to build hydrographs for the three gain sources are justified based on dataset limitations, appropriate predictor variables, and the independence of $Q_{non\text{-}ESPA}$ components.

The $Q_{non\text{-}ESPA}$ forecast is best fit to observed data in the critical low flow period. The general shape of the runoff peak timing and magnitude is reconstructed. However, the spring runoff period has large intra-annual and inter-annual variability that the statistical method should not be expected to replicate. Additionally, the statistical method cannot predict rare events. These limitations of the method are acceptable given the adequate performance during spring runoff, the fit of the critical low flow period, and the irrigation season volume validation.

5.Estimation of Consumptive Diversions

This section details the procedures used to calculate consumptive diversions, $Q_{DivET,}$ in the Milner to Murphy reach of the Snake River. Q_{DivET} is diverted water that is consumed by ET in the Milner to Murphy reach and is the third component of equation 2-1. Q_{DivET} is subtracted from the Q_{ESPA} and $Q_{non-ESPA}$ gains to calculate the total reach gain target.

5.1. Consumptive Diversion Calculation

Q_{DivET} of the SFFT is the quantity of the water diverted below Milner Dam that is used consumptively. All water diverted in excess of Q_{DivET} is assumed to be returned within the reach during the forecast period. Deep aquifer recharge was not considered to be a significant portion of the water budget because there are few significant gains or losses in this reach of the Snake River (Wood et al., 2014). The SFFT does not track diversions occurring in the reach or returns from these diversions to quantify water loss. Instead, the SFFT estimates consumptive demand (water loss) by estimating irrigation requirements.

Water consumed by crop evapotranspiration originates from both irrigation diversions and precipitation; Q_{DivET} estimations only estimate ET from irrigation diversions. Q_{DivET} is quantified by determining the irrigation requirements necessary to maintain adequate soil moisture. Irrigation requirements are modeled with Washington State University's Irrigation Scheduler Mobile, (WSU, Peters, 2017) and hosted by the Bureau of Reclamation's Agrimet[5] website. Irrigation requirements are estimated for seven crop types: alfalfa (no cuttings), dry beans, silage corn, spring grain, winter grain, potatoes, and sugar beets.

The crop types grown in the Milner to Murphy reach were identified using the USDA's National Agricultural Statistical Services crop data layer. The crop type determination was limited to only those lands irrigated with Snake River or Bruneau River water. The lands irrigated with Snake River (Water District 02, WD02) or Bruneau River (Bruneau Irrigation District, BID) water were identified with water right place of use GIS data layer maintained by IDWR. The average crop type for years 2010 – 2014 was determined to be 54% Alfalfa/Pasture, 15% corn, 10% spring grain, 8% winter grain, 6% sugar beets, 5% potatoes, and 2% dry beans (Table 5-1). The crop type mix will be updated periodically and will be based on a five-year average of the most recently available years. The five year average may be adjusted if anomalous conditions affect the crop mix in a given year.

Table 5-1. The acreage and percent crop mix within the BID and WD02 for the period from 2010 to 2014.

Crop Type	2010	2011	2012	2013	2014	Average
Alfalfa/Pasture	73,400 (60%)	65,800 (53%)	65,600 (55%)	58,400 (49%)	69,100 (56%)	54%
Beans, Dry	4,400 (4%)	1,400 (1%)	2,900 (2%)	2,300 (2%)	1,200 (1%)	2%
Corn, Silage	16,100 (13%)	18,100 (15%)	20,000 (17%)	21,900 (18%)	16,400 (13%)	13%
Grain, Spring	13,100 (11%)	14,300 (12%)	9,800 (8%)	10,800 (9%)	11,300 (9%)	10%

5 (https://www.usbr.gov/pn/agrimet/h2ouse.html)

Grain, Winter	7,300 (6%)	12,300 (10%)	9,200 (8%)	10,300 (8%)	9,000 (7%)	8%
Potatoes	4,400 (4%)	6,100 (5%)	6,200 (5%)	6,300 (5%)	5,800 (5%)	5%

The irrigation requirement of each crop type was estimated for an idealized 40-acre field and upscaled using the crop mix percentages to determine Q_{DivET} at the reach scale. The steps to calculate Q_{DivET} are as follows:

1) Calculate the irrigation requirement. The daily irrigation requirement is calculated for each of the seven crop types using the Irrigation Scheduler Mobile. The application rate is assumed to be 0.49 inches/day. The application rate was based on a standard pivot sprinkler with a length of 1,290 ft and a pumping rate of 1,100 gpm, which is the standard for a 40-acre field.

   The 7-day Daily Budget Table (Figure 5-1) is an example of the irrigation requirement for dry beans. The user input 0.49 inches/day of irrigation on July 5th and July 7th which results in an adequate irrigation application shown by the green shading. On July 8th the crop water use was 0.36 inches and the available soil moisture was 54.1% of capacity. July 8th is highlighted in yellow to indicate the need to schedule another irrigation. The user would then enter 0.49 inches in the irrigation text box and then hits save. The irrigation scheduler then adds the irrigation water to the soil profile on the 8th and recalculates soil moisture for the proceeding days and the next recommended irrigation is highlighted in yellow. The Soil Water Chart (Figure 5-2) is a feature of the Irrigation Scheduler Mobile and shows the fluctuation in soil moisture with irrigations scheduled through July 7th. When all irrigations are scheduled soil moisture is maintained within the green zone.

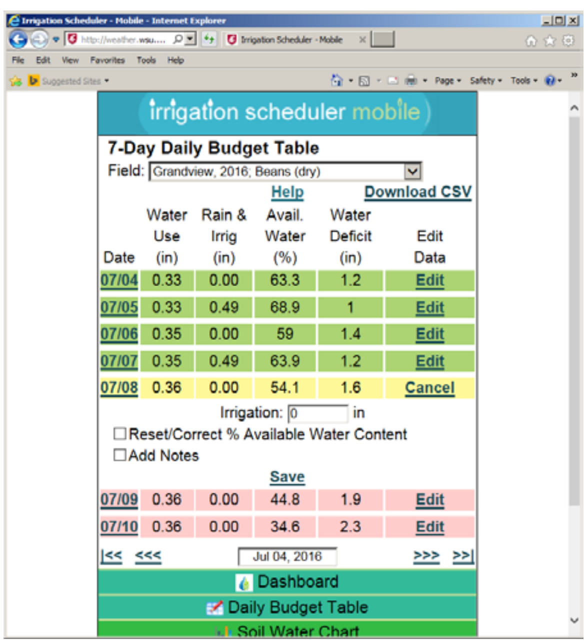

Figure 5-1. Irrigation Scheduler Mobile 7 Day Daily Budget Table.

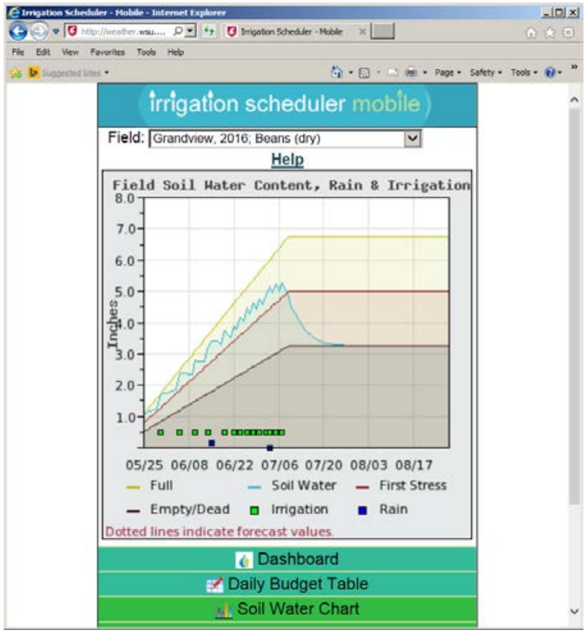

Figure 5-2. Irrigation Scheduler Mobile Soil Water Chart.

2) Download the Irrigation Scheduler Mobile output file once all irrigations are scheduled for a given crop type. This csv file contains the irrigation schedule and irrigation depth (I). Q_{DivET} is calculated for each crop on a daily time step by multiplying irrigation depth (converted from inches to feet) by total irrigated acres in the reach ($A_{Irrigated}$ = 120,000 acres) and the crop percent (CP) as follows:

$$Q_{DivET} = (I/12) * A_{Irrigated} * CP \tag{5-1}$$

Q_{DivET} is then converted to from AF/day to CFS.

3) Average Q_{DivET} to account for irrigation and spatial variability in the reach. A seven-day, centered, moving average is first applied to address irrigation schedule variability from different planting and irrigation schedules throughout the reach. A second 7-day, centered, moving average is then applied to account for different diversion locations and travel times to the Snake River at Murphy Gage. The resulting Q_{DivET} hydrograph is an estimate of total consumptive water demand for each crop type in the Milner to Murphy reach at the Murphy Gaging Station.

4) The irrigation (Q_{DivET}) for the seven crop types was combined to estimate the daily Q_{DivET} for all crops for the irrigation season. Figure 5-3 shows the cumulative irrigation rate for each crop in 2005.

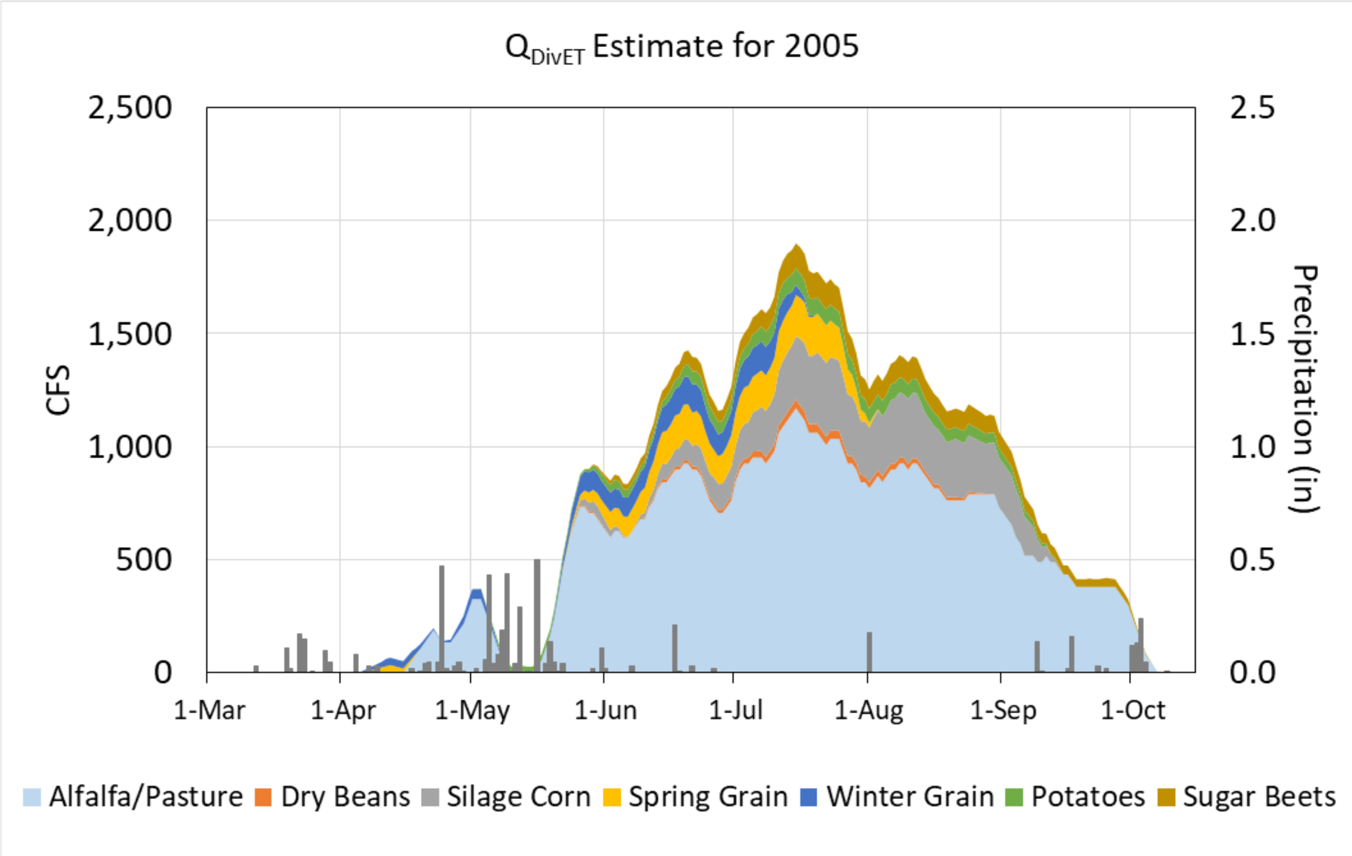

Figure 5-3. Q_{DivET} for the Milner to Murphy reach of the Snake River in 2013 by crop type and daily precipitation amounts on the secondary axis from the Grand View Agrimet Station.

An analysis of the crop mixes within WD02 and BID found that there was approximately 122,000 acres under irrigation. Whereas WD02 irrigates using water from the Snake River, the much smaller BID irrigates out of the Bruneau River below the Bruneau River near Hot Springs, gage (USGS 13168500). For our calculation of Q_{DivET}, the 122,000 acres was rounded down to 120,000 acres (≈ 2%) because crops are not irrigated optimally. It should also be noted that uncut alfalfa was applied as a surrogate for a combination of alfalfa and pasture because pasture is not an option in the WSU Irrigation Scheduler Mobile and because pasture, unlike alfalfa, is not cut during the season. However, this assumption potentially overestimates consumptive diversions because uncut alfalfa has higher ET than either alfalfa or pasture.

Q_{DivET} varies considerably from year to year because of climatic conditions. A graphical comparison of consumptive diversions from 2005 (see Figure 5-3, above) and 2013 (see Figure 5-4, below) highlights the variability. In May 2005, Q_{DivET} was less than 1,000 cfs because of precipitation and cool temperatures. This is contrasted by Q_{DivET} in May 2013 that generally exceeds 1,000 cfs. Likewise, Q_{DivET} estimates in 2005 and 2013 were 310,300 ac-ft and 390,900 ac-ft, respectively, an approximately 20% difference.

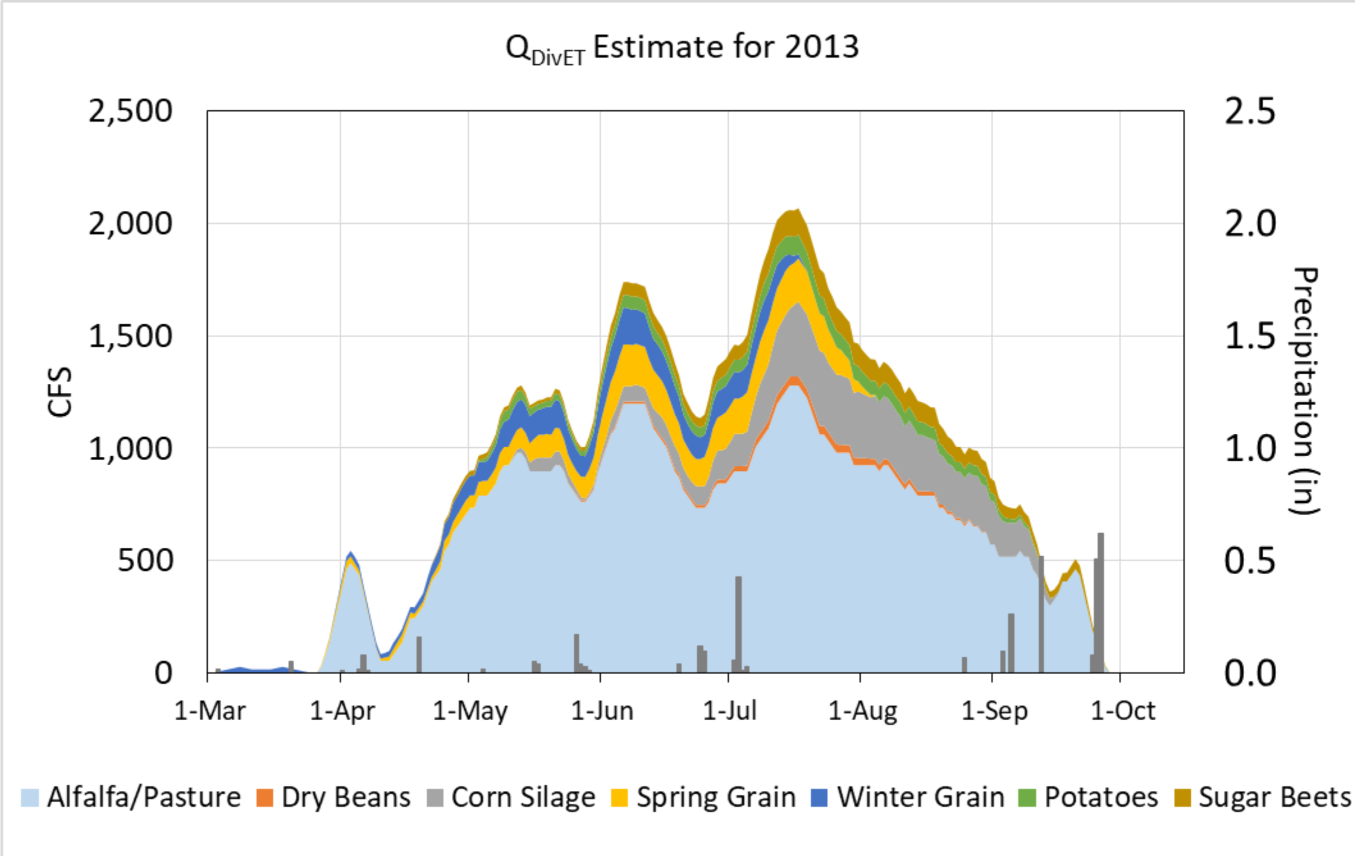

Figure 5-4. Q_{DivET} for the Milner to Murphy reach of the Snake River in 2013 by crop type and daily precipitation amounts on the secondary axis from the Grand View Agrimet Station.

The WSU Irrigation Scheduler Mobile is limited to the years 2003 - 2016. The irrigation requirements were run from March 1 through early October for each year and the SFFT estimated Q_{DivET} as the median daily value from 2003 through 2016.

5.2. Consumptive Diversion Calculation Validation

As explained below, the reasonableness of the Q_{DivET} calculation was validated by three methods.

5.2.1. Consumptive Diversion Comparison to Actual Diversions (2016)

The first validation is a comparison of the estimated Q_{DivET} for WD02 against actual diversions. It is expected that Q_{DivET} when multiplied by the regional delivery efficiency will approximate total volume diverted at the headgate. Based on the method discussed in the previous section, Q_{DivET} in 2016 was 379,600 acre-ft. WD02, the major water district in the reach that has complete diversion data, represents approximately 95% of the diversions in the reach. Thus, Q_{DivET} for just WD02 should be approximately 360,620 acre-ft. Assuming a reach-wide irrigation delivery efficiency of 75%, total diversions for WD02 should approximate 480,800 acre-ft. The actual diversion volume reported in the WD02 annual report for the 2016 irrigation season was 478,287 acre-ft (Whitney, 2017). The calculated Q_{DivET} for 2016 is reasonable based on the actual measured diversions within WD02.

The 75% delivery efficiency used above was based on the assumption that project delivery efficiency ranges between 50-60% for gravity-based surface water systems near Grandview and 85-95% for high lift pump systems. Thus, 75% efficiency falls in the middle of these ranges. Also the Idaho Water Supply Bank (WSB) assumes that headgate deliveries need to be 1 acre-foot greater than consumptive demand and the WSB sets consumptive demand at 3 to 3.5 acre-feet with in this region. With 1 acre-foot of excess diversion, the efficiency would be between 75% and 78%.

5.2.2. Consumptive Diversion Comparison to METRIC ET (2000)

A second validation of the Q_{DivET} estimate was based on a comparison to evapotranspiration estimates made with METRIC (Allen et al., 2007a; Allen et al., 2007b). METRIC estimates the total ET from irrigated land. If effective precipitation is added to QDivET then the volume should provide a close match to METRIC estimates of total ET. In 2000, METRIC ET was calculated for all irrigated areas in the state of Idaho. Using ArcGIS layers, the consumptive use within the POUs for BID and WD02 was 352,887 acre-ft. The Q_{DivET} estimate was 324, 830 acre-ft. Adding effective precipitation during the irrigation season to Q_{DivET} results in a total consumptive use in the Milner to Murphy reach of 360,940 acre-ft, which is 2% higher than the METRIC estimate at the irrigation season scale.

METRIC was also used to estimate consumptive use on a monthly time scale. The METRIC model shifted consumptive use later in the season. The shift could be due to a discrepancy in crop mix. The crop mix used by the Q_{DivET} estimate was based on the average crop mix for the period from 2010-2014. The actual crop mix within the Milner to Murphy reach for 2000 is unknown. It should be noted, however, that the reconstructed hydrograph of the Snake River (see third validation exercise below), suggests that Q_{ET} estimates from the methodology presented here were strongly shifted toward the early part of the season, and that the monthly Q_{ET} from METRIC is probably more accurate.

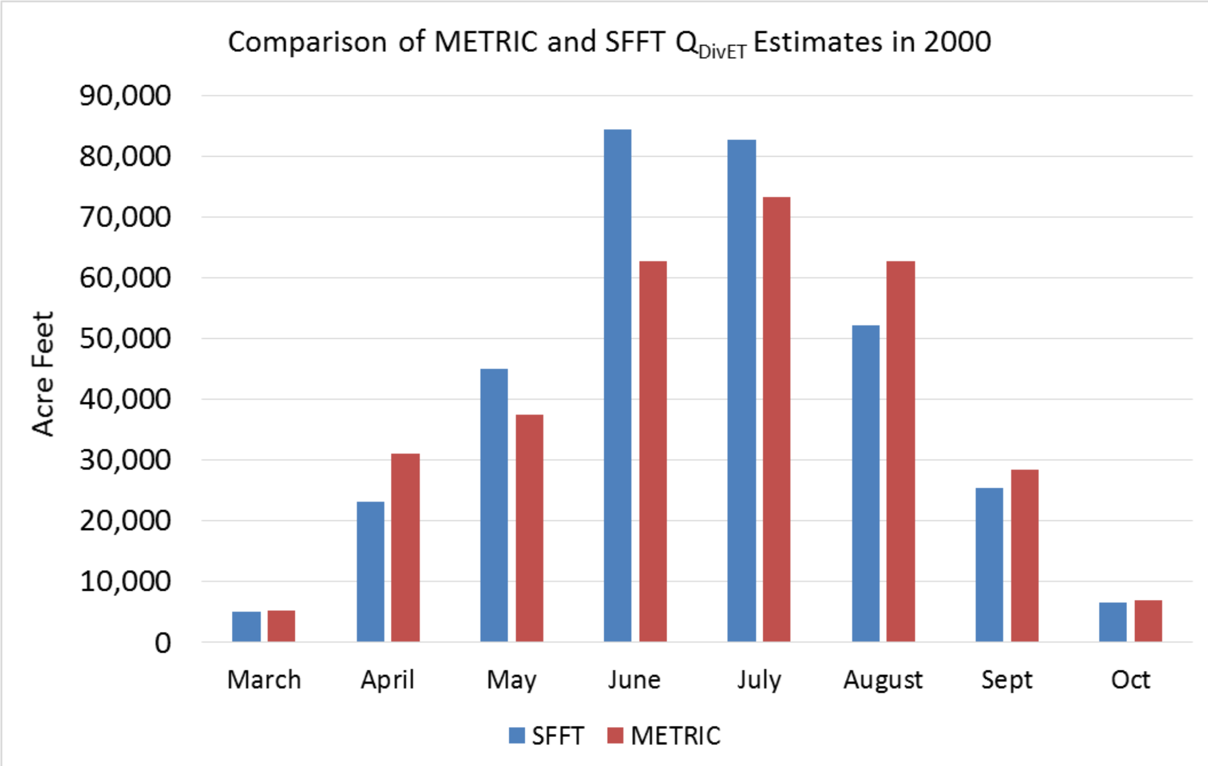

Figure 5-5. Comparison of total consumptive use (Q_{ET}) estimates based on the IDWR spreadsheet in IDWR and Q_{ET} estimates from METRIC. The Q_{ET} estimate from IDWR is based on adding effective precipitation to Q_{DivET}.

5.2.3. Consumptive Diversions Comparison to Reach Gains (2002 to 2012)

Finally, a more robust validation of Q_{DivET} was carried out using an estimate of aquifer discharge (Q_{ESPA}), return flow measurements ($Q_{returns}$), tributary inflow (Q_{tribs}), and the estimated Q_{DivET} values. Of the three components that make up the Milner to Murphy reach gain, only Q_{DivET} is completely unmeasured. Qnon-ESPA, which includes tributary inflow and return flows are mostly measured and QESPA can be estimated reasonably well from the measured discharge of Box Canyon Springs near Wendell, ID (USGS 13095500). Box Canyon Springs was up-scaled by a factor of 18 to represent Q_{ESPA} for the years from 2002 to 2016. The factor of 18 was based on a visual best fit to winter reach gains when consumptive demand is zero and tributary discharge is relatively stable. Box Canyon Springs is a major discharge point of the ESPA within the Snake River Canyon. It has a long period of record and is considered a good indicator of conditions in the ESPA (Boggs et al., 2010; Hoekema and Sridhar 2013). Validation steps for the year 2005 are shown in Figures 5-6, 5-7, 5-8, and 5-9 Figure 5-6, represented by Box Canyon up-scaled by 18, shows a minimum discharge at the beginning of June and a maximum discharge toward the beginning of October in 2005.

Having estimated Q_{ESPA} and having measurements for $Q_{non-ESPA}$, leaves only Q_{DivET} as an unknown. If Q_{DivET} is estimated correctly than when the three components are added together they should match the reach gain $Q_{Murphy} - Q_{Milner}$ with reasonable correlation.

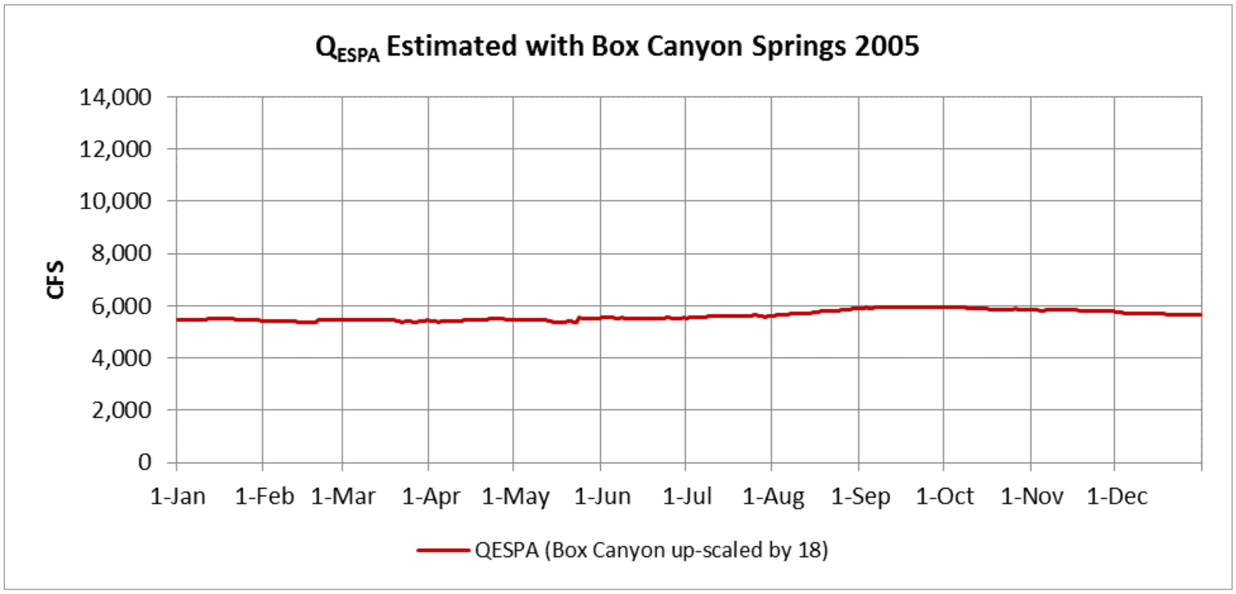

Figure 5-6. Estimated discharge from the ESPA (Q_{ESPA}) based on up-scaling of the discharge from Box Canyon Springs (USGS 13095500).

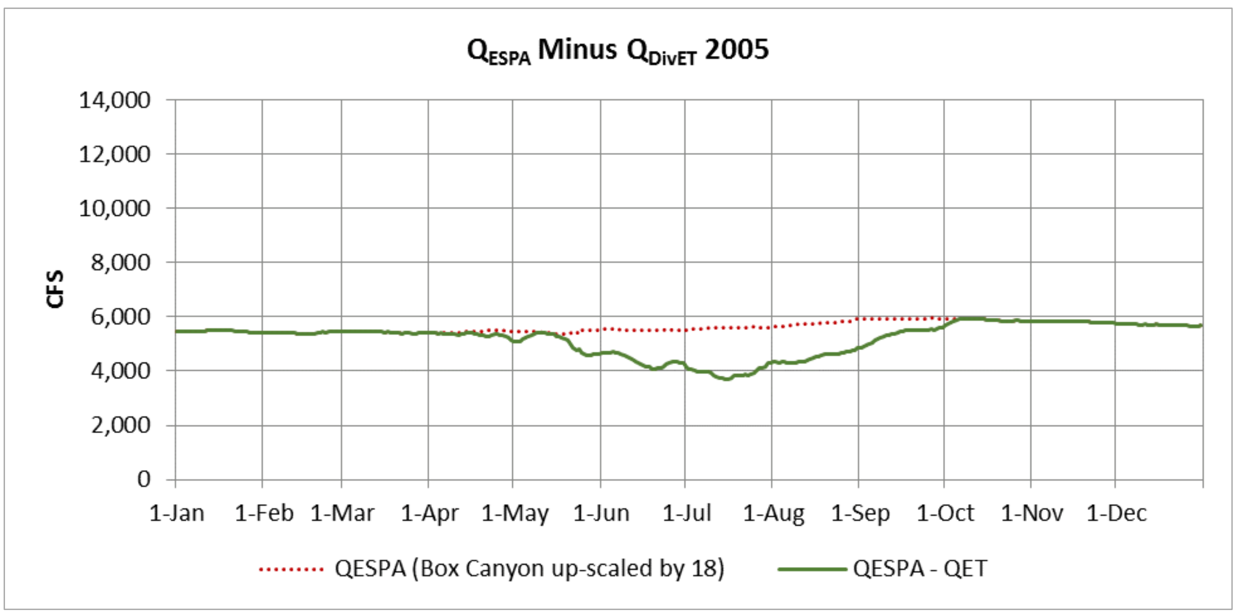

Figure 5-7. Estimated ESPA discharge (Q_{ESPA}) is shown by the dotted red line and Q_{ESPA} with the consumptive irrigation diversions, Q_{DivET}, removed is shown by the green line.

The components of the Milner to Murphy reach gain are shown in Figure 5-7 and Figure 5-8. . Subtracting consumptive diversions (Q_{DivET}) from Q_{ESPA} (as shown by the solid line in Figure 5-7 and the dotted line in Figure 5-8), the minimum discharge is reached in mid-July. The discharge drops below the Swan Falls minimum streamflow of 3,900 cfs during the irrigation season. However, when tributary discharge and discharge from irrigation drains returning excess diversions from above the reach are added into the Milner to Murphy reach gains, the flow is above the Swan Falls minimum streamflow. Since tributary inflow is minimal in July, most of the difference between the blue line (the modeled reach gain) and the green dotted line (Q_{ESPA} – Q_{DivET}) is return flow and non-ESPA aquifer discharge from the south side of the Snake River canyon. The $Q_{non\text{-}ESPA}$ play a critical role in maintaining the Swan Falls minimum streamflow.

Figure 5-9 compares the modeled reach gains (blue line) to the measured reach gains (black line). The measured reach gain is based on a 7-day moving average of Q_{Milner} subtracted from Q_{Murphy}, with a 2-day lag in flow from Murphy to Milner. The 7-day moving average limits the impact of Idaho Power Company's reservoir operations and imprecise travel time estimates on the reach gain. The modeled versus measured reach gains for the period 2002-2012 validate the concept that the Milner to Murphy reach gains are reasonably calculated by subtracting the calculated Q_{DivET} from the up-scaled Box Canyon Springs discharge (Figure 5-9). The Pearson product moment correlation coefficient, r, of 0.91 establishes that there is strong correlation between modeled and measured return flows (Figure 5-10).

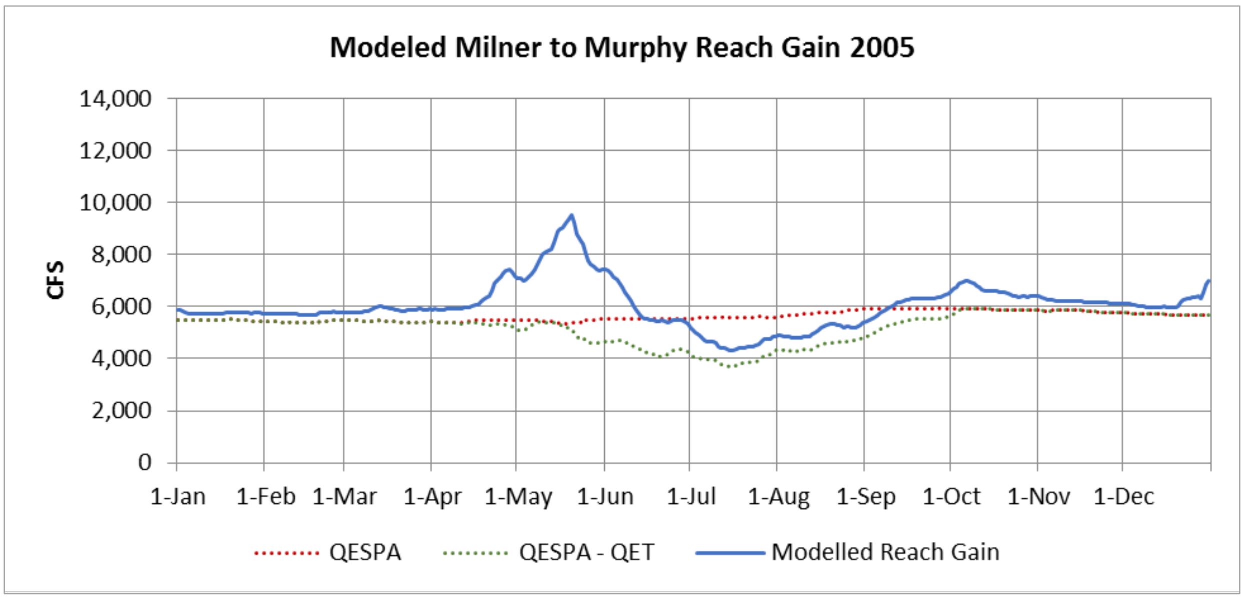

Figure 5-8. Modeled reach gain for Milner to Murphy based on Equation 4c.

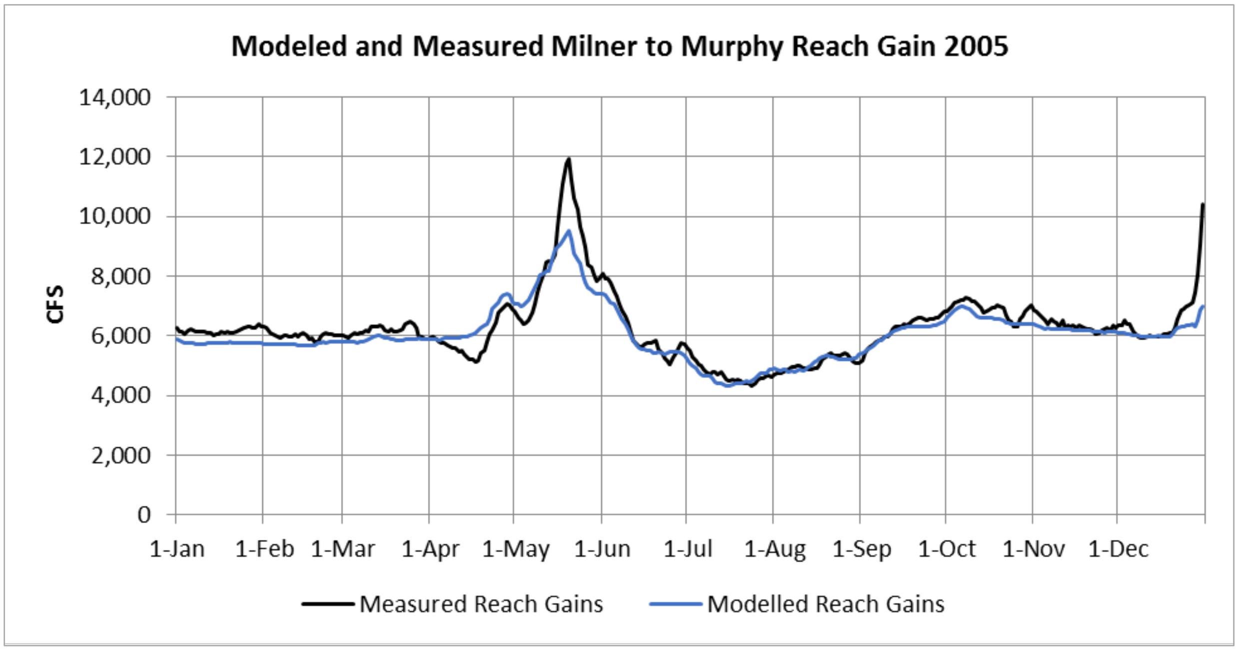

Figure 5-9. Comparison of the measured reach gains ($RG_{Milner2Murphy} = Q_{Murphy} - Q_{Milner}$) to the modeled reach gains ($RG_{Milner2Murphy} = Q_{ESPA} - Q_{DivET} - Q_{trib} + Q_{ReturnsAbvReach}$).

It should be noted that while it is possible to utilize Box Canyon Springs as a proxy for Q_{ESPA}, because the spring has a very constant flow with very limited annual variability any shift applied by the USGS to the rating table has a significant impact on discharge statistics. Significant shifts to the gage by the USGS in recent years makes it more difficult to determine the correct scale for adjusting Box Canyon discharge. Thus, in Figure 5.3 we only show the comparison of modeled versus measured reach gains from 2002-2012. Any attempt to utilize the springs to forecast the Milner to Murphy reach gains would require several years of measurements between shifts in order to be able to remove shift impacts from the statistics. Therefore while this method was found to have value in validating $Q_{DivET,}$ no attempt was made to directly incorporate Box Canyon Springs discharge in the forecast of the Milner to Murphy reach gain.

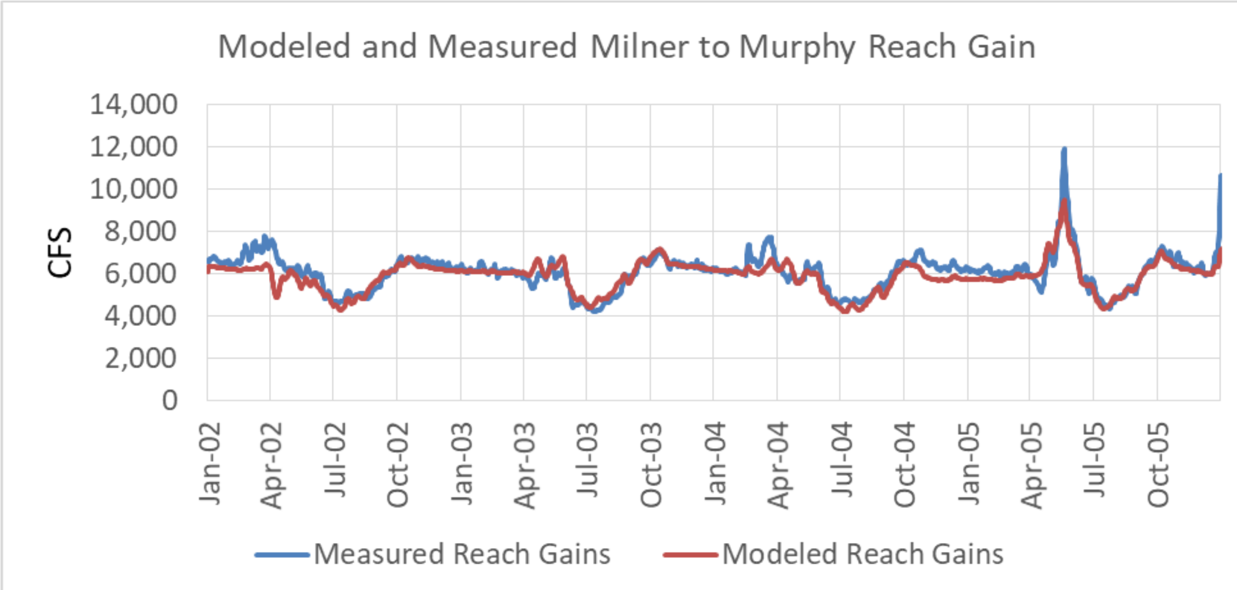

Figure 5-10. A comparison of the modeled versus measured Milner to Murphy reach gains from 2002 through 2005. The correlation coefficient, r, is 0.91 (for the entire comparison 2002-2012).

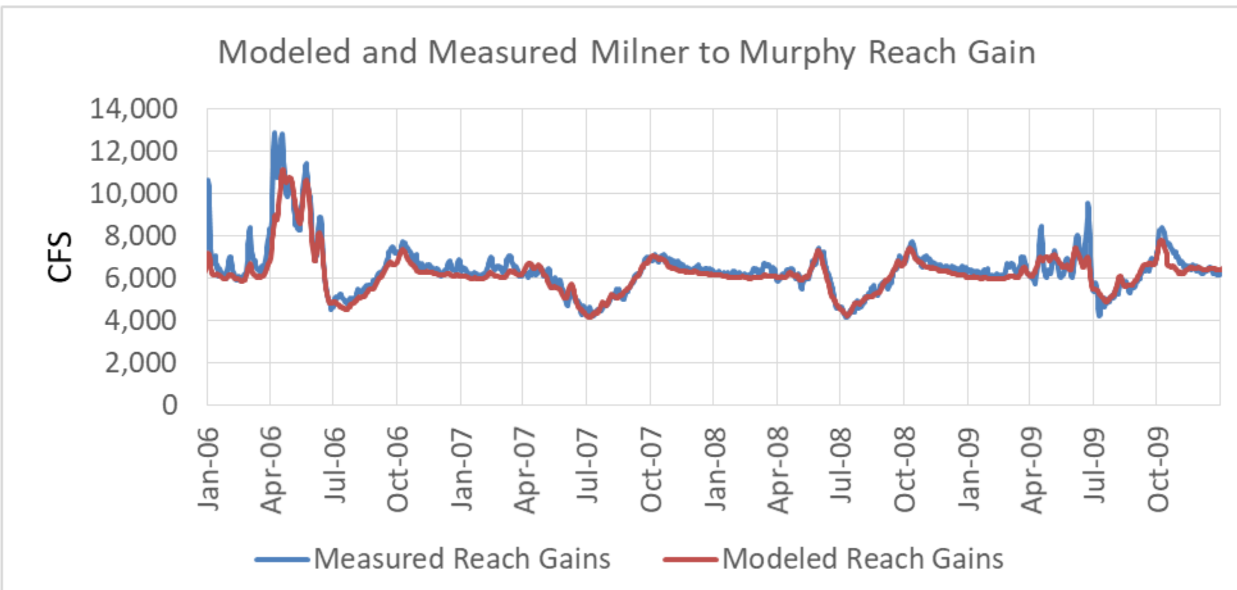

Figure 5-11. A comparison of the modeled versus measured Milner to Murphy reach gains from 2006 through 2009. The correlation coefficient, r, is 0.91 (for the entire comparison 2002-2012).

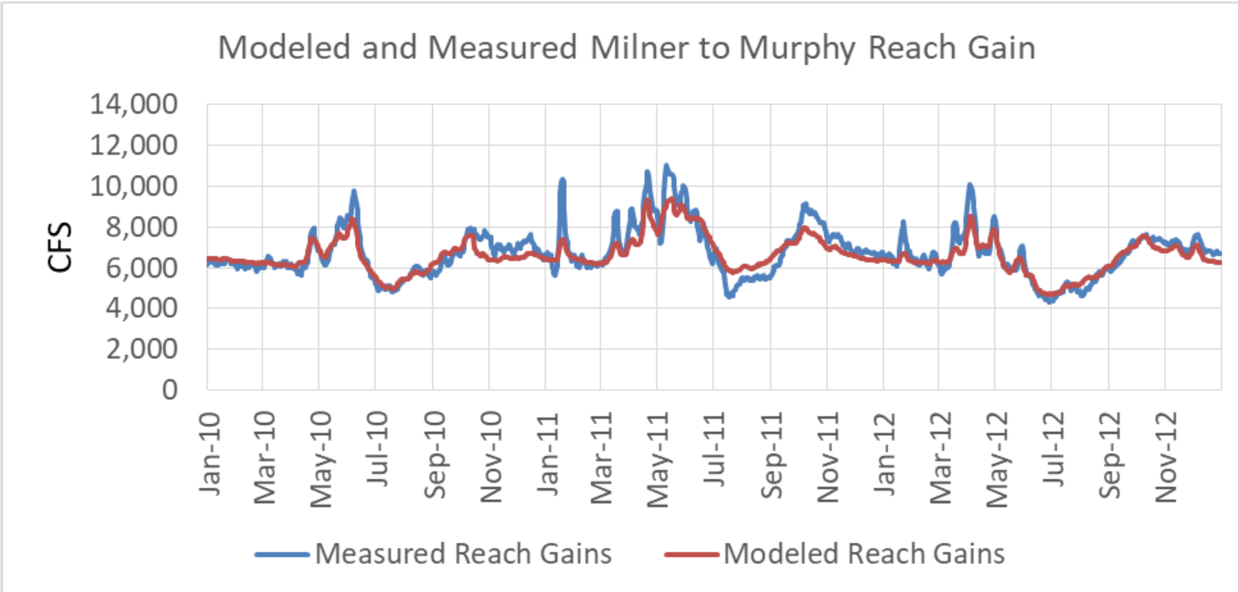

Figure 5-12. A comparison of the modeled versus measured Milner to Murphy reach gains from 2010 through 2012. The correlation coefficient, r, is 0.91 (for the entire comparison 2002-2012).

All three methods (comparison to actual diversions, reach gains, and METRIC) provide a reasonable validation of our Q_{DivET} estimates.

6. SFFT Hindcast Validation and Model Fit

The three components of Equation 2.1, Q_{ESPA}, $Q_{non\text{-}ESPA}$, and Q_{DivET} sum to generate the Swan Falls Forecast Tool prediction. The performance of the three components have been validated individually in the previous sections. This section discusses the validation procedure used to evaluate the overall ability of the SFFT to predict the Milner to Murphy reach gain and the corresponding uncertainty analysis. The validation procedure used to assess SFFT performance is a hindcast analysis. The difference between the hindcast and the observed reach gain are calculated as the residuals and are used to quantify SFFT uncertainty. The residuals are also added to the final forecast tool to account for bias within both the January and May forecast tool. A 15 day centered moving average of the 50th percentile daily residual from year 2002-2017 is applied to the forecast tool output to generate the Swan Falls Forecast tool results for both the January and May forecast tool. Residual exceedance probabilities are also fit to the SFFT output to estimate the SFFT forecast and the range of expected values.

$$SFFT_{Output} = Q_{ESPA} + Q_{non\text{-}ESPA} - Q_{DivET} \qquad (6\text{-}1)$$

where,

Q_{ESPA} = discharge from the ESPA between Milner Dam and King Hill

$Q_{non\text{-}ESPA}$ = Milner to Murphy reach gains from non-ESPA sources

Q_{DivET} = Milner to Murphy consumptive use of diverted flow

6.1. SFFT Hindcast Validation

SFFT performance was assessed using hindcast validation for the irrigation years 2002 - 2017. The historical extent is limited by the groundwater level database in the SFFT that contains data starting in IY 2002. Hindcasting procedure used the January and May forecast tool and applied only data that would have been available at the time of the forecast. No knowledge of future conditions is assumed.

Hindcast performance evaluation is qualitative with a focus on the ability of the SFFT to capture the priority area of the summer low flow period and rebound. The ability to capture runoff timing and magnitude were less important. Figure 6-1 shows the hindcast validation for three years and contains an average water year (2009), a dry water year (2014), and wet year (2017).

The SFFT accurately portrays the majority of the Milner to Murphy reach gain hydrograph. Most importantly, the hindcast and the observed data closely match during the receding limb of the runoff period into the summer critical low flow period and during the late summer recovery. The SFFT also captures the November through February winter flow. Hindcast disagreement to observed data is most pronounced during the spring and early summer runoff period. In high water years the SFFT generally underestimates flow during the runoff period while in the low water years, hindcasted runoff slightly overestimates the observed. In all but extreme cases the observed hydrograph is within or tracks near the forecast lower bound (Section 6.3). There is general agreement in the hindcasted and observed hydrographs in average water years. In all hindcasts, the SFFT has the greatest difficulty mimicking abrupt peaks and troughs.

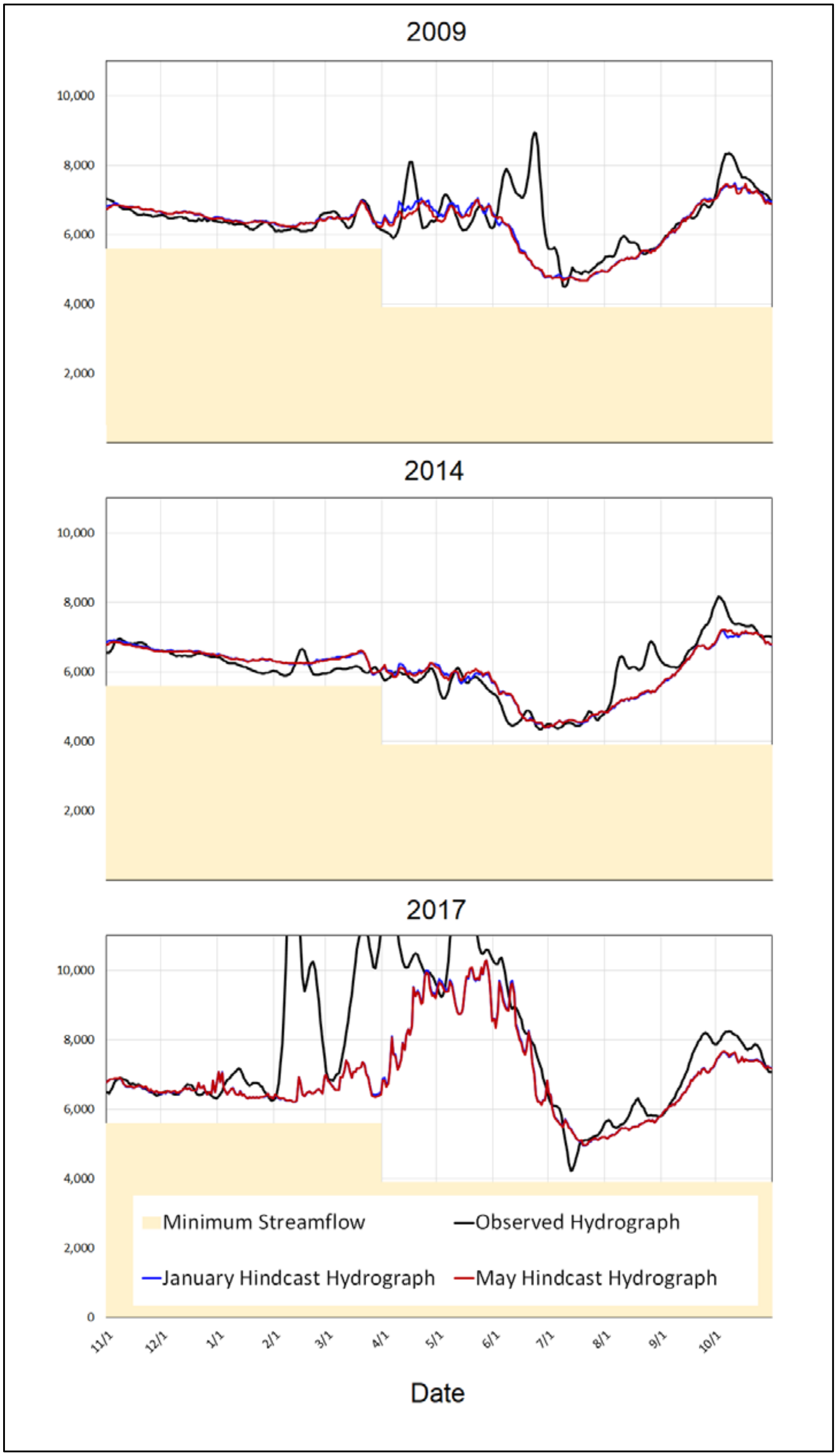

Figure 6-1. Observed and hindcasted hydrographs for an average (2009), dry (2014) and wet (2017) water year for the January and May forecasts.

6.2. Residual Analysis and Uncertainty Quantification

A residual analysis was performed to quantify SFFT performance. The residual matrix consists of the daily difference of the observed and hindcasted hydrographs for each year in the study period. The residual interquartile range (25th percentile, median, 75th percentile) are plotted for each day. Non-normality of the daily residual distribution is assumed and non-parametric statistics are used to estimate expected values. The residual analysis plot (Figure 6-2) contains key information about hindcast output performance including uncertainty range, hindcast bias and daily distribution skewness. Positive values in the plot are hindcast output overestimation of observed data and negative values are hindcast output underestimation of observed data.

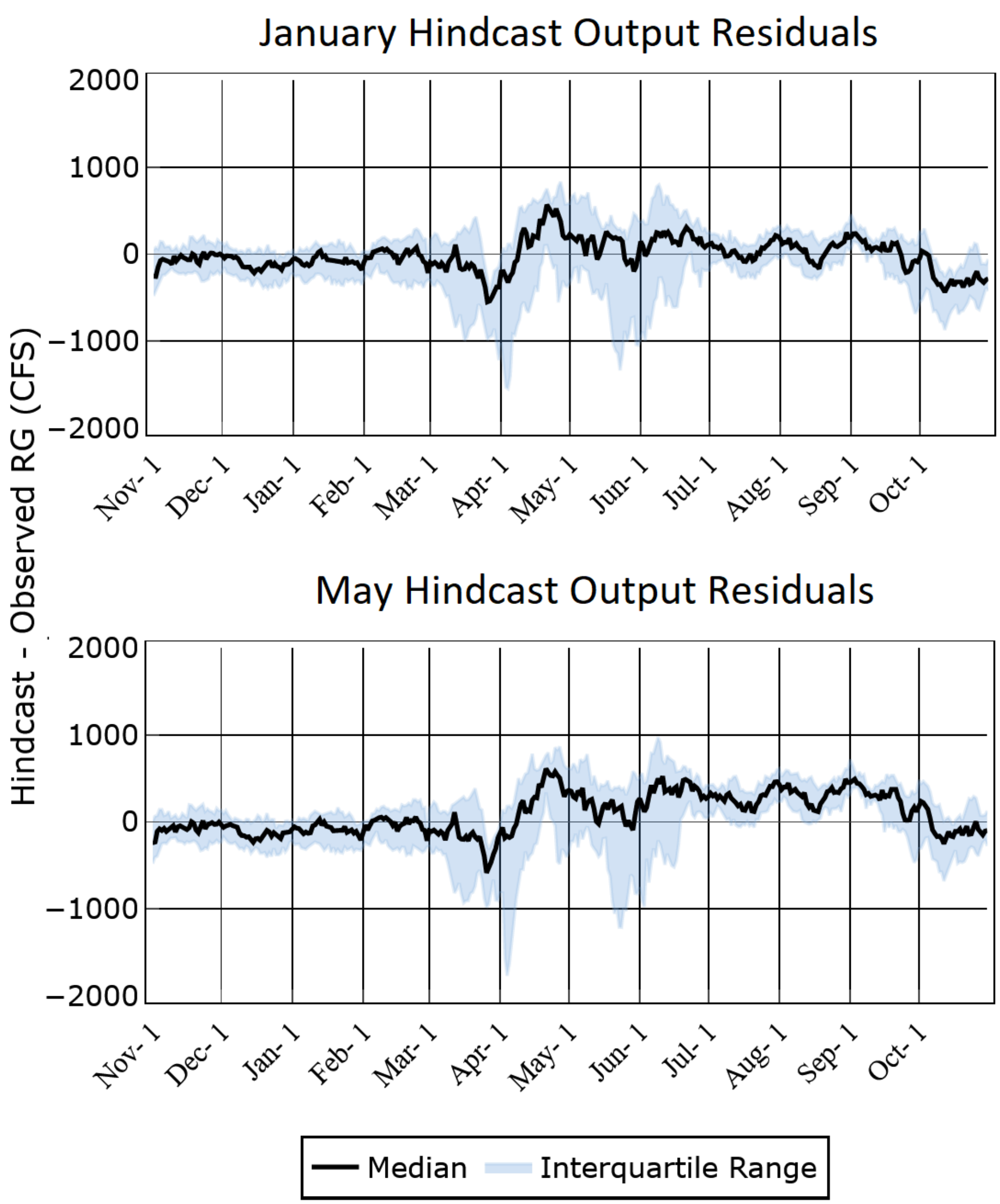

Figure 6-2. Hindcast residual analysis plot for Milner to Murphy reach gain for January and May hindcasts.

The residual interquartile range (IQR) is a measure of the hindcast ability to replicate observed flow and quantifies hindcast uncertainty. The IQR is the shaded area in the residual analysis plot and is bound by the 25^{th} percentile and the 75^{th} percentile for a given day. The IQR contains 50% of the data points, 25% of the data points fall below the lower bound, and 25% of the data points are above the upper bound. Large IQRs correspond to large hindcast uncertainty and result from significant hindcast over/under estimation. Conversely, narrow IQRs are portions of the hydrograph the hindcast is able to reliably reproduce historic flows with low uncertainty. If the median and IQR depart from the zero line on the residual plot, this indicates a significant bias in the model. Bias can be the result of the model not fully capturing all components of the hydrograph.

The residual analysis of the January forecast indicates that the model performs well from November 1^{st} to the end of February. During this period, the median residual tracks closely to zero and the zero residual value is within the IQR. Starting in March the IQR begins to expand and remain large until the latter half of June. This expansion in the IQR corresponds to the timing of Spring runoff when the snowmelts in the mountains surrounding the Snake River Plain. In addition to having a large IQR, from mid-March to mid-April the January forecast contains a strong negative bias. After mid-March the IQR once again includes the zero residual error value. Both the large IQR and negative bias of the model indicates that this model will have difficulty in predicting a shortfall in late March just before the minimum streamflow drops from 5600 cfs to 3900 cfs on April 1^{st}. From July 1 to the end of September the model has a low IQR and exhibits limited bias as the zero residual value falls consistently within the IQR. Interestingly, the model once again displays a negative bias in October.

The residual analysis of the May forecast indicates that the May forecast has low uncertainty and bias during the non-irrigation season from November through mid-March. The model suffers the same increase in IQR during the runoff period from March to June and the brief negative bias at the end of March and beginning of April. However, the May forecast is biased high for the entire irrigation season until October.

6.3. Residual Analysis Fit to SFFT Prediction

The output of the SFFT in terms of the three components in Equation 2.1, Q_{ESPA}, $Q_{non\text{-}ESPA}$, and Q_{DivET} is a deterministic hydrograph. This deterministic hydrograph, however does not represent our best understanding of the system, because we know from the residual analysis that the forecast expresses some bias at certain times of the year. The SFFT output hydrograph is therefore fitted by the residual analysis IQR to correct the known bias in the deterministic forecast hydrograph. Residual analysis quartiles are added to the SFFT output hydrograph to generate a forecast with a range of expected values (Figure 6-3).

$$SFFT_{Forecast} = Q_{ESPA} + Q_{non\text{-}ESPA} - Q_{DivET} + R_{percentile} \qquad (6\text{-}2)$$

where,

Q_{ESPA} = discharge from the ESPA between Milner Dam and King Hill

$Q_{non\text{-}ESPA}$ = Milner to Murphy reach gains from non-ESPA sources

Q_{DivET} = Milner to Murphy consumptive use of diverted flow

$R_{percentile}$ = Percentile of the residuals from the Hindcast analysis

To account for bias in the January and May forecasts a 15-day centered moving average of the 50th percentile was added to the forecast output to reduce the bias within each model. This, in theory, would help to correct any bias in the January and May forecasts. Figure 6-3 shows that once corrected for bias, the forecast tool performs better without significantly increasing the uncertainty within the model. The main bias correction that adding the residuals corrected was the excess flow predicted by the May forecast in the summer.

Similar to before the residuals were added, large uncertainty exists during the runoff period and during the increase in flow during October. These areas are both negatively skewed and therefore are underestimating the amount of flow in the reach. This outcome is preferred so that the forecast tool does not overestimate low flow events, because high flow events are not a significant concern for maintaining the minimum streamflow of the Snake River near Murphy. Analyzing the interquartile range for select years (Figure 6-4) shows that the range captures even more of the observed hydrograph then just relying on the 50th percentile.

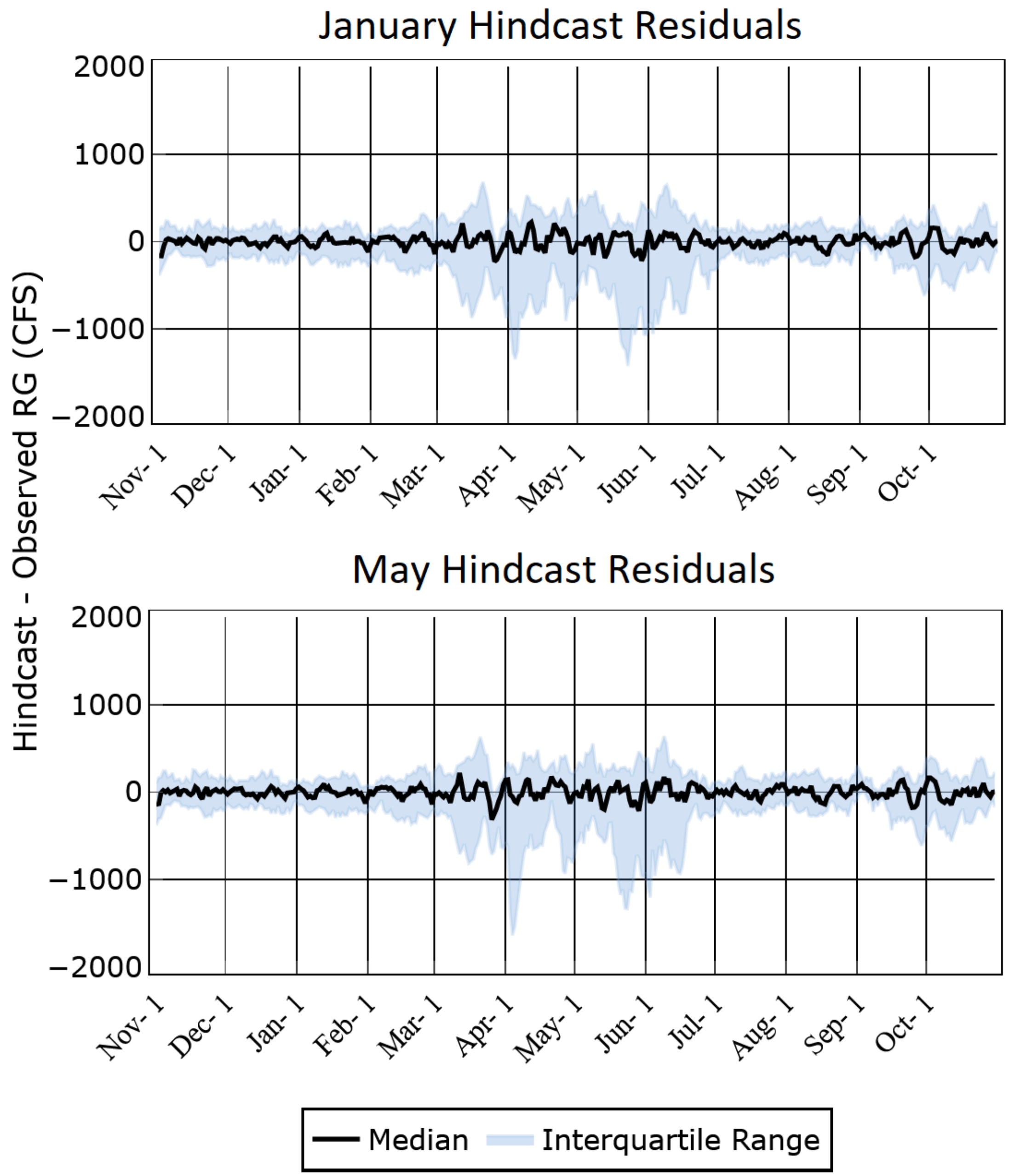

Figure 6-3. Hindcast residual analysis plot for Milner to Murphy reach gain for January and May hindcast after including a 15-day centered average of the 50th percentile of residuals for each day to correct for bias

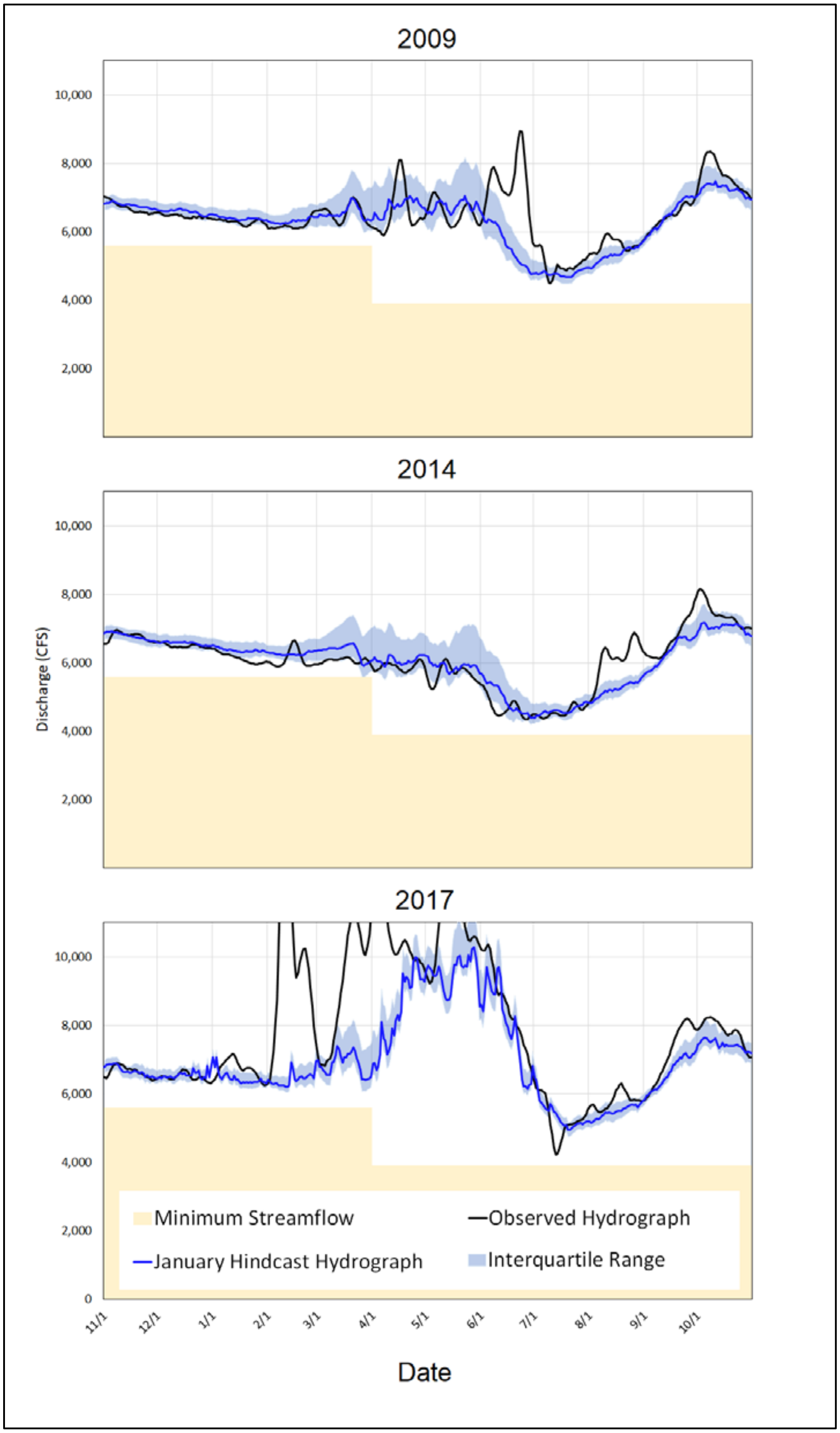

Figure 6-4. Observed and January hindcasted hydrographs with model uncertainty for an average (2009), dry (2014) and wet (2017) water year.

7.SFFT Calculations – Spreadsheet Details

7.1. Aquifer Discharge—Spreadsheet Methods and Procedures

Excel Worksheet Title	Function	Link to Other Worksheets
User	• User-defined input – enter upcoming year (or current year for May Tool) in Cell C4 User-defined input – enter the number of wells for inclusion in interpolation neighborhood (between 1 and 100) in Cell D4 Uncertainty Range – Lower Bound in Cell F4 Uncertainty Range – Upper Bound in Cell G4 Bruneau SWSI (50% exceedance) in Cell H4 Big Wood SWSI (50% exceedance) in Cell I4 Snake River (Heise) SWSI (50% exceedance) in Cell J4 Upper Snake River Reservoir Storage in Cell K5	• Cell C4 in *User* worksheet is linked to cell B6 in the *Head – Well Selection* Worksheet • Cell D4 in *User* worksheet is linked to cell D6 in the *Head – Well Selection* Worksheet • Uncertainty Range Lower and Upper Bound are linked to the ResidualMatrix Worksheet and define the residual percentiles for uncertainty bounds • Bruneau SWSI is linked to ReturnFlow – Forecast Worksheet • Big Wood SWSI is linked to ReturnFlow – Forecast Worksheet
Raw RFs	Database of response functions for each ESPAM 2.1 model cell. Determined using ESPAM 2.1 transient superposition data sets. Each cell stressed at 1,000,000 cfd for one month to determine responses. Responses are the collective gains from all spring and ghb cells in the Milner to King Hill reach of the Snake River	
Head – Well Selection	Looks up the depth to water for select wells for the forecast year the user enters in Cell C4 of the *User* worksheet	• Cell range A8 through C107 (Well ID and X, Y coordinates) is linked to *Head – Well Data* worksheet cell range A12 through D111 (excludes the altitude data in column B of the *Head – Well Data* worksheet) • Cell range H8 through H107 (2008 depth to water values) is linked to *Head – Well Data* worksheet range I12 through I111 • Cell range I8 through I107 (depth to water value for each well) is a "lookup" Excel function, looking up the year value in cell B6 (user-defined forecast year), returning the depth to water value located in the *Head – Well Data* worksheet K6 through BA111 for the user-defined year • Cell range T13 through T5039 (sum of weights multiplied by the change in water level for each neighborhood cell divided by the sum of

Excel Worksheet Title	Function	Link to Other Worksheets
		the weights) is linked to *Head – Interpolation* worksheet cell range DD10087 to DD15113
Head – Well Data	Database of raw depth to water values for wells in column 100 or less of the ESPAM 2.1 mode domain • There is a placeholder for future water levels in columns AW through BA • Additional wells can be added, starting in row 77 of this worksheet • A value of 9999 is assigned to missing data • When new data are entered, users should review the map of head changes (worksheet *Head – Map*) to make sure data are representative	
Head – Interpolation	• Head differences (as compared to 2008 reference year) are interpolated for each model grid cell (columns 100 and less) from the entered well data • There are tree tables in this worksheet. The first table (rows 8-5040) is calculation of values used to weight each well observation (inverse square of distance between well and cell). The second table (rows 5045 - 10074) is a ranking of the distance between each well and the specific cell. This is used to find wells in the neighborhood of the cell. The third table (after row 10075) determines the product of the well change in water level and weighting from the first table for wells in the neighborhood selected on the *Head - Well Selection* worksheet. • The final result is determined in column DD adjacent to the third table as the sum of weights multiplied by the change in water level for each neighborhood cell divided by the sum of the weights	• Cell range A14 through D5040 (ESPAM 2.1 model cell column and row, and X,Y coordinates) is linked to *Head – Well Selection* worksheet cell range N13 through S5039 • Cell range F10 through DA12 (Well ID and X,Y coordinates) is linked to *Head – Well Selection* worksheet cell range A8 through C107
Head – Map	• Visual representation of water level difference from reference year (2008) to review when new water level data are entered • One must <u>Refresh</u> the map when a different year is chosen (Analyze, then Refresh)	The visual representation shown is based on data in the *Head – Map Data* worksheet
Head - Map Data	Calculates a minimum and maximum head difference between the forecast year and the reference year (2008). Provides a separate worksheet used for the visual representation of the water level difference displayed in the *Head – Map* worksheet.	• Cell range C7 through C5033 is linked to *Head – Well Selection* worksheet cell range T13 through T5039

Excel Worksheet Title	Function	Link to Other Worksheets
Head – Discharge Sum	Multiplies the head difference (interpolated forecast year head minus 2008 reference year head) by the head response function for each ESPAM 2.1 model cell in Column 1 through 100. The result is the effect of November or April aquifer head on discharge in the Kimberly to King Hill reach of the Snake River.	• Cell range A8 through B5034 (ESPAM 2.1 model cell column and row) is linked to *Head – Well Selection* worksheet cell range N13 through O5039 • Cell range C8 through C5034 (change in water level compared to 2008 value) is linked to *Head – Well Selection* worksheet cell range T13 through T5039
Head – Response Functions	Database of bi-weekly (15.2 day) initial head response functions for each ESPAM 2.1 model cell in Column 1 through 100	
Head- Recession Graph	Plot of the forecast year and reference year (2008) head contribution to Snake River discharge between Kimberly and King Hill.	Data plotted is in the *Head – Discharge Sum* worksheet
Irr Rech - Canal Seepage Calc	Multiplies monthly diversion volumes for three irrigation entities by the entity's canal seepage constant, a constant that matches what was used in ESPAM 2.1	Cell range B7 through D18 is linked to *Data* worksheet cell range B7 through D18; cell range K7 through M18 is linked to *Data* worksheet cell range W7 through Y18.
Irr Rech - On-Farm Rech Calc	Calculates on-farm recharge for each of the three irrigation entities using monthly diversions and canal seepage values. Mimics on-farm recharge calculations implemented for ESPAM 2.1.	• **50% exceedance:** Cell range B14 through B77 is linked to each entity's diversion data in cell ranges B7 through B18, C7 through C18, and D7 through D18 in the *Data* worksheet. • **User-defined uncertainty range:** Cell range Q14 through Q77 is linked to each entity's diversion data in cell ranges W7 through W18, X7 through X18, and Y7 through Y18 in the *Data* worksheet. • **50% exceedance:** Cell range C14 through C77 is linked to each entity's canal seepage data in cell ranges E7 through E18, F7 through F18, and G7 through G18 in the *Irr Rech - Canal Seepage Calc* worksheet. • **User-defined uncertainty range:** Cell range R14 through R77 is linked to each entity's canal seepage data in cell ranges N7 through N18, O7 through O18, and P7 through P18 in the *Irr Rech - Canal Seepage Calc* worksheet. • **50% exceedance:** Cell range E14 through E77 is linked to each entity's average monthly ET calculated in *Irr Rech ET_PPT_Statistics* worksheet. • **User-defined uncertainty range:** Cell range T14 through T77 is linked to each entity's average monthly ET calculated in *Irr Rech ET_PPT_Statistics* worksheet. • **50% exceedance:** Cell range F14 through F77 is linked to each entity's average monthly precipitation calculated in *Irr Rech ET_PPT_Statistics* worksheet.

Excel Worksheet Title	Function	Link to Other Worksheets
		• **User-defined uncertainty range:** Cell range U14 through U77 is linked to each entity's average monthly precipitation calculated in *Irr Rech ET_PPT_Statistics* worksheet.
Entity RFs	Database of monthly response functions for each irrigation entity and each managed recharge site.	• Cell range B14 through M41 is linked to response functions for each recharge site located in *Managed Recharge_RFs* worksheet cell range B8 through M240
Irr Rech DivsPredict_Data	Database of historic total irrigation entity diversions, January and April Snake (Heise) SWSI values, January and April Upper Snake Storage, January and April Big Wood SWSI values, the mean distribution of annual diversion across months (values sum to 1), and predictive model coefficients for January and April for each irrigation entity.	
Irr Rech ET_PPT_Statistics	Calculates median monthly ET and precipitation over water years 1980-2016.	Calculations use data in the ET and precipitation worksheets for each irrigation entity; that is, the data in the worksheets listed in the next six entries in this table.
Irr Rech Northside.ET	Database of monthly ET values for Northside Irrigation Entity	Data is used to calculate average monthly ET in the *Irr Rech ET_PPT_Statistics* worksheet
Irr Rech AFRD2.ET	Database of monthly ET values for AFRD2 Irrigation Entity	Data is used to calculate average monthly ET in the *Irr Rech ET_PPT_Statistics* worksheet
Irr Rech GoodingRichfield.ET	Database of monthly ET values for Gooding Richfield Irrigation Entity	Data is used to calculate average monthly ET in the *Irr Rech ET_PPT_Statistics* worksheet
Irr Rech Northside.PP	Database of monthly precipitation values for Northside Irrigation Entity	Data is used to calculate average monthly precipitation in the *Irr Rech ET_PPT_Statistics* worksheet
Irr Rech AFRD2.PP	Database of monthly precipitation values for AFRD2 Irrigation Entity	Data is used to calculate average monthly precipitation in the *Irr Rech ET_PPT_Statistics* worksheet
Irr Rech GoodingRichfield.PP	Database of monthly precipitation values for Gooding Richfield Irrigation Entity	Data is used to calculate average monthly precipitation in the *Irr Rech ET_PPT_Statistics* worksheet
Irr Rech - ObservedGains	Database of observed river reach gains from IDWR's "new" ESPAM2.2 method; also includes "raw modeled gains," using reach gains from irrigation recharge and starting heads, less average annual pumping. These data are used in the calibration calculator to generate a forecast year prediction (Nov - Oct, irrigation year XXXX). This prediction requires observed gains and raw modeled gains through October of the previous irrigation year (XXXX - 1).	

Excel Worksheet Title	Function	Link to Other Worksheets
Irr Rech - calib model - 50%	Calculates a forecasted reach gain for the 50% exceedance value from recharge associated with irrigation.	• Cell range C2 through C25 is linked to *Irr Rech Input and Output - 50%* worksheet cell range C5 through C28 • Cell range K2 through K13 is linked to *Irr Rech Input and Output - 50%* worksheet cell range D5 through D16
Irr Rech - Daily interp - 50%	Generates daily Snake River reach gains between Kimberly and King Hill using the forecasted monthly Kimberly and King Hill reach gains for the 50% exceedance value.	• Cell range B2 through B16 is linked to *Irr Rech - calib model - 50%* worksheet cell range K11 through K25 • Cell range D2 through D16 is linked to *Irr Rech - calib model - 50%* worksheet cell range D2 through D16
Irr Rech Input and Output - 50%	50% Exceedance: This worksheet has the Snake River reach gains between Kimberly and King Hill for the forecast year and the prior year, along with the observed Snake River reach gains between Kimberly and King Hill for the year prior to the forecast year.	Data in this sheet is used in the calibration model (*Irr Rech - calib model - 50%)*
Irr Rech - Predict_Calcs	Calculates a forecast of monthly irrigation diversions for each irrigation entity for the 50% exceedance and the user-defined uncertainty range using predictor variables (Big Wood SWSI, Snake (Heise) SWSI, and Upper Snake Reservoir Storage.	Cell range B5 through B8 is linked to *User worksheet cells I5, J5, K5, and G4*
Managed Recharge_RFs	Calculates a spatially averaged, monthly response function for each managed recharge site.	
Convolution	Calculates monthly Snake River reach gains between Kimberly and King Hill associated with on-farm irrigation recharge, canal seepage, managed recharge, and pumping. Generates these gains for the 50% exceedance value and the user-defined uncertainty range value.	• **50% Exceedance:** Cell range B6 through B53 is linked to *Irr Rech - On-Farm Rech Calc* worksheet cells M14 through M25 (Northside on-farm recharge), M40 through M51 (AFRD 2 on-farm recharge), and M66 through M77 (Gooding Richfield on-farm recharge). • **User-defined uncertainty range:** Cell range S6 through S53 is linked to *Irr Rech - On-Farm Rech Calc* worksheet cells AB14 through AB25 (Northside on-farm recharge), AB40 through AB51 (AFRD 2 on-farm recharge), and AB66 through AB77 (Gooding Richfield on-farm recharge). • **50% Exceedance:** Cell range B60 through B107 is linked to *Irr Rech - Canal Seepage Calc* worksheet cells E7 through E18 (Northside canal recharge), F7 through F18 (AFRD 2 canal recharge), and G7 through G18 (Gooding Richfield canal recharge). • **User-defined uncertainty range:** Cell range B60 through B107 is linked to *Irr Rech - Canal Seepage Calc* worksheet cells N7 through N18 (Northside canal recharge), O7 through O18

Excel Worksheet Title	Function	Link to Other Worksheets
		(AFRD 2 canal recharge), and P7 through P18 (Gooding Richfield canal recharge). • Cell range B114 through B218 is linked to *Data* worksheet cells B59 through B70 (SW Irrigation District managed recharge), C59 through C70 (Milner Gooding Main Canal managed recharge), D59 through D70 (Shoshone Site managed recharge), E59 through E70 (Milepost 31 Site managed recharge), F59 through F70 (Northside Main Canal including Wilson Lake managed recharge), G59 through G70 (Twin Falls Canal Co. - Murtaugh Canal managed recharge). • Cell range B225 through B290 is linked to *Data* worksheet cells B41 through B52 (IEGW501 Pumping), C41 through C52 (IEGW507 Pumping), D41 through D52 (IEGW508 Pumping), E41 through E52 (IEGW509 Pumping). • Cell range B97 through B308 is linked to *Data* worksheet cells H59 through H70 (Big Wood Canal Co. – Richfield managed recharge).
Data	Worksheet contains the data used to generate monthly Snake River reach gains between Kimberly and King Hill associated with on-farm irrigation recharge, canal seepage, managed recharge, and pumping. The worksheet also sums the monthly Snake River reach gains between Kimberly and King Hill associated with on-farm irrigation recharge, canal seepage, managed recharge, and pumping.	• **50% Exceedance:** Cell range B7 through D18 is linked to *Irr Rech - Predict_Calcs* worksheet cells B12 through M14 (forecasted monthly diversions for each irrigation entity). • **User-defined uncertainty range:** Cell range W7 through Y18 is linked to *Irr Rech - Predict_Calcs* worksheet cells B17 through M19 (forecasted monthly diversions for each irrigation entity). • **50% Exceedance:** Cell range B25 through B36 is linked to *Irr Rech - Canal Seepage Calc* worksheet cells E7 through E18 (Northside Canal seepage); cell range D25 through D36 is linked to *Irr Rech - Canal Seepage Calc* worksheet cells F7 through F18 (AFRD2 Canal seepage); cell range F25 through F36 is linked to *Irr Rech - Canal Seepage Calc* worksheet cells G7 through G18 (Gooding Richfield Canal seepage). • **User-defined uncertainty range:** Cell range W25 through W36 is linked to *Irr Rech - Canal Seepage Calc* worksheet cells N7 through N18 (Northside Canal seepage); cell range Y25 through Y36 is linked to *Irr Rech - Canal Seepage Calc* worksheet cells O7 through O18 (AFRD2 Canal seepage); cell range AA25 through AA36 is linked to *Irr Rech - Canal Seepage Calc* worksheet cells P7 through P18 (Gooding Richfield Canal seepage).

Excel Worksheet Title	Function	Link to Other Worksheets
		• **50% Exceedance:** Cell range C25 through C36 is linked to *Irr Rech - On-Farm Rech Calc* worksheet cells M14 through M25 (Northside on-farm recharge); cell range E25 through E36 is linked to *Irr Rech - On-Farm Rech Calc* worksheet cells M40 through M51 (AFRD2 on-farm recharge); cell range G25 through G36 is linked to *Irr Rech - On-Farm Rech Calc* worksheet cells M66 through M77 (Gooding Richfield on-farm recharge). • **User-defined uncertainty range:** Cell range X25 through X36 is linked to *Irr Rech - On-Farm Rech Calc* worksheet cells AB14 through AB25 (Northside on-farm recharge); cell range Z25 through Z36 is linked to *Irr Rech - On-Farm Rech Calc* worksheet cells AB40 through AB51 (AFRD2 on-farm recharge); cell range AB25 through AB36 is linked to *Irr Rech - On-Farm Rech Calc* worksheet cells AB66 through AB77 (Gooding Richfield on-farm recharge). • Cell range L41 through O52 is linked to *Convolution* worksheet cell range O255 through O290. • Cell range B59 through J70 is linked to *User* worksheet cell range B9 through J20. • **50% Exceedance:** Cell range B77 through N88 is linked to *Convolution* worksheet cell range O61 through O308. • **User-defined uncertainty range:** Cell range W77 through AB88 is linked to *Convolution* worksheet cell range AF60 through AF53.

8.References

Allen, R.G.; M. Tasumi; R. Trezza. 2007a. "Satellite-Based Energy Balance for Mapping Evapotranspiration with Internalized Calibration (METRIC)—Model." *Journal of Irrigation and Drainage Engineering* 133, no. 4: 380-395. doi.org/10.1061/(ASCE)0733-9437(2007)133:4(380).

Allen, R.G., M. Tasumi; A. Morse, R. Trezza, J.L. Wright, W. Bastiaanssen, W. Kramber, I. Lorite, C.W. Robison. 2007b. "Satellite-Based Energy Balance for Mapping Evapotranspiration with Internalized Calibration (METRIC)—Application." *Journal of Irrigation and Drainage Engineering* 133, no. 4: 395-406. doi.org/10.1061/(ASCE)0733-9437(2007)133:4(395).

Anderson, D.R. 2008. Model Based Inference in the Life Sciences: A Primer on Evidence. Springer, New York.

Backus, J. W.; H. Stern, I. Ziller, R. A. Hughes, R. Nutt, R. J. Beeber, S. Best, R. Goldberg, L. M. Haibt, H. L. Herrick, R. A. Nelson, D. Sayre, P. B. Sheridan. 1957. "The FORTRAN Automatic Coding System". Western joint computer conference: Techniques for reliability. Los Angeles, California: Institute of Radio Engineers, American Institute of Electrical Engineers, ACM: 188–198. doi:10.1145/1455567.1455599

Boggs, K.G., R.W. Van Kirk, G.S. Johnson, J.P. Fairley, and P.S. Porter. 2010. Analytical solutions to the linearized Boussinesq equation for assessing the effects of recharge on aquifer discharge. *Journal of the American Water Resources Association* 46, no. 6: 1116 – 1132. DOI:10.1111/j.1752-1688.2010.00479.x

Burnham, K.P., and D.R. Anderson. 2002. Model Selection and Multimodel Inference: A Practical Information-Theoretic Approach, 2nd ed. Springer, New York.

Claeskens, G., and H.L. Hjort. 2008. Model Selection and Model Averaging. Cambridge University Press, Cambridge.

Cosgrove, D.M., and G.S. Johnson. 2004. Transient response functions for conjunctive water management in the Snake River Plain, Idaho. *Journal of the American Water Resources Association* 40, no. 6: 1469 – 1482.

Crawley, M.J. 2007. The R Book. Wiley, West Sussex, UK.

Doherty, J., 1995. PEST Utilities for MODFLOW and MT3D Parameter Estimation. Watermark Computing.

Efron, B. 1982. The Jacknife, the Bootstrap, and Other Resampling Plans. Society for Industrial and Applied Mathematics, Philadelphia, PA.

Fredericks, J.W., and J.W. Labadie. 1995. Decision support system for conjunctive stream-aquifer management. Colorado Water Resources Research Institute Open File Report No. 10. Ft. Collins, Colorado: Colorado State University, 124.

Helsel, D.R., and R.M. Hirsch. 1992. Statistical Methods in Water Resources. Studies in Environmental Science Vol. 49. Elsevier, Amsterdam.

Hoekema, D.J., V. Sridhar (2013). "A System Dynamics Model for Conjunctive Management of Water Resources in the Snake River Basin." *Journal of the American Water Resources Association* 49, no. 6: 1327-1350.

Idaho Department of Water Resources. 2013. Enhanced Snake Plain Aquifer Model Version 2.1. Final Report. January.

Maddock, T. III. 1972. Algebraic technological functions from a simulation model. *Water Resources Research* 8, no. 1: 129 – 134.

Maddock, T. III, and L.J. Lacher. 1991. MODRSP: A program to calculate drawdown, velocity, storage, and capture response functions for multi-aquifer systems. Department of Hydrology and Water Resources, University of Arizona, Tucson, Arizona, HWR 91-020.

Morel-Seytoux, H.J., and C.J. Daly. 1975. A discrete Kernel generator for stream-aquifer studies. *Water Resources Research* 11, no. 2: 253 – 260.

Nash, J.E., and J.V. Sutcliffe. 1970. River flow forecasting through conceptual models: Part I—A discussion of principles. *Journal of Hydrology*, 10(3): 282–290.

Pawitan, Y. 2001. In All Likelihood: Statistical Modelling and Inference Using Likelihood. Clarendon Press, Oxford.

Peters TR (2017). Irrigation Scheduler Mobile: Documentation and User Manual. http://weather.wsu.edu/is/ISMManualOptimized.pdf.

R Core Team. 2014. R: A language and environment for statistical computing. R Foundation for Statistical Computing, Vienna, Austria. URL http://www.R-project.org/.

Shumway, R.H., and D.S. Stoffer. 2011. Time Series Analysis and Its Applications, With R Examples, 3rd ed. Springer, New York.

Whitney, R. 2017. *Water District 02 (Milner to Murphy) 2016 Annual Report*. February 21, 2017. https://idwr.idaho.gov/files/districts/WD02-20170221-2016-Annual-Report.pdf

Wood, M.S., M.L. Williams, D.M. Evetts, and P.J. Vidmar (2014). *Evaluation of seepage and discharge uncertainty in the middle Snake River, southwestern Idaho:* U.S. Geological Survey Scientific Investigations Report 2014–5091, 34 p., *http://dx.doi.org/10.3133/sir20145091*.

Appendix A. Head Response Function Validity

Head Response Functions – Hypothetical Model Demonstration

A transient Modflow model of a hypothetical system is used to provide a simple demonstration of head response functions. The model consists of a 10x10 model grid with river boundaries along rows 1 and 10 (Figure A-1). The entire domain is represented as homogeneous and isotropic. River head is constant at 90 feet along the row 1 boundary, and at 0 feet along the row 10 (lower) boundary. In the unperturbed state, the initial aquifer heads are in a steady state condition between the two head dependent boundaries. The model grid is 5280 feet on each side of a cell, and aquifer properties are set to a transmissivity of 50,000 ft^2/day, storativity of 0.15, and river conductance of 68,000 ft^2/day.

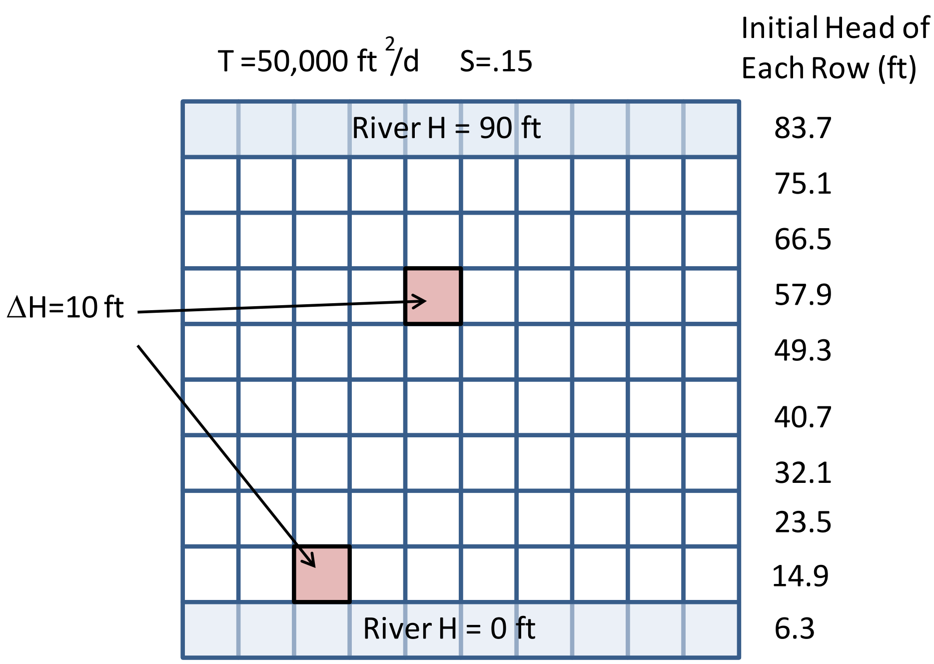

Figure A-1. Simulation conditions of the hypothetical model used to demonstrate the validity of using head response functions

We used the four simulations of the hypothetical model to evaluate validity of head response functions:

1. A steady state background simulation with head gradient and aquifer flow between the two bounding rivers on opposing sides of the grid. Gains on the lower river represent conditions of no perturbations in initial head.

2. The same conditions as simulation 1 except an additional 10 feet of head are imposed on the cell at row 4, column 5 in the initial conditions.
3. The same conditions as simulation 1 except an additional 10 feet of head are imposed on the cell at row 9, column 3 relative to the initial conditions.
4. The conditions of simulation 1 except 10 feet of additional head are imposed on both cells specified in for simulations 2 and 3.

The effects of the head perturbations were determined by subtracting river gains on the lower elevation river in Simulation 1 from calculated gains in Simulations 2, 3, and 4. The additive property of superposition is demonstrated by showing that the differences from simulations 2-1 and 3-1 can be summed to produce the differences determined from simulation 4-1 (**Figure A-2**). The additive property of superposition is apparent from the nearly identical river gains determined by summing the effects of individual initial head perturbations (green line on **Figure A-2**) and the gains determined by simulation of the combined perturbation (black markers on **Figure A-2**). It is this linearity of results that is an essential requirement for application of response functions.

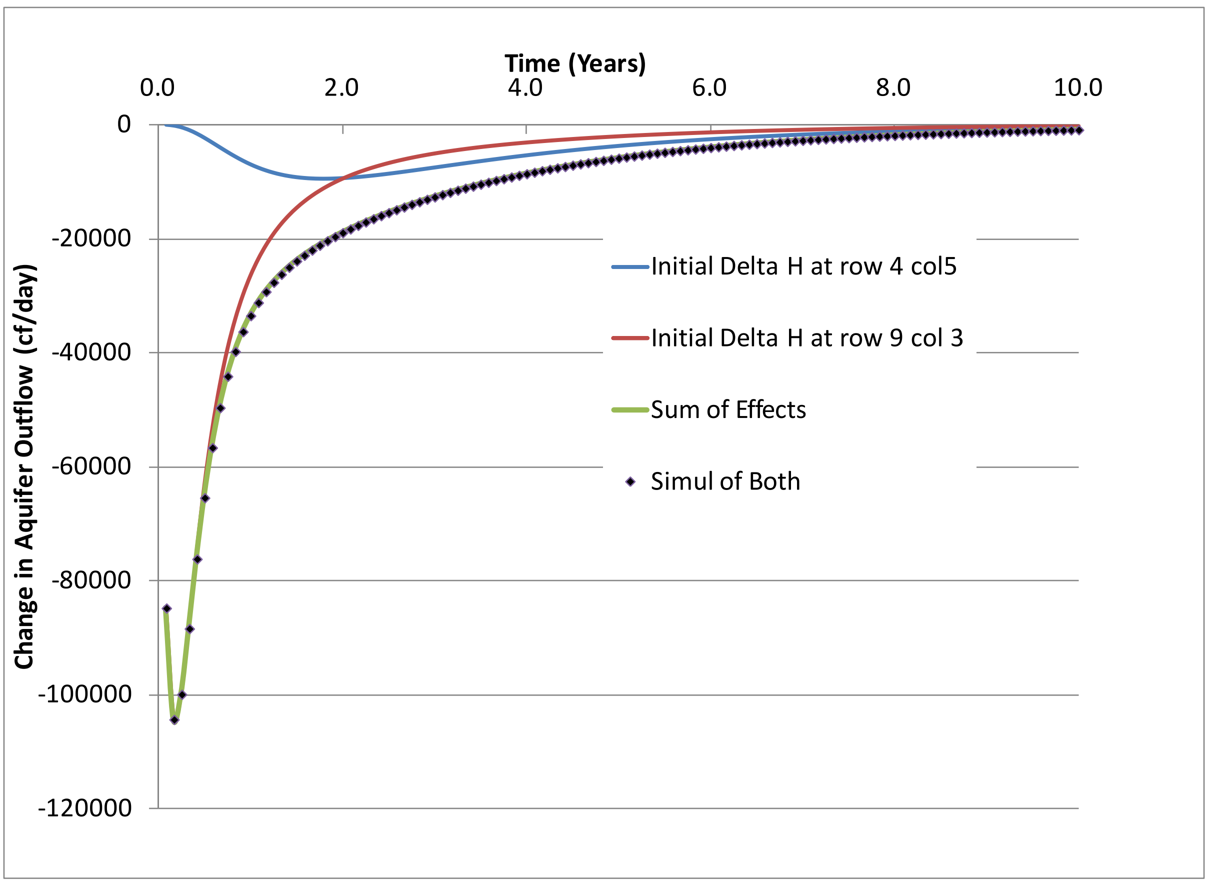

Figure A-2. Comparison of lower river gains from hypothetical model simulations with initial head perturbations

The red and blue lines show the change in river gains from initial head perturbation in individual cells. The green line presents the sum of effects from the red and blue lines. The black markers show the change in gains from simultaneous simulation of both perturbations.

Head Response Functions – ESPAM 2.1 Demonstration

We used the ESPAM 2.1 model to demonstrate how initial head response functions may be applied to the Snake River Plain aquifer model in a forecasting application. This approach is needed to provide an estimate of the effects of November or April aquifer water levels on future Snake River gains. This demonstration compares the effect of changes in initial aquifer head on Snake River gains in the Kimberly to King Hill reach from two approaches. In the demonstration, January is used for initial heads, however, response functions are not affected by the period in which they are developed or employed. We used two methods to demonstrate the validity of using head response functions using ESPAM 2.1:

1. Method 1. Differencing the river gains from two simulations:
    a. Recession of river gains from initial heads established as the 1992-2008 average January heads (determined from the ESPAM 2.1 model calibration simulation) with no recharge from head independent sources.
    b. Recession of river gains from the conditions of the simulation specified in step a) but with 1 foot of head added to the initial head of all model cells.
2. Method 2. Summing unit initial head response functions (response to one foot of added initial head) for each model cell. We developed response functions by simulating a horizontal initial head surface with a head perturbation at a single cell, repeating that simulation for each active cell in the model grid. The horizontal initial head simulation represents an equivalent of all physical conditions of the original model, except there is no recharge or discharge. Head at all head dependent model features (excluding the perturbation) is set equal to the initial aquifer head.

If gains from Method 1 above compare well with that obtained by summing all unit initial head response functions in Method 2, the initial head response function application may be considered verified. Changes in river gains determined from the response function approach must be added to the average discharge recession used in step 1a above to estimate the recession in any specific year. In this case, the head perturbations must be determined from interpolation of measured well water levels (differences from average or another reference period).

Base recession curve (no initial head perturbation) determination

The theoretical gains in the Kimberly to King Hill reach of the Snake River resulting from an average January aquifer head distribution were determined by 1) identifying the average January head distribution, and 2) by performing a simulation with that initial head distribution and no head-independent recharge or discharge (no well package in the ESPAM 2.1 model). The recession curve is theoretical in that it ignores real-system non-linearities that may come into play as aquifer head falls dramatically. This, however, is not a concern since effects of other aquifer recharge elements included in the forecast will maintain aquifer water levels in a range where linear relationships prevail.

The average January aquifer head distribution was determined from simulation of the ESPAM 2.1 calibration data set and recording and averaging head at every model cell for each January in the 1992 to 2008 period. Average heads were determined by a FORTRAN (Backus et al. 1957) program written specifically to read the Modflow output binary head file and average January head in each cell. This head array was then used as a starting head distribution for recession simulations.

The river gain recession includes Snake River gains determined from both the drain (springs) and general head boundary (baseflow in the Snake River) packages in Modflow. These discharges were determined by application of the utility program bud2smp (Doherty 1995) to the binary budget file output from Modflow. A one-year simulation of ESPAM 2.1 with a single stress period and 24 timesteps was executed with no head-independent recharge and discharge (.wel package). The average January head values described above served as the starting heads for the simulation. The simulated recession of Kimberly to King Hill river gains from average January starting heads is shown in Figure A-3.

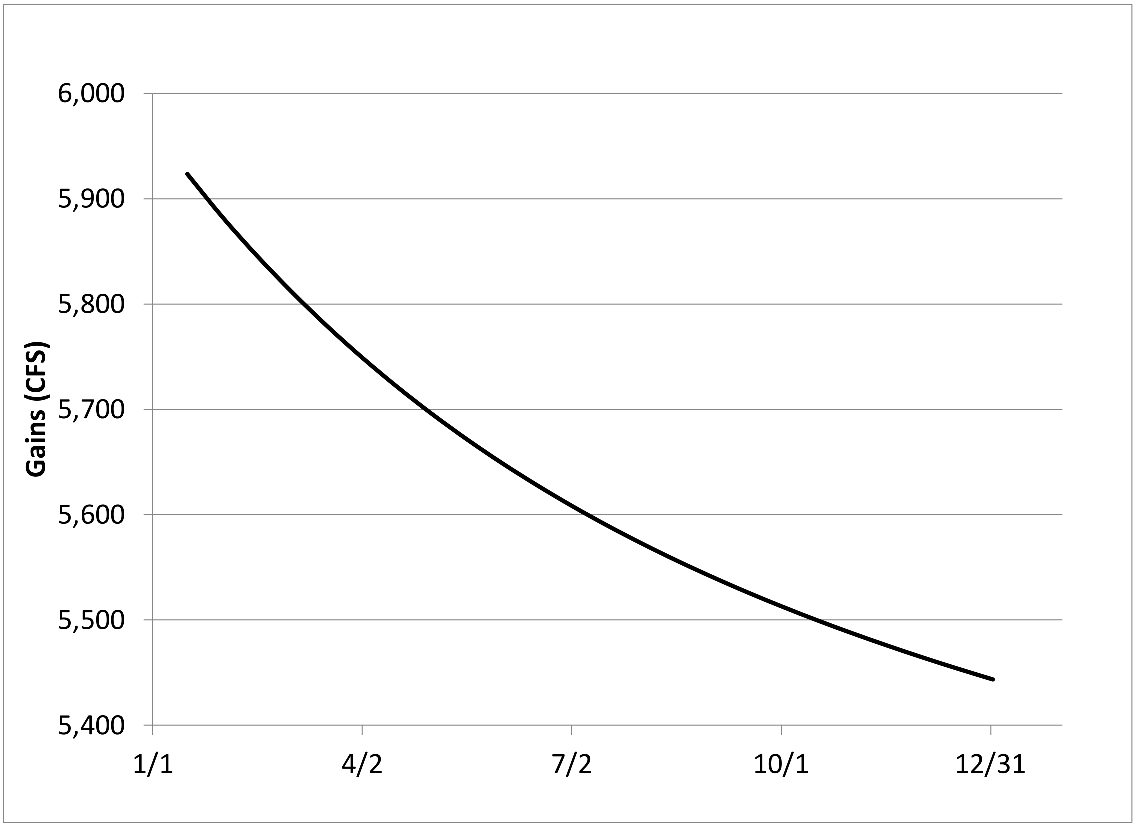

Figure A-3. Simulated Kimberly to King Hill river gain recession from average January starting heads

Perturbed recession curve determination

The starting heads for the perturbed head simulations were created by adding one foot of head to the starting head of each cell from the base simulation (1992 through 2008 average heads). The simulation was then performed in a manner parallel to that described above for the base recession simulation. The river gain results of the perturbed head simulation, along with those of the base simulation are presented in **Figure A-4**. As expected, the higher aquifer heads of the perturbed simulation resulted in greater river gains throughout the one-year simulation period.

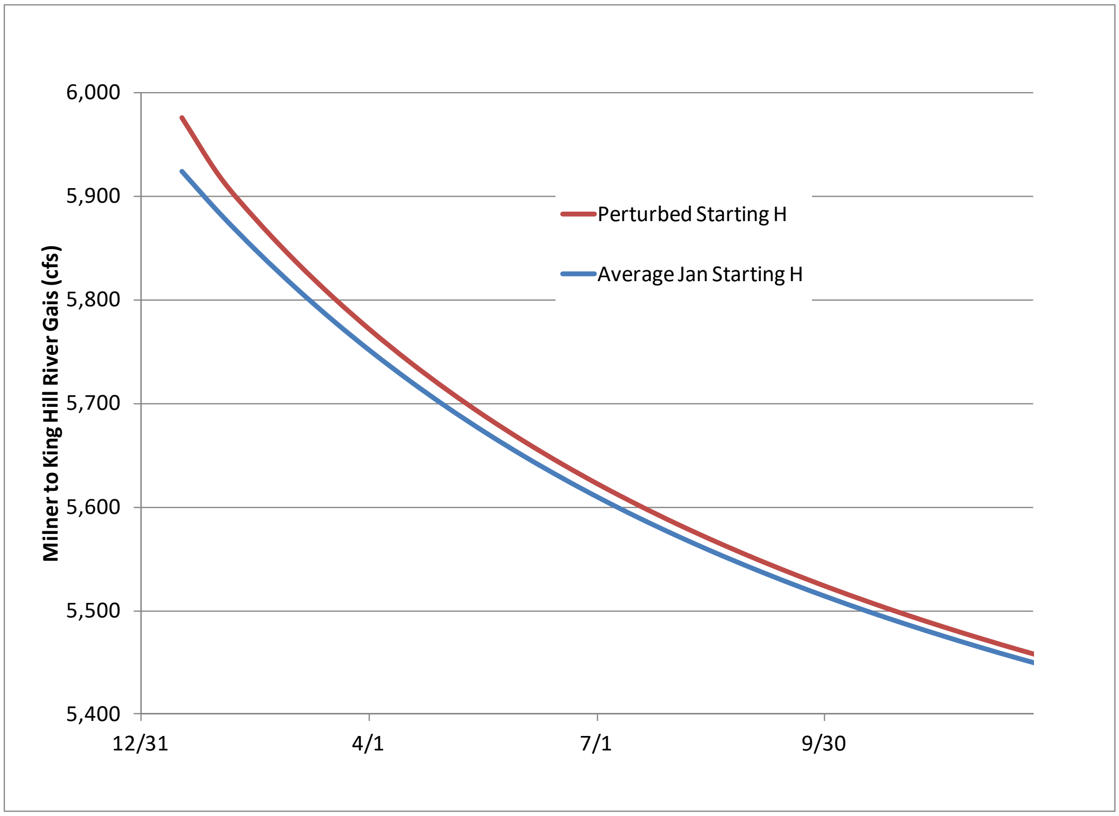

Figure A-4. Simulated river gain recession from both the average January and perturbed starting heads
The perturbed starting heads were elevated one foot at all model cells relative to the average January heads.

Comparison of River Gains Estimated by the Two Methods

The validity of initial head response functions is demonstrated by comparison of the sum of response functions from all cells to gains determined as the difference between base and perturbed head simulations. Both provide estimates of river gains resulting from an aquifer-wide initial head change of one foot. The difference in river gains between simulations with an initial head equal to the average January head and a simulation with an initial head surface elevated by one foot does not impose any superposition assumptions. The sum of response functions for that same added one-foot increment in initial head, however, does require validity of superposition. Response functions determined under conditions of no background gradient produce the same effect on river gains as simulation of a one-foot uniform change in initial head under typical hydraulic gradient (Figure A-5).

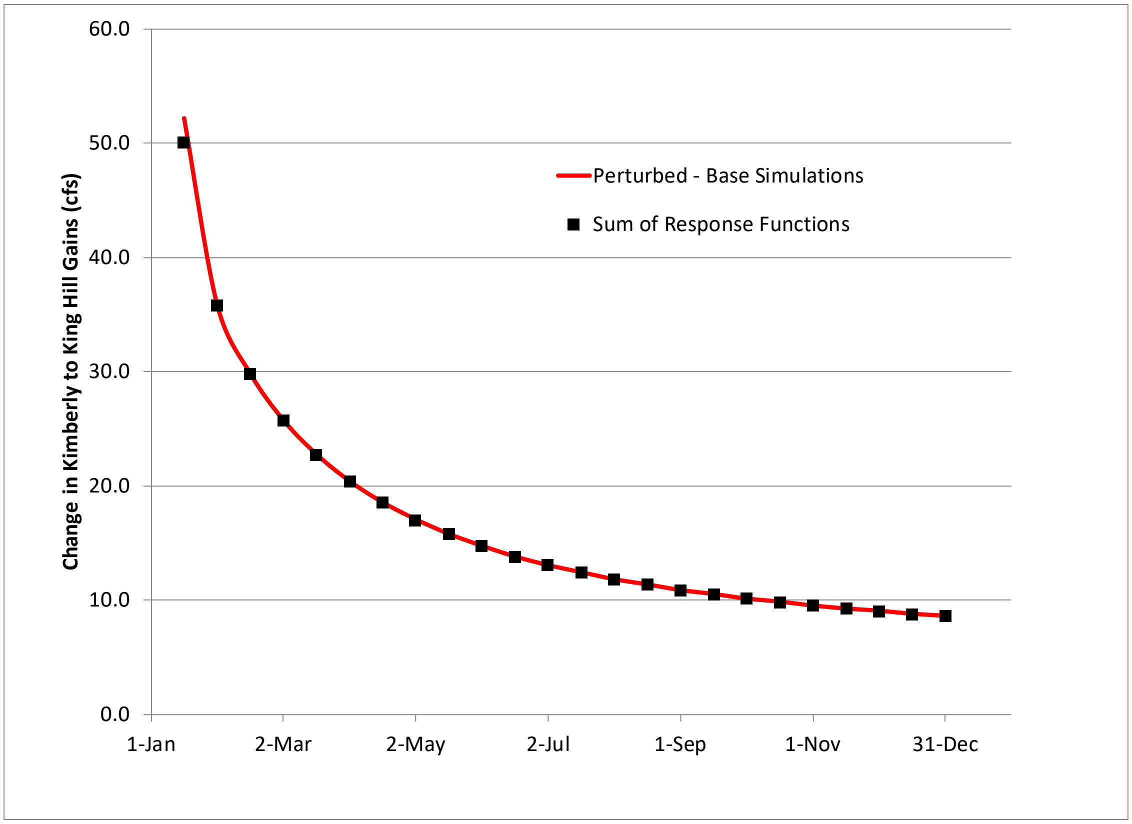

Figure A-5. Comparison of the sum of response functions to differences between simulation results from an average January initial head and a simulation with a one foot uniformly higher initial head

Conclusions on the Validity of Initial Head Response Functions

The use of initial head response functions is a valid and viable approach to estimating the component of future river gains in the Snake River Plain from earlier aquifer water level observations. It provides a means of understanding and estimating the relationship between aquifer water levels in any month and subsequent river gains. This will be best implemented by differencing measured aquifer water levels in a specific month (November or April for this project) from either a chosen year reference (2008 in this project) or multi-year average. The differences between the reference and observed head values are then interpolated to all effective cells in the model grid and multiplied by the initial head response functions. This process will develop an estimate of the change in river gains relative to the reference condition. To determine total gains from initial head conditions it is necessary to add the estimated change in gains to the reference condition gains (see Figure A-1).

Appendix B. Forecast Tool Inputs

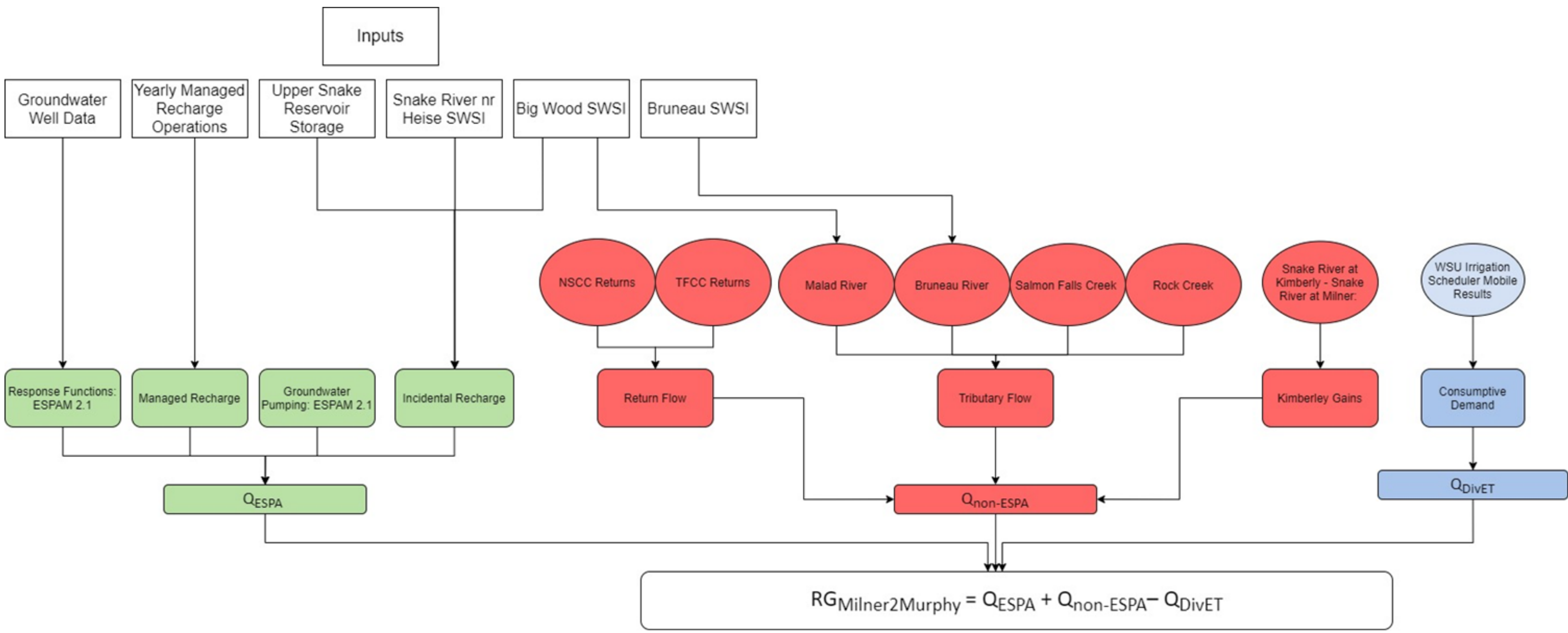

	Type of Data	Input	Date Range	Statistic	Notes
Q_{ESPA}	Starting Head Component	Response Functions			ESPAM 2.1
		Groundwater Water Level Data	Preceding Fall or Spring synoptic		
	Managed Recharge		Current year recharge operations	Actual/ Forecasted values	
	Incidental Recharge	SWSI: (Big Wood & Snake nr Heise) & Reservoir Storage	1981 to 2014	Correlation to SWSI value	Correlation built with ESPAM 2.1
	Groundwater Pumping	ESPAM 2.1	2001 to 2010	Average	
$Q_{non\text{-}ESPA}$	Tributary Flow	Salmon Falls Creek	1986 to Present	Median	
		Rock Creek	1993 to Present	Median	
		Bruneau River	1986 to Present	Analog SWSI	
		Malad River	1987 to Present	Analog SWSI	
	Return Flow	Northside Returns	2002 - Present	Median	
		Southside Returns	2002 - Present	Median	
	Kimberley Reach Gains	Snake River at Kimberly	1993 to 2016	Median	Smoothed with a 5 day moving average (centered)
Q_{DivET}	WSU Irrigation Scheduler Mobile Results		2010 - 2014	Median	

Appendix C. Hindcast Validation

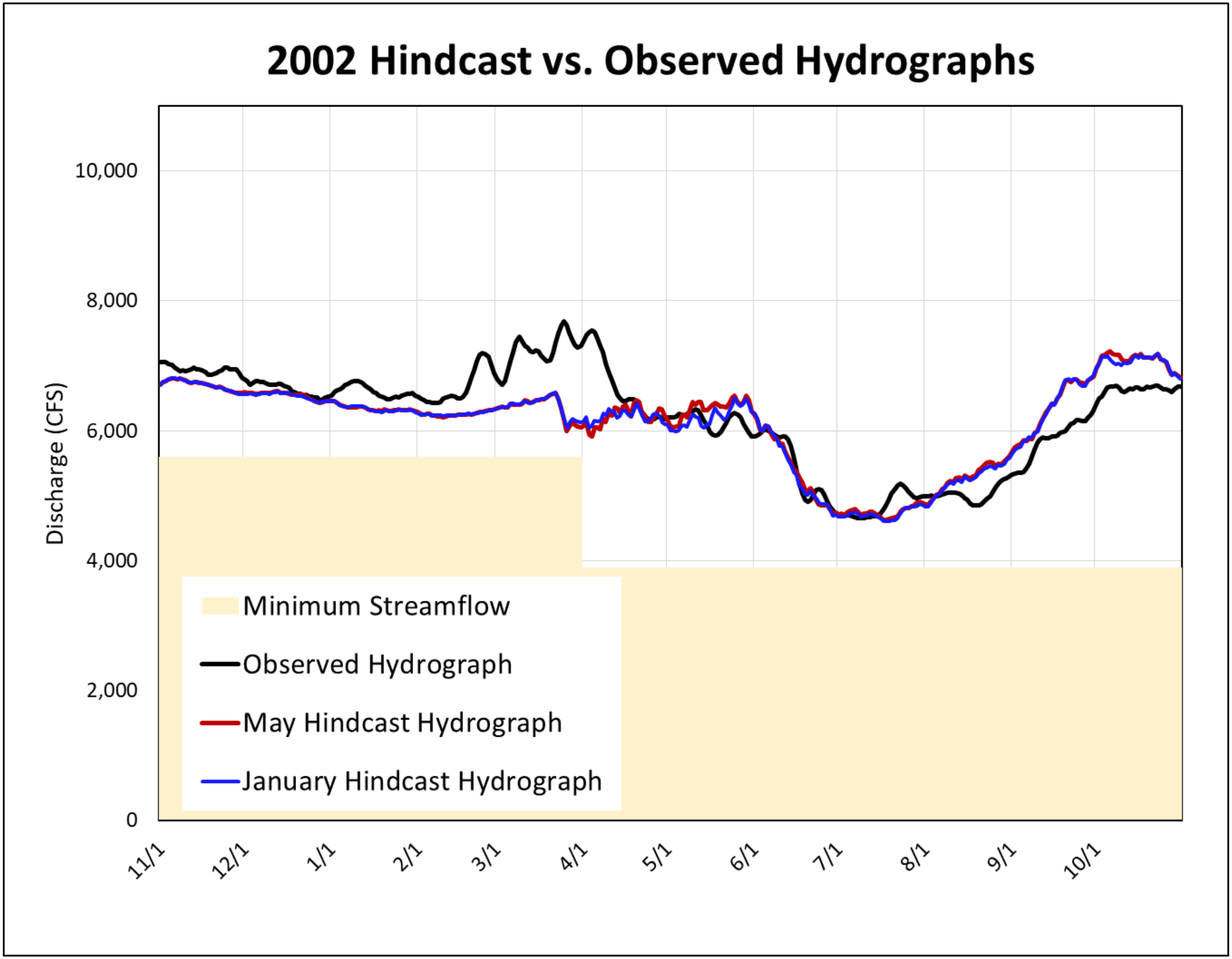
2002 Hindcast vs. Observed Hydrographs
10,000
8,000
6,000
4,000
2,000
0
Discharge (CFS)
11/1
12/1
1/1
2/1
3/1
4/1
5/1
6/1
7/1
8/1
9/1
10/1
Minimum Streamflow
Observed Hydrograph
May Hindcast Hydrograph
January Hindcast Hydrograph

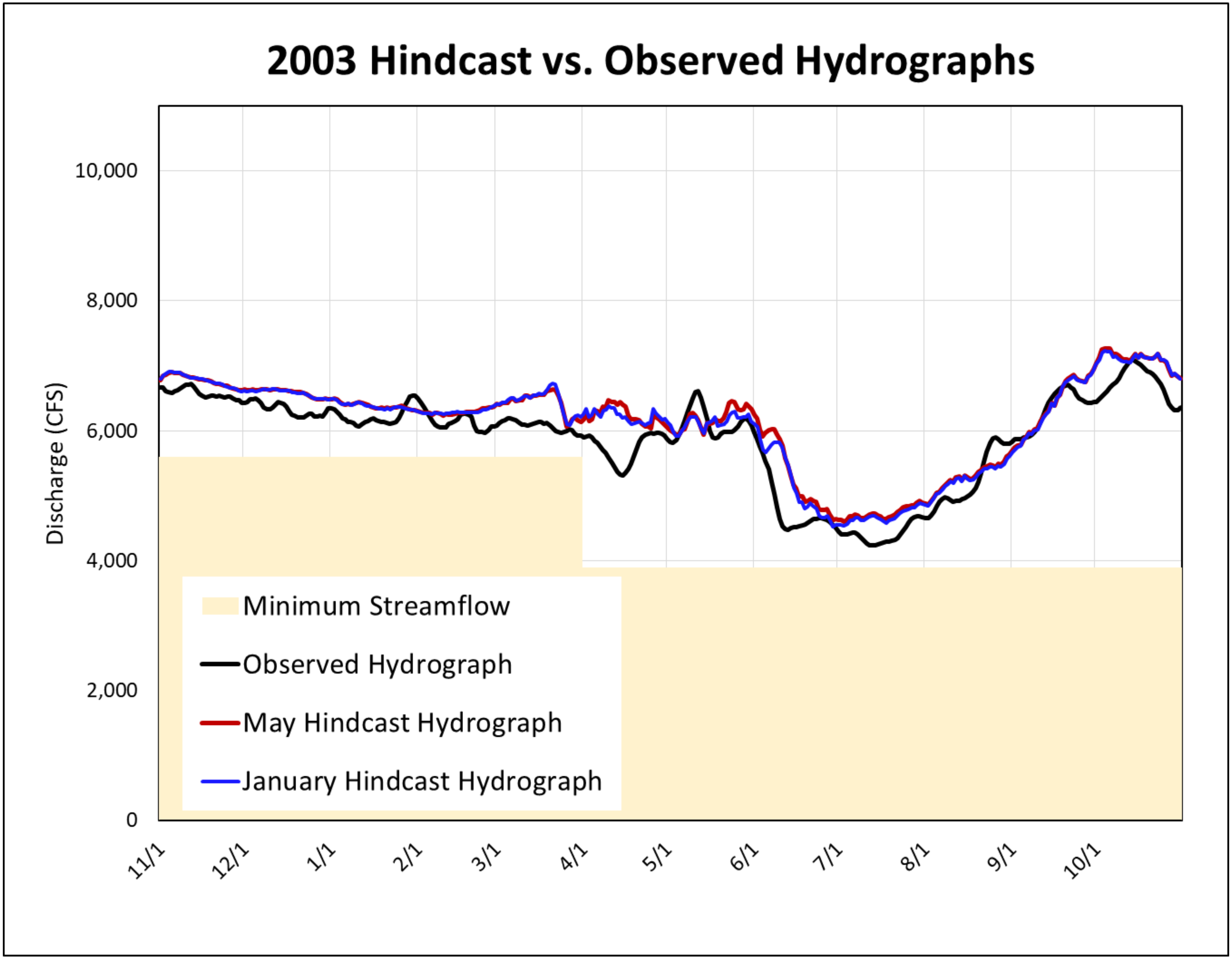
2003 Hindcast vs. Observed Hydrographs
Discharge (CFS)
10,000
8,000
6,000
4,000
2,000
0
11/1
12/1
1/1
2/1
3/1
4/1
5/1
6/1
7/1
8/1
9/1
10/1
Minimum Streamflow
Observed Hydrograph
May Hindcast Hydrograph
January Hindcast Hydrograph

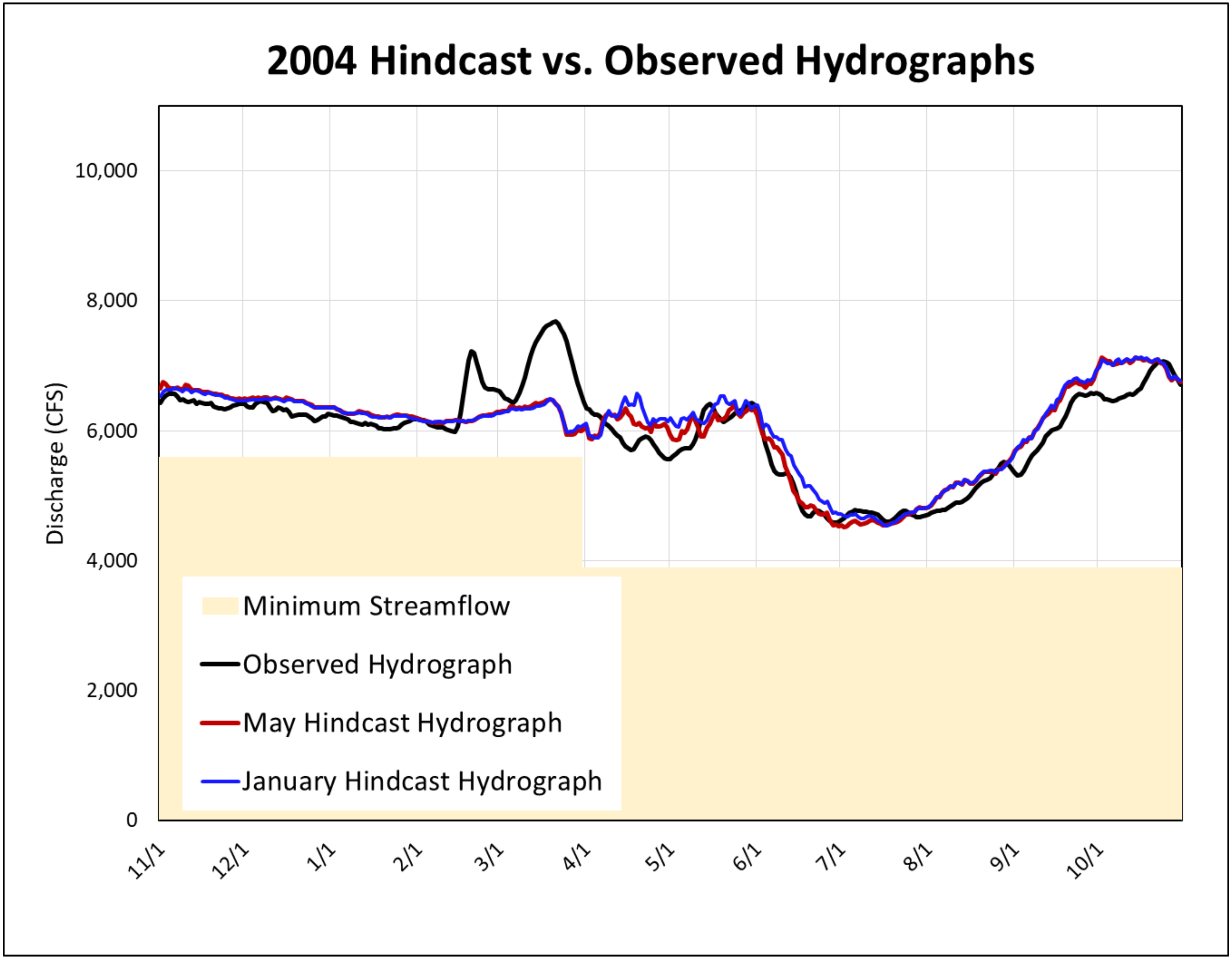
2004 Hindcast vs. Observed Hydrographs
10,000
8,000
6,000
4,000
2,000
0
Discharge (CFS)
11/1
12/1
1/1
2/1
3/1
4/1
5/1
6/1
7/1
8/1
9/1
10/1
Minimum Streamflow
Observed Hydrograph
May Hindcast Hydrograph
January Hindcast Hydrograph

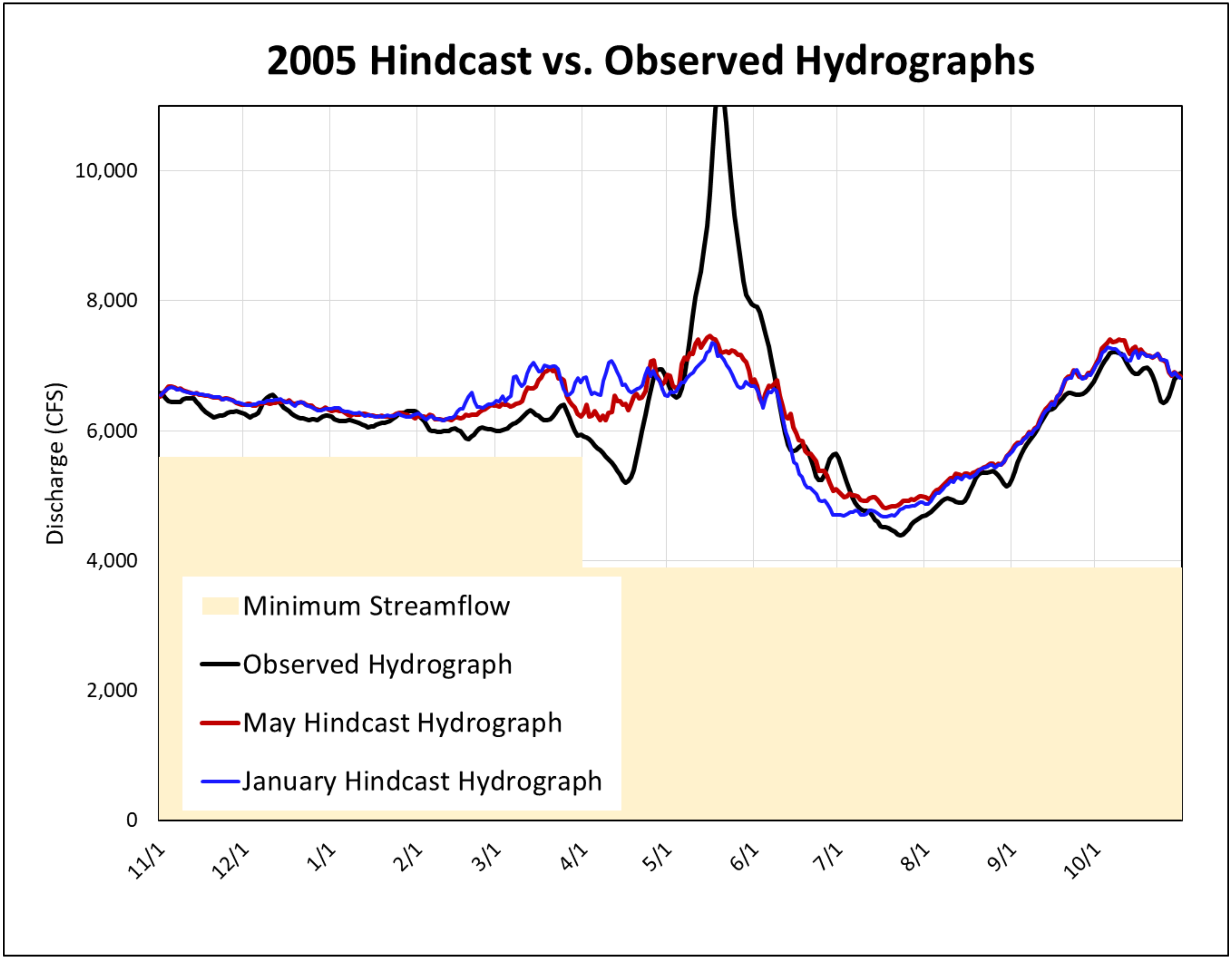

2005 Hindcast vs. Observed Hydrographs
Discharge (CFS)
10,000
8,000
6,000
4,000
2,000
0
11/1
12/1
1/1
2/1
3/1
4/1
5/1
6/1
7/1
8/1
9/1
10/1
Minimum Streamflow
Observed Hydrograph
May Hindcast Hydrograph
January Hindcast Hydrograph

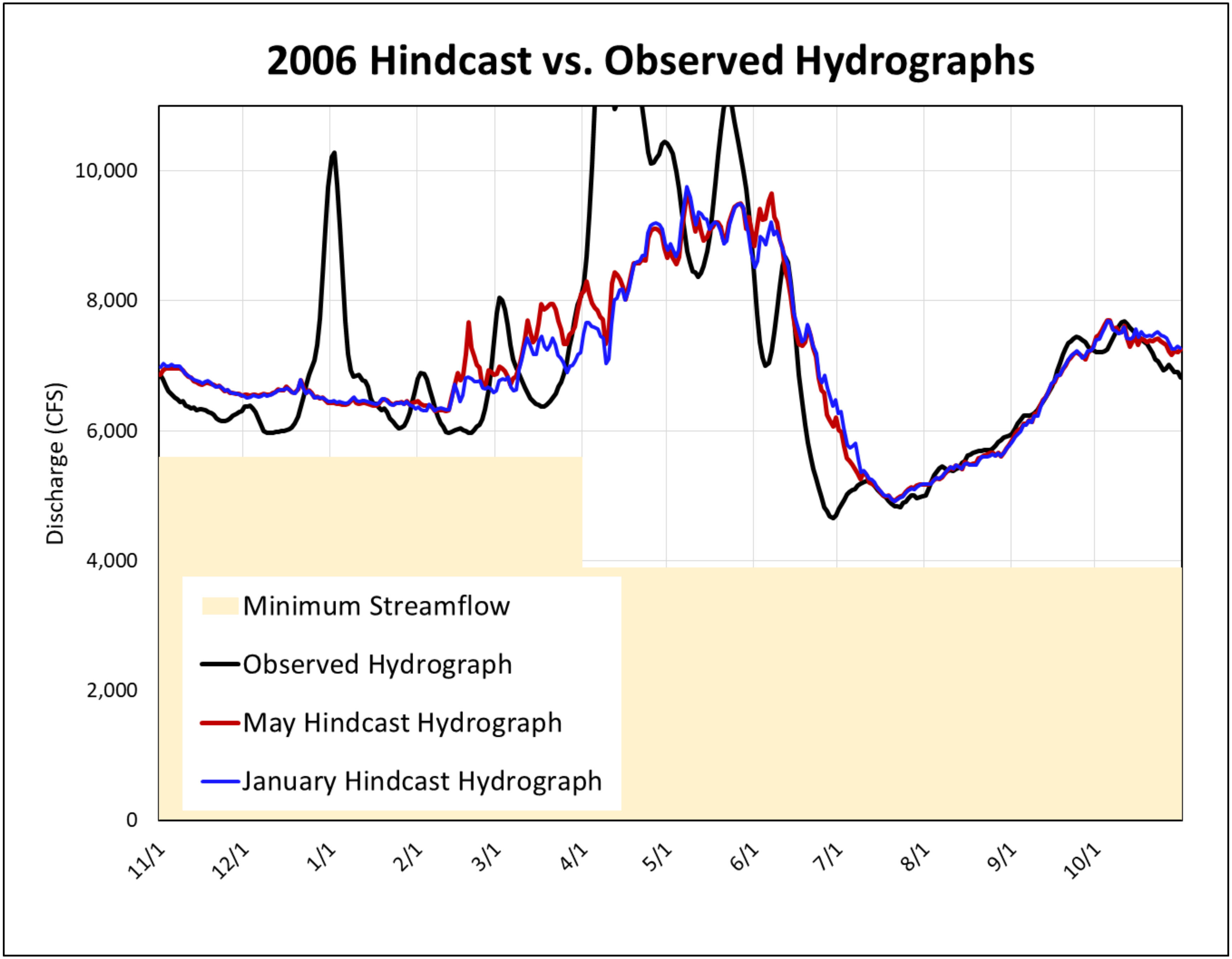

2006 Hindcast vs. Observed Hydrographs
Discharge (CFS)
10,000
8,000
6,000
4,000
2,000
0
11/1
12/1
1/1
2/1
3/1
4/1
5/1
6/1
7/1
8/1
9/1
10/1
Minimum Streamflow
Observed Hydrograph
May Hindcast Hydrograph
January Hindcast Hydrograph

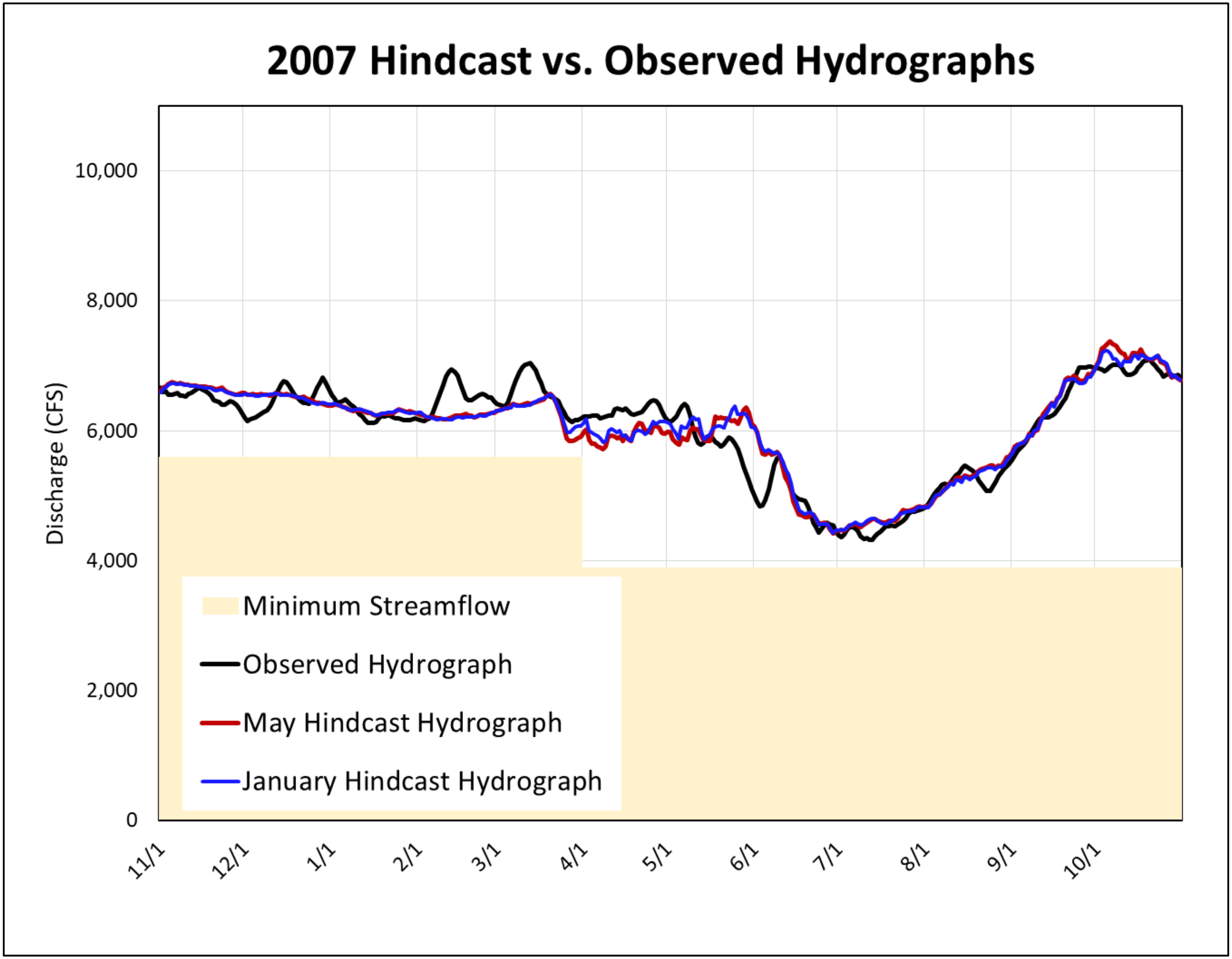
2007 Hindcast vs. Observed Hydrographs
Discharge (CFS)
10,000
8,000
6,000
4,000
2,000
0
11/1
12/1
1/1
2/1
3/1
4/1
5/1
6/1
7/1
8/1
9/1
10/1
Minimum Streamflow
Observed Hydrograph
May Hindcast Hydrograph
January Hindcast Hydrograph

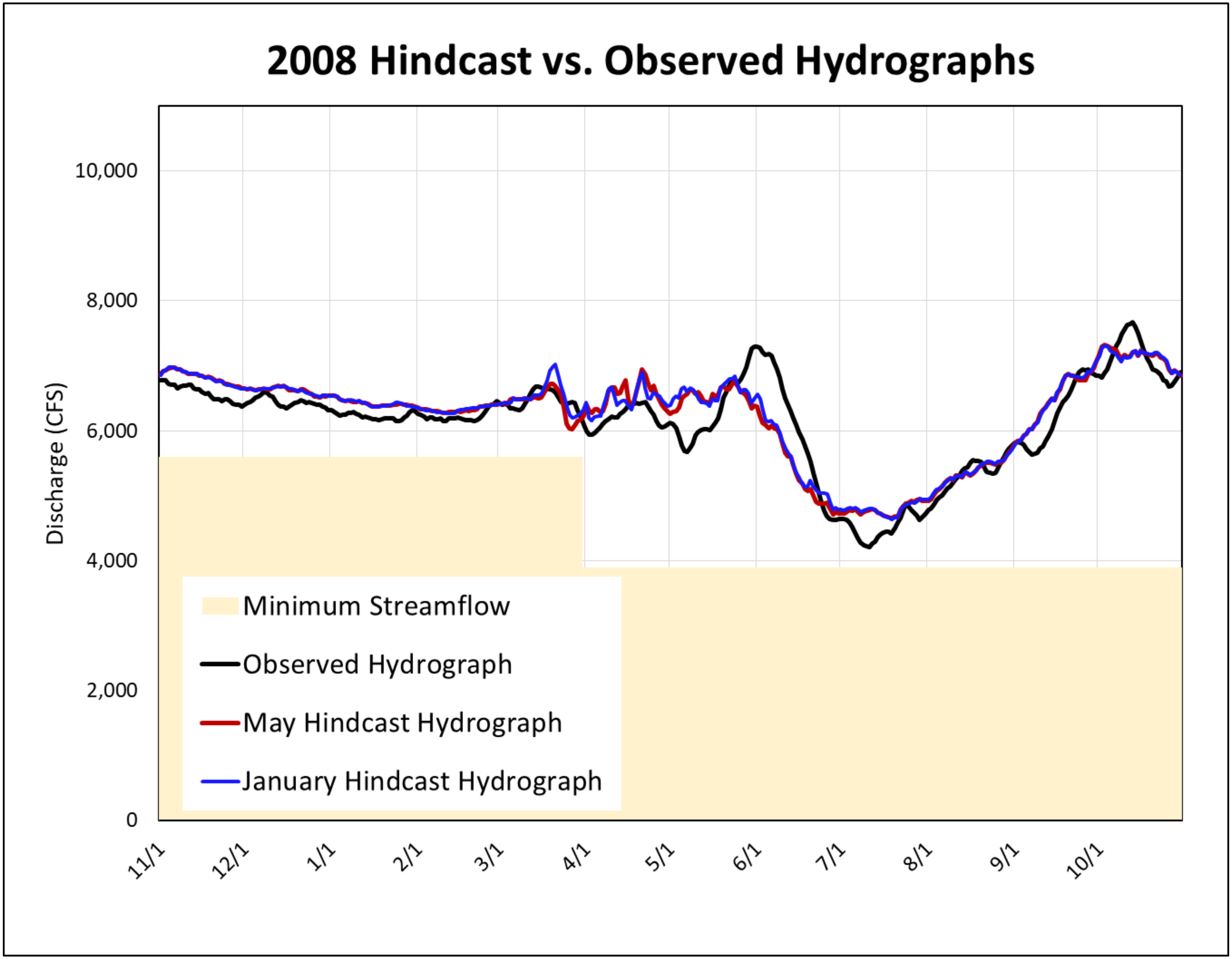
2008 Hindcast vs. Observed Hydrographs
Discharge (CFS)
10,000
8,000
6,000
4,000
2,000
0
11/1
12/1
1/1
2/1
3/1
4/1
5/1
6/1
7/1
8/1
9/1
10/1
Minimum Streamflow
Observed Hydrograph
May Hindcast Hydrograph
January Hindcast Hydrograph

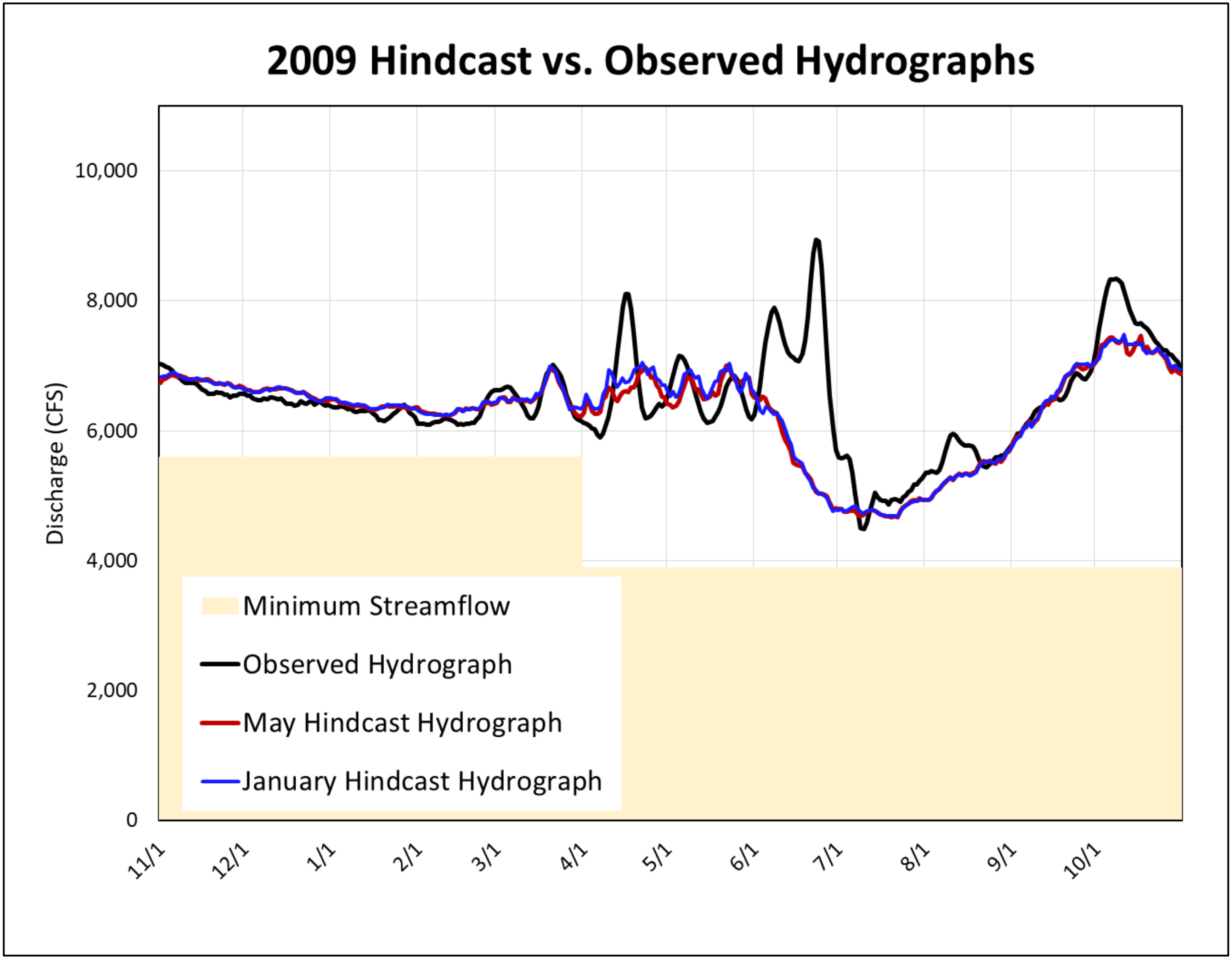
2009 Hindcast vs. Observed Hydrographs
Discharge (CFS)
10,000
8,000
6,000
4,000
2,000
0
11/1
12/1
1/1
2/1
3/1
4/1
5/1
6/1
7/1
8/1
9/1
10/1
Minimum Streamflow
Observed Hydrograph
May Hindcast Hydrograph
January Hindcast Hydrograph

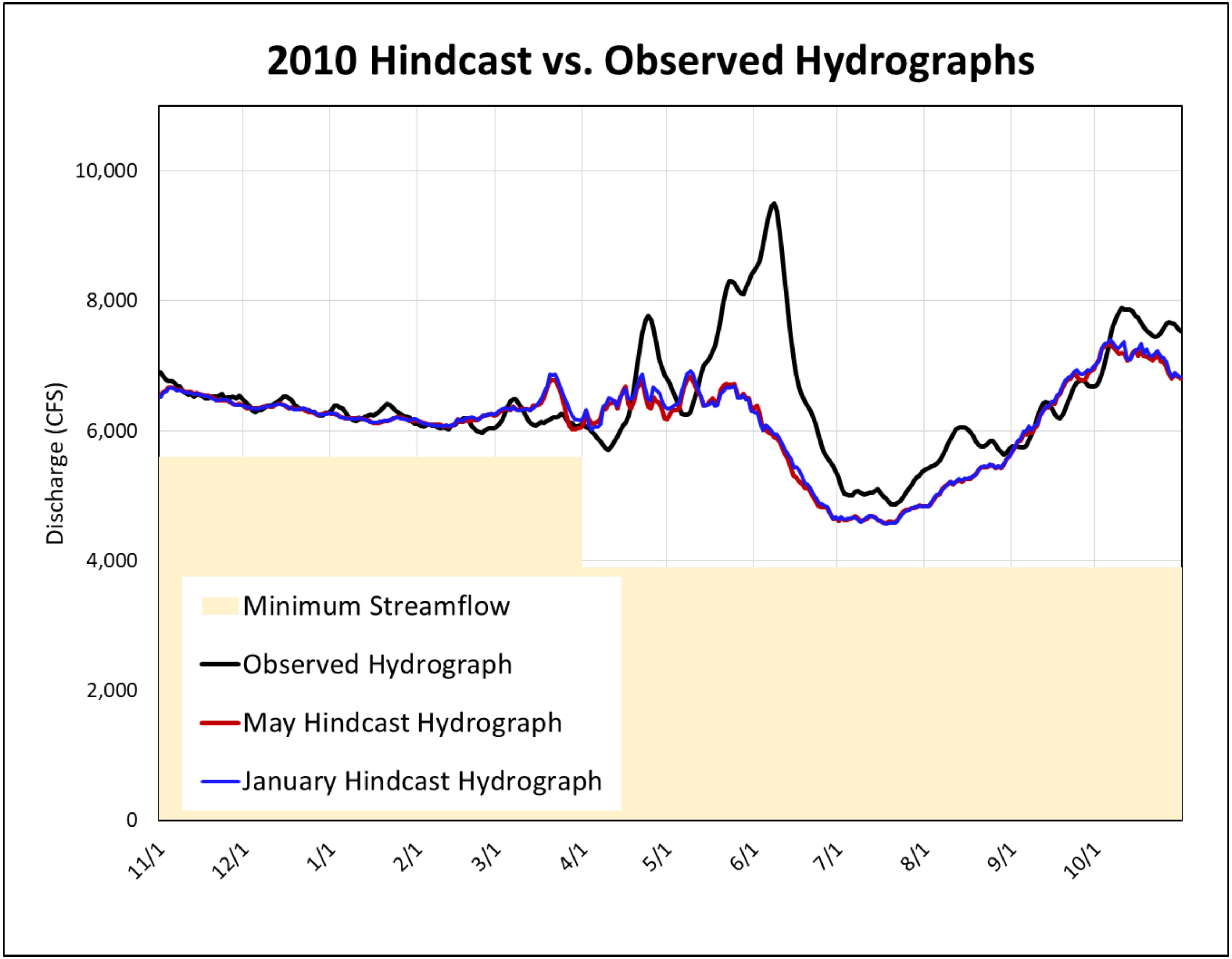

2010 Hindcast vs. Observed Hydrographs
Discharge (CFS)
10,000
8,000
6,000
4,000
2,000
0
11/1
12/1
1/1
2/1
3/1
4/1
5/1
6/1
7/1
8/1
9/1
10/1
Minimum Streamflow
Observed Hydrograph
May Hindcast Hydrograph
January Hindcast Hydrograph

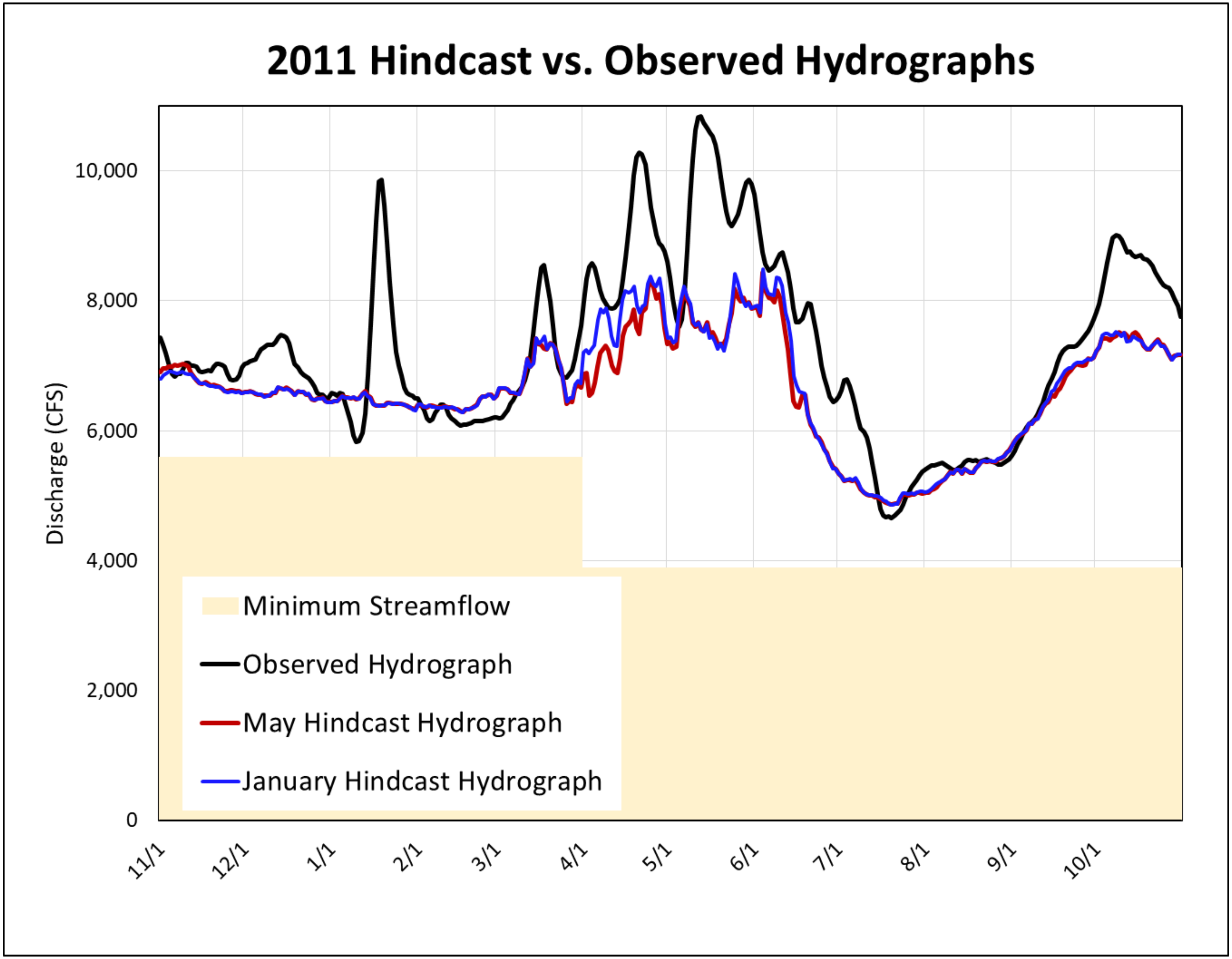
2011 Hindcast vs. Observed Hydrographs
Discharge (CFS)
10,000
8,000
6,000
4,000
2,000
0
11/1
12/1
1/1
2/1
3/1
4/1
5/1
6/1
7/1
8/1
9/1
10/1
Minimum Streamflow
Observed Hydrograph
May Hindcast Hydrograph
January Hindcast Hydrograph

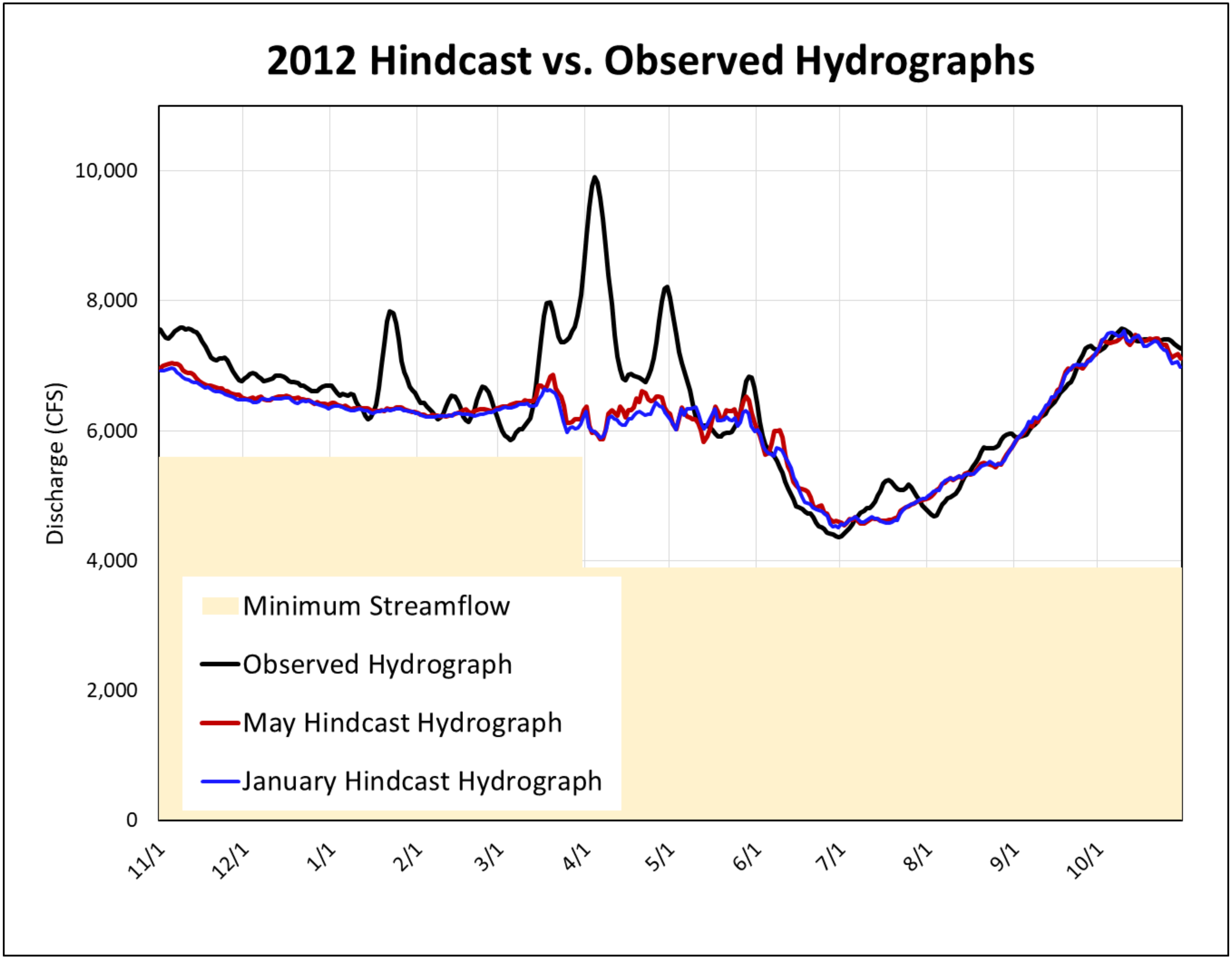
2012 Hindcast vs. Observed Hydrographs
Discharge (CFS)
10,000
8,000
6,000
4,000
2,000
0
11/1
12/1
1/1
2/1
3/1
4/1
5/1
6/1
7/1
8/1
9/1
10/1
Minimum Streamflow
Observed Hydrograph
May Hindcast Hydrograph
January Hindcast Hydrograph

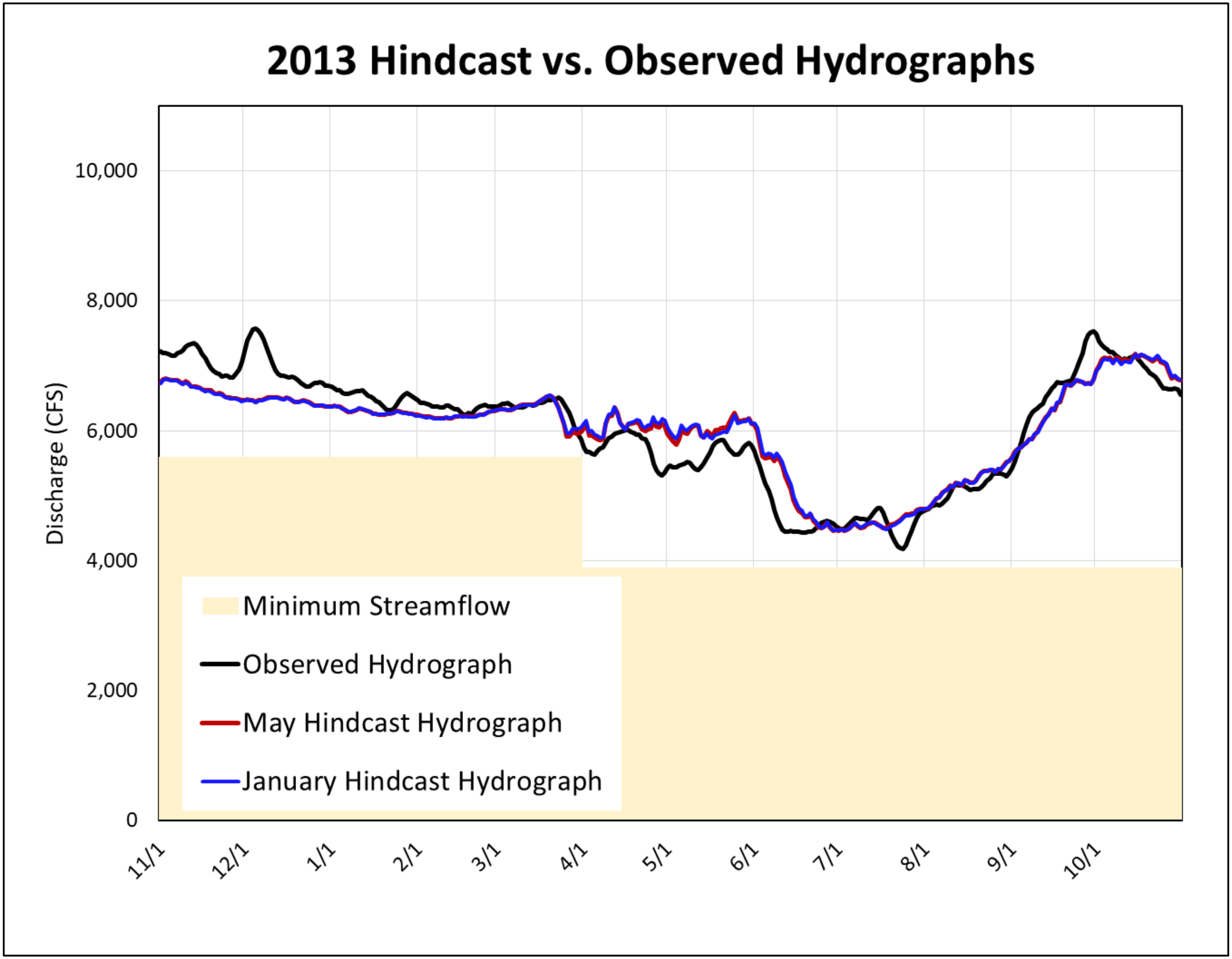
2013 Hindcast vs. Observed Hydrographs
Discharge (CFS)
10,000
8,000
6,000
4,000
2,000
0
11/1
12/1
1/1
2/1
3/1
4/1
5/1
6/1
7/1
8/1
9/1
10/1
Minimum Streamflow
Observed Hydrograph
May Hindcast Hydrograph
January Hindcast Hydrograph

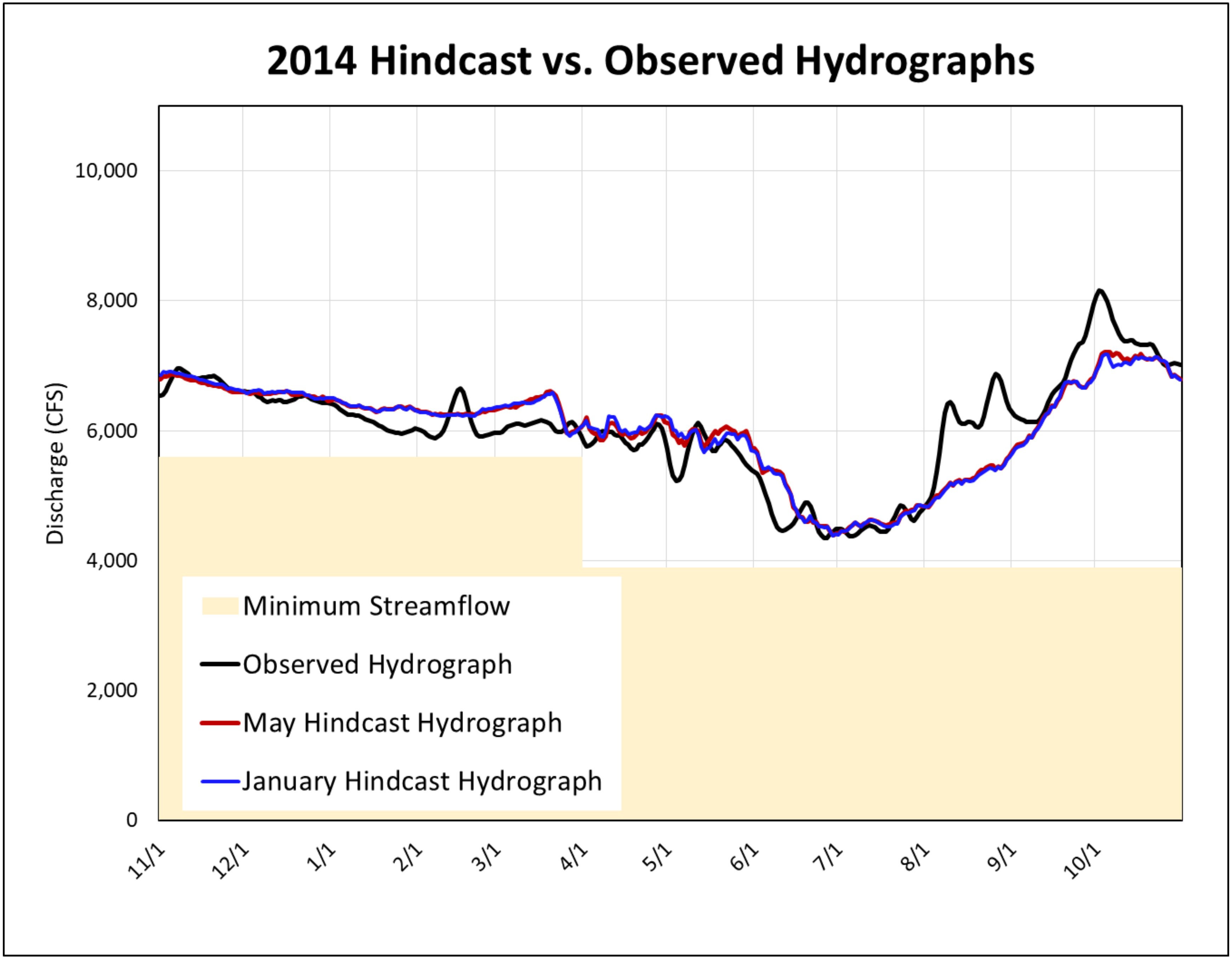

2014 Hindcast vs. Observed Hydrographs
Discharge (CFS)
10,000
8,000
6,000
4,000
2,000
0
11/1
12/1
1/1
2/1
3/1
4/1
5/1
6/1
7/1
8/1
9/1
10/1
Minimum Streamflow
Observed Hydrograph
May Hindcast Hydrograph
January Hindcast Hydrograph

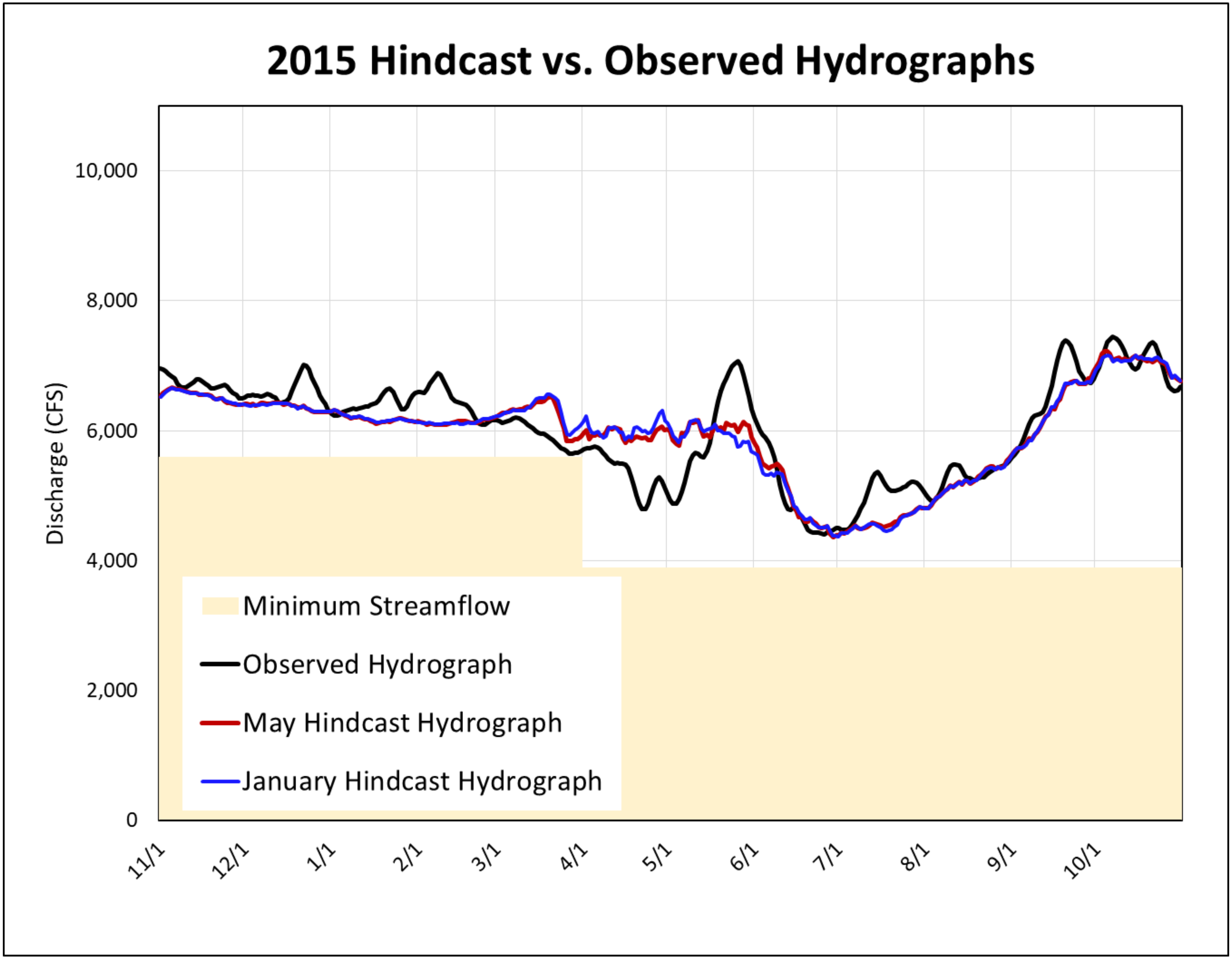
2015 Hindcast vs. Observed Hydrographs
Discharge (CFS)
10,000
8,000
6,000
4,000
2,000
0
11/1
12/1
1/1
2/1
3/1
4/1
5/1
6/1
7/1
8/1
9/1
10/1
Minimum Streamflow
Observed Hydrograph
May Hindcast Hydrograph
January Hindcast Hydrograph

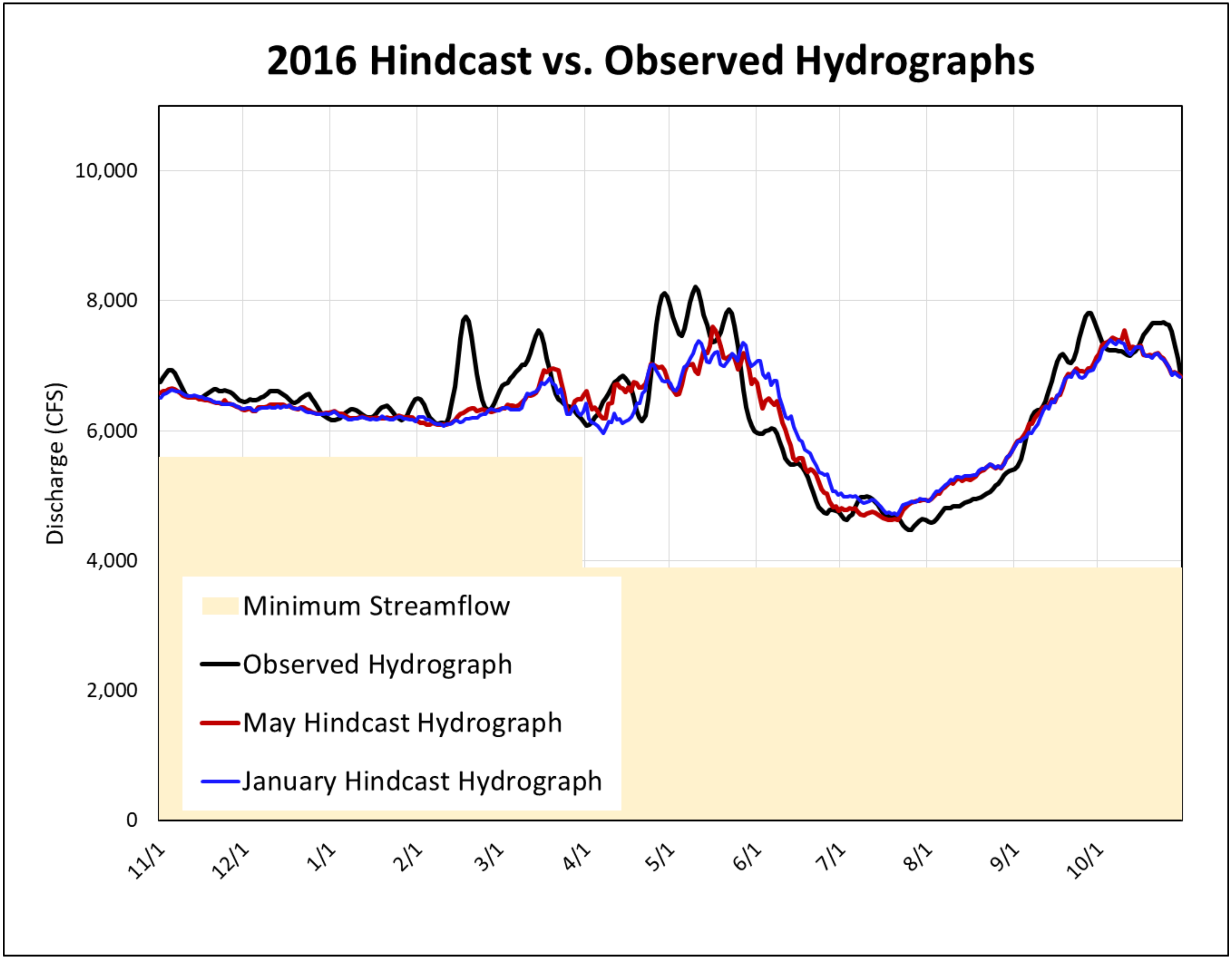
2016 Hindcast vs. Observed Hydrographs
Discharge (CFS)
10,000
8,000
6,000
4,000
2,000
0
11/1
12/1
1/1
2/1
3/1
4/1
5/1
6/1
7/1
8/1
9/1
10/1
Minimum Streamflow
Observed Hydrograph
May Hindcast Hydrograph
January Hindcast Hydrograph

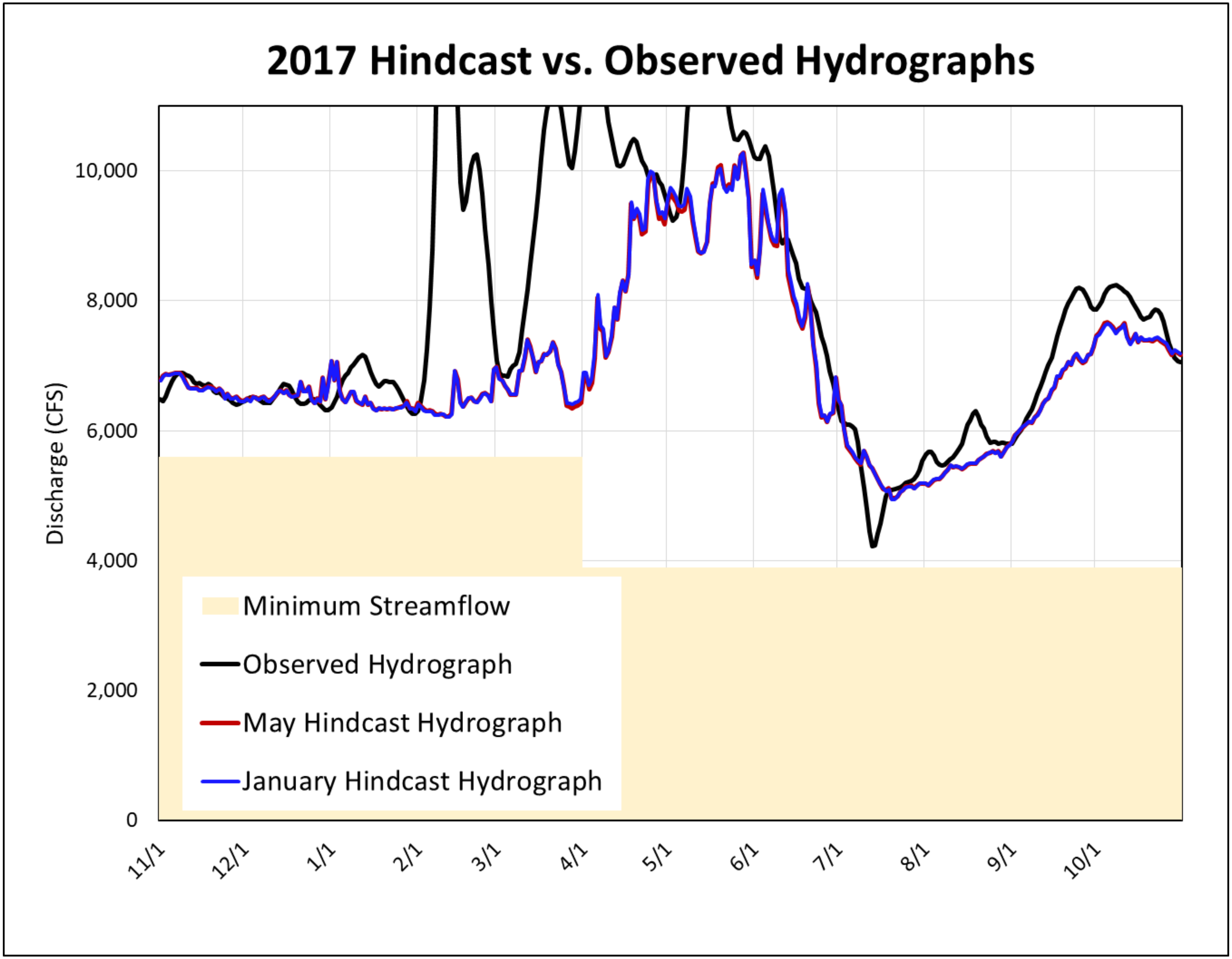
2017 Hindcast vs. Observed Hydrographs
Discharge (CFS)
10,000
8,000
6,000
4,000
2,000
0
11/1
12/1
1/1
2/1
3/1
4/1
5/1
6/1
7/1
8/1
9/1
10/1
Minimum Streamflow
Observed Hydrograph
May Hindcast Hydrograph
January Hindcast Hydrograph